

2016

Evaluation and prediction of hydrology and nitrate-nitrogen transport in tile-drained watersheds

Charles David Ikenberry
Iowa State University

Follow this and additional works at: <http://lib.dr.iastate.edu/etd>

 Part of the [Agriculture Commons](#), [Bioresource and Agricultural Engineering Commons](#), [Civil Engineering Commons](#), and the [Water Resource Management Commons](#)

Recommended Citation

Ikenberry, Charles David, "Evaluation and prediction of hydrology and nitrate-nitrogen transport in tile-drained watersheds" (2016). *Graduate Theses and Dissertations*. 15003.
<http://lib.dr.iastate.edu/etd/15003>

This Dissertation is brought to you for free and open access by the Graduate College at Iowa State University Digital Repository. It has been accepted for inclusion in Graduate Theses and Dissertations by an authorized administrator of Iowa State University Digital Repository. For more information, please contact digirep@iastate.edu.

Evaluation and prediction of hydrology and nitrate-nitrogen transport in tile-drained watersheds

by

Charles David Ikenberry

A dissertation submitted to the graduate faculty
in partial fulfillment of the requirements for the degree of

DOCTOR OF PHILOSOPHY

Major: Agricultural and Biosystems Engineering

Program of Study Committee:
Michelle L. Soupir, Major Professor
Matthew J. Helmers
William G. Crumpton
Philip W. Gassman
Roy R. Gu

Iowa State University

Ames, Iowa

2016

Copyright © Charles David Ikenberry, 2016. All rights reserved.

TABLE OF CONTENTS

	Page
LIST OF FIGURES	v
LIST OF TABLES	viii
NOMENCLATURE	x
ACKNOWLEDGEMENTS	xii
ABSTRACT.....	xiii
CHAPTER 1 GENERAL INTRODUCTION	1
1.1 Introduction	1
1.1.1 Overview of tile drainage.....	1
1.1.2 Water quality issues	3
1.1.3 Wetlands and tile drainage.....	3
1.2 Justification of Research	4
1.3 Organization of the Dissertation	6
1.4 Research Hypotheses and Objectives	7
1.4.1 Nitrate-nitrogen export: magnitude and patterns from drainage districts to downstream river basins.....	8
1.4.2 Simulating short-term fluctuations in subsurface flow and nitrate- nitrogen in small, tile-drained watersheds using SWAT.	9
1.4.3 Modification of SWAT to improve simulation of nitrate-nitrogen removal wetlands.....	10
1.5 References	10
CHAPTER 2 NITRATE-NITROGEN EXPORT: MAGNITUDE AND PATTERNS FROM DRAINAGE DISTRICTS TO DOWNSTREAM RIVER BASINS	13
2.1 Abstract	13
2.2 Introduction.....	14
2.3 Materials and Methods	18
2.3.1 Study area	18
2.3.2 Data collection and analysis	20
2.4 Results	22
2.4.1 Hydrology	22
2.4.2 Nitrate concentrations	24
2.4.3 Nitrate loads and yields.....	24

2.4.4 Cumulative analysis of nitrate yields	25
2.4.5. Nitrate and discharge relations.....	27
2.5 Discussion	29
2.5.1 Hydrologic patterns and relationships	29
2.5.2 Tile nitrate concentrations: magnitudes and implications	31
2.5.3 Nitrate losses: magnitude and context	33
2.5.4 Scaling drainage district losses to river basin exports	34
2.6 Conclusions	39
2.7 Acknowledgements.....	39
2.8 References	40
CHAPTER 3 SIMULATING SHORT-TERM FLUCTUATIONS IN SUBSURFACE FLOW AND NITRATE-NITROGEN IN SMALL, TILE- DRAINED WATERSHEDS USING SWAT	43
3.1 Abstract	43
3.2 Introduction	44
3.3 Materials and Methods	48
3.3.1 Study area	48
3.3.2 SWAT model development	50
3.3.3 Crop rotation and fertilizer application	52
3.3.4 Hydrologic parameterization and calibration	53
3.3.5 Nitrogen input parameterization	56
3.4 Results and Discussion	58
3.4.1 Evaluation of hydrologic simulation	58
3.4.2 Evaluation of NO ₃ -N simulation.....	62
3.4.3 Simulation with modified NO ₃ -N algorithms.....	69
3.4.4 Re-calibration with modified NO ₃ -N algorithms.....	75
3.5 Conclusions	81
3.6 Acknowledgements	83
3.7 References	83
CHAPTER 4 MODIFICATION OF SWAT TO IMPROVE SIMULATION OF NITRATE-NITROGEN REMOVAL WETLANDS	89
4.1 Abstract	89
4.2 Introduction	90
4.3 Materials and Methods	95
4.3.1 The SWAT model.....	95
4.3.2 Case study wetlands	98
4.3.3 Modified wetland equations	100
4.3.4 Hydrologic calibration	104
4.3.5 NO ₃ -N calibration	105
4.3.6 Integration of wetlands and watershed/tile drainage.....	106
4.4 Results and Discussion	107
4.4.1 Simulation of wetland hydrology	107

4.4.2 Simulation of wetland NO ₃ -N concentration	113
4.4.3 Simulation of wetland NO ₃ -N loads	116
4.4.4 Sensitivity analysis using modified wetland equations	128
4.4.5 Integrated watershed/wetland simulation	137
4.5 Conclusions	140
4.6 Acknowledgements	141
4.7 References	142
 CHAPTER 5 GENERAL CONCLUSIONS	 145
5.1 Review of central themes	145
5.2 Review of the magnitude and patterns of NO ₃ -N exports from drainage districts to downstream river basins	146
5.3 Review of simulating short-term fluctuations in subsurface flow and NO ₃ -N in small, tile-drained watersheds using SWAT	146
5.4 Review of the modification of SWAT to improve simulation of NO ₃ -N removal wetlands	148
5.5 Implications/recommendations	148
5.6 Recommendations for future research	149
 APPENDIX A FORTRAN CODE MODIFICATIONS FOR CHAPTER 3	 151
APPENDIX B FORTRAN CODE MODIFICATIONS FOR CHAPTER 4	152

LIST OF FIGURES

	Page
Figure 1.1 Subsurface tile drainage in the Upper Midwest	1
Figure 1.2 Common subsurface field tile configurations	2
Figure 2.1 Map of the Boone River and Lyons Creek watersheds	19
Figure 2.2 Monthly time series plots of precipitation, water yields, NO ₃ -N concentrations, and NO ₃ -N yields from tiles and the Boone River	23
Figure 2.3 Annual cumulative precipitation, water yields, and NO ₃ -N yields for each drainage district	26
Figure 2.4 Load duration curves for Lyons Creek tiles and the Boone River	28
Figure 2.5 Average annual and monthly NO ₃ -N loads in the Boone River with potential contributions from drainage districts	36
Figure 3.1. Location of CREP wetland watersheds simulated in this study	49
Figure 3.2. Daily time series SSF for the KS watershed	60
Figure 3.3. Daily time series SSF for the AL watershed	61
Figure 3.4. Daily time series NO ₃ -N concentration for the KS watershed	63
Figure 3.5. Daily time series NO ₃ -N concentration for the AL watershed	64
Figure 3.6. Simulated soil profile NO ₃ -N for corn-soybean rotations in the KS watershed	66
Figure 3.7. Simulated soil profile NO ₃ -N for corn-soybean rotations in the AL watershed	67
Figure 3.8. Daily time series NO ₃ -N concentration for the KS watershed using modified algorithms	70
Figure 3.9. Daily time series NO ₃ -N concentration for the AL watershed using modified algorithms	71
Figure 3.10. Simulated soil profile NO ₃ -N for corn-soybean rotations in the KS watershed with modified soil-NO ₃ algorithms	73
Figure 3.11. Simulated soil profile NO ₃ -N for corn-soybean rotations in the AL watershed with modified soil-NO ₃ algorithms	74

Figure 3.12. Re-calibrated daily time series NO ₃ -N concentration for the KS watershed using modified algorithms	76
Figure 3.13. Re-calibrated daily time series NO ₃ -N concentration for the AL watershed using modified algorithms	77
Figure 3.14. Simulated soil profile NO ₃ -N for corn-soybean rotations in the KS watershed with modified soil-NO ₃ algorithms after re-calibration.....	79
Figure 3.15. Simulated soil profile NO ₃ -N for corn-soybean rotations in the AL watershed with modified soil-NO ₃ algorithms after re-calibration.....	80
Figure 4.1 SWAT model structure illustrating relationship between subbasins, reaches, hydrologic response units, ponds/wetlands, and reservoirs	97
Figure 4.2 Location of case study CREP wetland sites.....	99
Figure 4.3 Observed flow into KS Wetland, simulated flow out of the wetland using modified wetland equations, and precipitation	109
Figure 4.4 Observed flow into AL Wetland, simulated flow out of the wetland using modified wetland equations, and precipitation	110
Figure 4.5 KS Wetland simulated outflows vs. measured inflows	111
Figure 4.6 AL Wetland simulated outflows vs. measured inflows	112
Figure 4.7 Calibration and validation results for KS Wetland NO ₃ -N concentration using original SWAT equations	114
Figure 4.8 Calibration and validation results for KS Wetland NO ₃ -N concentration using modified SWAT equations	115
Figure 4.9 Calibration and validation results for AL Wetland NO ₃ -N concentration using original SWAT equations	117
Figure 4.10 Calibration and validation results for AL Wetland NO ₃ -N concentration using modified SWAT equations	118
Figure 4.11 Calibration and validation results for KS Wetland NO ₃ -N loads using original SWAT equations	119
Figure 4.12 Calibration and validation results for KS Wetland NO ₃ -N loads using modified SWAT equations	120
Figure 4.13 Simulated vs. observed NO ₃ -N loads for the KS Wetland using	

original SWAT equations and modified wetland equations	121
Figure 4.14 Plot of NO ₃ -N load errors against observed loads for KS Wetland.....	122
Figure 4.15 Calibration and validation results for AL Wetland NO ₃ -N loads using original SWAT equations	124
Figure 4.16 Calibration and validation results for AL Wetland NO ₃ -N loads using modified SWAT equations	125
Figure 4.17 Simulated vs. observed NO ₃ -N loads for the AL Wetland using original SWAT equations and modified wetland equations	126
Figure 4.18 Plot of NO ₃ -N load errors against observed loads for AL Wetland.....	127
Figure 4.19 Sensitivity of NO ₃ -N concentrations in the KS wetland with variation of removal rate	130
Figure 4.20 Sensitivity of NO ₃ -N concentrations in the KS wetland with variation of temperature coefficient	131
Figure 4.21 Sensitivity of NO ₃ -N concentrations in the AL wetland with variation of removal rate	132
Figure 4.22 Sensitivity of NO ₃ -N concentrations in the AL wetland with variation of temperature coefficient	133
Figure 4.23 Simulation of NO ₃ -N concentrations in the KS wetland with variation of NDTARGR	135
Figure 4.24 Simulation of NO ₃ -N loads exported from the KS wetland with variation of NDTARGR	136
Figure 4.25 Simulated NO ₃ -N loads in wetland outflow for the best simulation of the KS watershed using modified lagging parameters	138
Figure 4.26 Simulated NO ₃ -N loads in wetland outflow for the KS watershed using the original NO ₃ -N algorithms	139

LIST OF TABLES

	Page
Table 2.1 Watershed characteristics for the Lyons Creek drainage districts	19
Table 2.2 Annual average data summary for tile-drained catchments and Boone River	22
Table 2.3 Percentage of total water yield and NO ₃ -N exported during various discharge conditions	29
Table 3.1 Watershed characteristics of simulated sites.....	49
Table 3.2 Simulated fertilizer-N application.....	53
Table 3.3 Hydrologic input parameters considered during model calibration and assessment	55
Table 3.4 Performance evaluation criteria	56
Table 3.5 Nitrogen-related parameters considered during model calibration and assessment	57
Table 3.6 Performance statistics for pathway-specific flow components.....	58
Table 3.7 Performance statistics for initial daily NO ₃ -N concentration calibration.	62
Table 3.8 Simulated soil-N dynamics for Webster and Clarion soil HRUs after calibration using existing NO ₃ -N algorithms.	68
Table 3.9 Performance statistics for modified daily NO ₃ -N concentration calibration.	69
Table 3.10 Simulated soil-N dynamics for Webster and Clarion soil HRUs after calibration using modified NO ₃ -N algorithms.....	72
Table 3.11 Performance statistics for modified daily NO ₃ -N concentration re-calibration	78
Table 3.12 Simulated soil-N dynamics for Webster and Clarion soil HRUs after re-calibration using modified NO ₃ -N algorithms.	81
Table 4.1 Watershed and wetland characteristics of case study sites	99
Table 4.2 Performance evaluation criteria	105

Table 4.3	Wetland parameters and calibration values using original SWAT equations	106
Table 4.4	Wetland parameters and calibration values using modified equations....	107
Table 4.5	Comparison of NO ₃ -N simulation performance using original and modified equations	128

NOMENCLATURE

ac	Acre
ARS	Agricultural Research Service
BMP	Best Management Practice
CREP	Conservation Reserve Enhancement Program
d	Day
EPA	Environmental Protection Agency
ha	Hectare
hr	Hour
HUC	Hydrologic Unit Code
in	Inch
kg	Kilograms
L	Liter
m	Meter
mm	Millimeter
mg	Milligram
N	Nitrogen
NO ₃ -N	Nitrate-nitrogen
NRCS	Natural Resources Conservation Service
NSE	Nash-Sutcliffe Efficiency
PBIAS	Percent Bias
ppb	Parts per billion

ppm	Parts per million
Q	Volumetric flow rate
SSF	Sum of tile flow, lateral flow, and groundwater flow
SURQ	Surface runoff (SWAT model output)
SWAT	Soil and Water Assessment Tool
μg	Microgram
USDA	United States Department of Agriculture
USGS	United States Geological Survey
WYLD	Water yield (SWAT model output)

ACKNOWLEDGEMENTS

I would like to take this opportunity to thank several individuals that played important roles in my graduate education and experience. First, I am extremely grateful to my Major Professor, Michelle Soupir, for giving me the opportunity to pursue my doctorate at Iowa State University. I am sincerely appreciative of her insight, advice, encouragement, and patience. I would also like to thank my committee members – Matt Helmers, Bill Crumpton, Phil Gassman, and Roy Gu – for their time and expertise in helping refine my research ideas and always encouraging me to dig deeper into the issues.

A special note of thanks to my supervisor, Allen Bonini, and the Department of Natural Resources, for seeing value in allowing me to pursue this opportunity. I must express both apologies and appreciation to all my colleagues at the DNR that have listened to me complain about nights, weekends, and vacation time spent studying, analyzing, or writing. I do hope that your patience has not worn too thin, and I thank you for your tolerance.

Finally and most importantly, I must thank my entire family, but especially my wife Kristen, who has made many sacrifices throughout this process. She has willingly taken on far more than her share of parental duties while I was working late or locked in a quiet room in a remote corner of the house. She has been selfless, supportive, encouraging, and always forgiving. I hope that this endeavor will ultimately benefit her and our children in some way, and I look forward to making up for lost time with them.

ABSTRACT

Implementation of artificial subsurface drainage (tile drainage) for cultivation of row crops in poorly-drained areas of the Upper Midwest of the United States has enabled the region to be one of the most agriculturally productive areas of the world; but has also resulted in loss of wetland ecosystems, altered hydrology, and increased transport of nitrate-nitrogen ($\text{NO}_3\text{-N}$) to surface water. The direct link between subsurface tile drainage and transport of nonpoint-source pollutants, particularly $\text{NO}_3\text{-N}$, to surface waters is a primary concern for downstream drinking water supplies and hypoxia in the Gulf of Mexico. The studies described in this dissertation include evaluation of $\text{NO}_3\text{-N}$ export from small, tile-drained watersheds typical of agricultural drainage districts on the Des Moines Lobe ecoregion of Iowa, evaluation of watershed-scale simulation of hydrology and $\text{NO}_3\text{-N}$ transport at the daily interval using the Soil and Water Assessment Tool (SWAT), investigation of important nitrogen pathways and processes simulated in SWAT, and the evaluation and improvement of SWAT algorithms for simulating water quality treatment wetlands in this landscape.

Specific objectives of the first study were to quantify hydrology and $\text{NO}_3\text{-N}$ export patterns from three tile-drained catchments and the downstream river over a 5-yr period, compare results to prior plot-, field-, and watershed-scale studies, and discuss implications for water quality improvement in these landscapes. The tile-drained catchments had an annual average water yield of 247 mm yr^{-1} , a flow-weighted $\text{NO}_3\text{-N}$ concentration of 17.1 mg L^{-1} , and an average $\text{NO}_3\text{-N}$ loss of nearly $40 \text{ kg ha}^{-1} \text{ yr}^{-1}$. Overall, water yields were consistent with prior tile drainage studies in Iowa and the upper Midwest, but associated $\text{NO}_3\text{-N}$ concentrations and losses were among the highest reported for plot studies and higher than those found in other small watersheds. More than 97% of the $\text{NO}_3\text{-N}$ export occurs

during the highest 50% of flows at both the small catchment and river basin scales. Findings solidified the importance of working at the drainage district scale to achieve $\text{NO}_3\text{-N}$ reductions necessary to meet water quality goals. They also point to the need for implementing strategies that address both hydrology and nitrogen supply in tile-drained landscapes.

The objectives of the second study were to develop and calibrate SWAT models for small, tile-drained watersheds, evaluate model performance for pathway-specific flow and $\text{NO}_3\text{-N}$ simulation at monthly and daily intervals, and document important intermediate processes and N-fluxes. For simulation in the KS and AL watersheds, Nash-Sutcliffe Efficiency (NSE) values were 0.79 and 0.71, respectively, for monthly water yield (WYLD); 0.55 and 0.66 for monthly subsurface flow (SSF); and 0.72 and 0.60 for monthly $\text{NO}_3\text{-N}$ load (using the modified $\text{NO}_3\text{-N}$ lagging algorithms). However, calibration efforts were extensive and detailed monitoring data allowing such efforts are not typically available. Simulation of daily surface runoff (SURQ) and SSF proved more challenging and were generally not satisfactory (NSE < 0.50) with the exception of daily SURQ in the KS watershed, for which NSE was 0.55 and percent bias (PBIAS) was -10.0%. Simulation of daily $\text{NO}_3\text{-N}$ concentration was not satisfactory even after modifying algorithms to lag $\text{NO}_3\text{-N}$ transport via tile flow. For daily $\text{NO}_3\text{-N}$ concentration the KS watershed NSE was 0.20 and AL watershed NSE was -1.12, indicating that simulation in the AL model was less accurate than using the average concentration. Important soil $\text{NO}_3\text{-N}$ processes such as mineralization, denitrification, and plant uptake are often overlooked in watershed modeling studies, but should be evaluated and reported as standard practice. These processes are highly variable

and difficult to measure. Better parameterization methods are needed, and related inputs and soil-N fluxes should be constrained within reasonable ranges.

The objectives of the third study were to modify wetland algorithms in SWAT by adapting proven CREP wetland models, compare model performance using both original SWAT algorithms and modified wetland equations, and evaluate the ramifications of watershed and tile drain simulation errors on prediction of $\text{NO}_3\text{-N}$ in Iowa CREP wetlands. The modified equations improved simulation of hydrology and $\text{NO}_3\text{-N}$ in the wetlands, with NSE values of 0.88 to 0.99 for daily load predictions, and PBIAS values generally less than 6%. The applicability of the modified equations to wetlands without detailed monitoring data was improved over the original SWAT equations due to more objectively-informed parameterization, reduced need for hydrologic calibration, and incorporation of an irreducible nutrient concentration and temperature correction factor. The $\text{NO}_3\text{-N}$ removal rate (NSETLR) is the critical input parameter for $\text{NO}_3\text{-N}$ reduction and strongly influences model performance. Isolating the KS wetland from the watershed resulted in an overall NSE of 0.98 and PBIAS of 2.6% for $\text{NO}_3\text{-N}$ load at the wetland outlet. When the wetland was integrated with the watershed simulation using existing soil and tile $\text{NO}_3\text{-N}$ algorithms, the NSE decreased to 0.30 and PBIAS increased to 53.3%, indicating that simulation of the BMP is limited by the ability of the model to reflect short-term fluctuations in flow and $\text{NO}_3\text{-N}$ concentration.

CHAPTER 1. GENERAL INTRODUCTION

1.1 Introduction

1.1.1 Overview of tile drainage

Alteration of the landscape of the Upper Midwest of the United States by the widespread installation of subsurface tile drainage infrastructure (Figure 1.1) and subsequent cultivation of wetland areas has enabled the region to become one of the most agriculturally productive areas in the world (McCorvie and Lant, 1993; Urban, 2005). Common configurations of subsurface drainage infrastructure include privately owned field tiles (Figure 1.2), which drain to a system of increasingly larger tiles (subcollectors and collector mains) that eventually discharge to a ditch or stream. Surface inlets are sometimes placed in poorly-drained depressions and ditches to

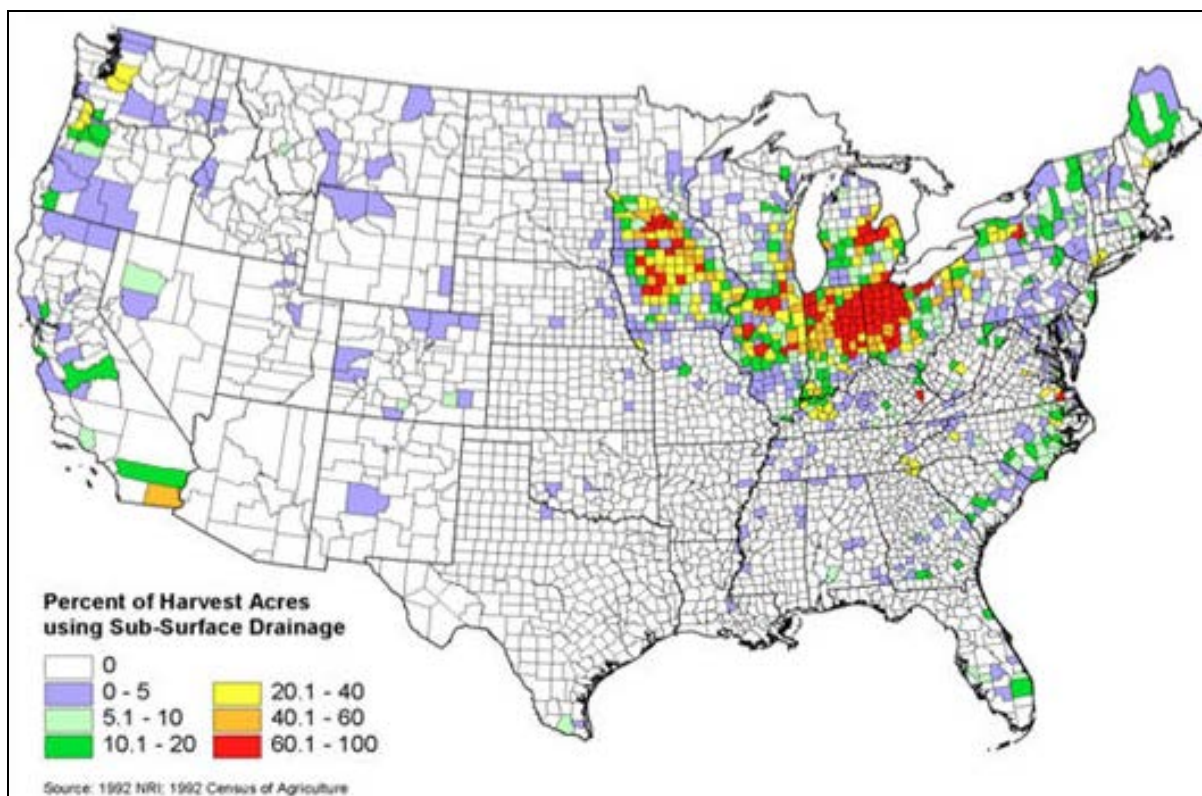


Figure 1.1 Subsurface tile drainage in the Upper Midwest (Census of Agriculture).

drain surface ponding through the tile system. The construction and maintenance of collector systems is facilitated by formation of agricultural drainage districts, which provide the financing and organization necessary to install drainage infrastructure across multiple tracts of land.

Subsurface tile drainage systems enable row crop production and improve crop yields in poorly-drained soils by lowering the water table, thereby limiting prolonged saturation of the root

zone to prevent root aeration stress (Hatfield et al., 1998; Goswami et al., 2008). Drainage also increases the planting and harvesting windows by creating drier soil conditions for planting and harvesting equipment (Fipps and Skaggs, 1991). In many areas of the Corn Belt, including north-central Iowa, cultivation of poorly-drained soils for corn (*Zea mays* L.) and soybean [*Glycine max* (L.) Merr.] would not be viable if not for the installation of subsurface tile drainage systems. Unfortunately, artificial subsurface drainage has some unintended and undesirable ecological and environmental consequences, including altered hydrology, loss of wetland habitat and function, and contributions of nonpoint source pollutants to surface waters.

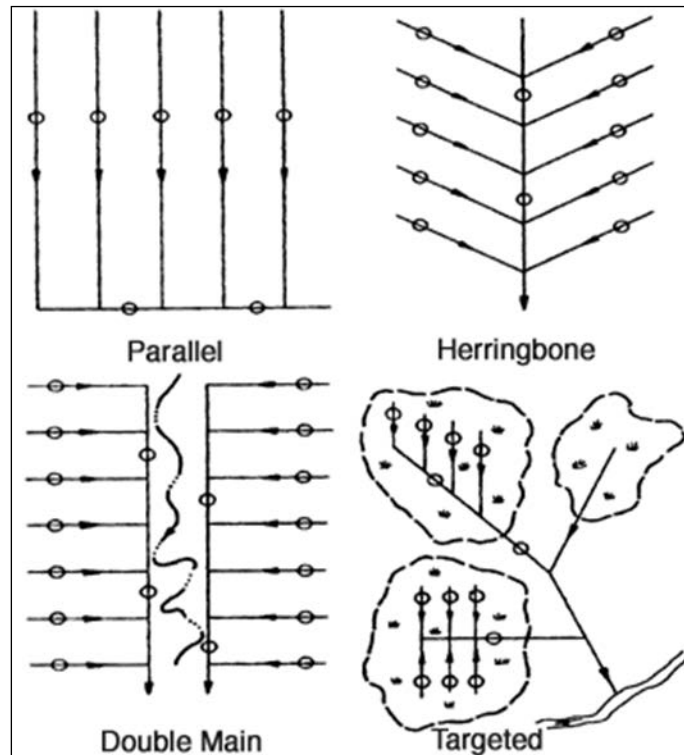


Figure 1.2 Common subsurface field tile configurations (University of Minnesota Extension)

1.1.2 Water quality issues

Streamflow and nutrient levels in watersheds with significant tile drainage are affected because tile drains alter the pathways and processes that govern hydrology and nutrient transport (Schilling and Helmers, 2008). Relative importance and magnitude of water balance components such as runoff, lateral flow, shallow groundwater flow, and aquifer recharge differ in tilled versus non-tiled watersheds (Gentry, 2007; Goswami et al., 2008; Sui and Frankenberger, 2008). Similarly, water quality processes such as erosion, nitrification/denitrification, and leaching are impacted by the presence of tile drain systems (El-Sadek et al., 2003; Lemke et al., 2011; Coelho et al., 2012). The direct link between subsurface tile drainage and transport of nonpoint-source pollutants, particularly nitrate-nitrogen ($\text{NO}_3\text{-N}$), to surface waters is a primary concern for drinking water systems using surface water supplies. Additionally, hypoxia in the Gulf of Mexico is attributed largely to N and phosphorus (P) exports from the Upper Mississippi River basin (UMRB) (Goolsby et al., 2000; Alexander et al., 2008; David et al., 2010). Recently, contributions of dissolved P from tile drains to surface water (King et al., 2014; Smith et al., 2014) and resulting eutrophication, particularly in Lake Erie, has received increased attention (Baker et al., 2014; Johnson et al., 2014).

1.1.3 Wetlands and tile drainage

During European settlement of the Midwest, “wet lands” were considered obstacles to settlement, a breeding ground for nuisance mosquitoes, and a hindrance to productive use of the landscape (Urban, 2005). It is not surprising, then, that by the mid-1800s, government policies and programs evolved to establish wide-spread drainage projects to remove these “undesirable” landscape features and allow cultivation of the rich prairie soils of the Corn Belt region. Because

drainage projects were expensive, states passed legislation that made possible the formation of drainage districts. The State of Iowa passed drainage district legislation in 1873, and by 1930, 22% of all farmland in the state was drained and 18% of farmland (over 2.4 million ha) was included in a drainage district. As a result, Iowa has lost over 95% of its wetland areas (Bishop et al., 1982; Miller et al., 2009) with similar losses in Indiana, Illinois, and Ohio (McCorvie and Lant, 1993). These programs were immensely successful in accomplishing their planned objectives and contributed to the agricultural and economic success of the region.

However, as scientists began to recognize the ecological, hydrological, and water quality benefits of wetlands, government policies began to reverse course in the 1970s, with provisions for wetland protection in the 1969 National Environmental Policy Act (NEPA) and 1972 Clean Water Act (CWA). In 1989, President George H.W. Bush signed a policy of “no net loss” of wetlands, and the 1990 U.S. Farm Bill included subsidies to restore wetlands that government once paid to remove (McCorvie and Lant, 1993). In addition to funding wetland mitigation programs for the purpose of ecosystem restoration, programs such as the Iowa Conservation Reserve Enhancement Program (CREP) have been initiated to strategically utilize wetland functions for water quality improvement in tile-drained landscapes (Crumpton et al, 2006).

1.2 Justification of Research

The central theme of this dissertation is the evaluation and simulation of hydrology and $\text{NO}_3\text{-N}$ transport in tile-drained watersheds in north-central Iowa. While it is widely known that artificial subsurface drainage of land in agricultural production and loss of wetland ecosystems affects hydrology and nutrient transport, accurate prediction and simulation of these landscapes remains challenging. The major biogeochemical processes and pathways involved have

generally been identified, but are often extremely complex, spatially and temporally variable, and therefore difficult to quantify. Long-term water yields and nutrient losses from large land areas can be estimated at annual or even seasonal time-steps using a variety of regression approaches and available flow, water quality, and land use data (Goolsby et al., 2000; Crumpton et al., 2006; Alexander et al., 2008; Stenback et al., 2011). Often, however, estimates of nutrient losses are desired when and where in-stream data is not available at the scale of interest.

At smaller spatial scales and time steps, variation in hydrology and nutrient transport is often difficult to explain and more difficult to simulate. Some uncertainty is caused by unknown differences in soil characteristics, such as particle size distribution, organic matter content, and pH (Cambardella et al., 1994). Additionally, dynamic processes such as microbial activity and the development of preferential pathways (i.e., cracks and fissures), can have a dramatic effect on the movement of water and nutrients but these processes are difficult to incorporate into simulation models. Agricultural practices specific to individual farms and fields (e.g., tillage, fertilizer type, and application rates) also impact hydrology and nutrient transport. In most instances, an accurate and complete record of agricultural management decisions is not available for modeling purposes.

In areas with tile drainage systems, the tile infrastructure itself is one of the most hydrologically dominant features of the landscape. It is often necessary to use general design guidance to estimate local tile size, depth, and spacing characteristics. In many cases, it is likely that modeling constructs and assumptions do not accurately reflect in situ drainage infrastructure. At large scales this variation is less important because general guidelines may reflect average conditions. But variation in tile infrastructure characteristics may be critical for predicting

hydrology and nutrient losses in smaller watersheds (i.e., drainage district scale) and at shorter time intervals.

These aforementioned uncertainties and variations in watershed characteristics, combined with simplifying model assumptions and limitations, confound efforts to accurately assess the impact of specific drainage catchments on stream flows, local water quality, and nutrient exports at smaller spatial and temporal scales. This has several important consequences for watershed management. First, it is often difficult to determine which drainage catchments contribute the highest water yields and nutrient losses without expensive and prolonged monitoring studies. This hinders timely and reliable prioritization of watersheds for the purpose of reducing nutrient losses to surface water. Second, it hampers selection and targeting agricultural best management practices (BMPs) aimed at reducing nutrient-driven water quality problems. Different BMPs are more or less suitable for treating distinct nutrient pathways, and the performance of some BMPs is sensitive to characteristics of the inflow. For example, wetlands should be placed where they have opportunity to intercept and treat the most $\text{NO}_3\text{-N}$. Models capable of accurately predicting differences in hydrology and nutrient export from specific watersheds would greatly benefit watershed management for water quality improvement.

1.3 Organization of the Dissertation

This research is focused on the evaluation and simulation of watershed-scale hydrology and $\text{NO}_3\text{-N}$ transport in tile-drained landscapes. The challenges associated with predicting spatial and temporal variation in hydrology and $\text{NO}_3\text{-N}$ transport are investigated through the analysis of monitoring data and through modeling efforts. Chapter 2: *Nitrate-Nitrogen Export: Magnitude and Patterns from Drainage Districts to Downstream River Basins* includes an

analysis of five years of flow and $\text{NO}_3\text{-N}$ data collected at the outlet of three adjacent, tile-drained agricultural drainage districts and the downstream river basin. This analysis sets the stage for the larger objective, which is to improve our ability to predict and simulate hydrology and nutrient transport at watershed scales in tile-drained landscapes. Chapter 3: *Simulating short-term fluctuations in subsurface flow and nitrate-nitrogen in small, tile-drained watersheds using SWAT* evaluates the ability of SWAT to simulate pathway-specific flow components, short-term fluctuations of $\text{NO}_3\text{-N}$ concentrations, and examines soil-N processes and fluxes. Chapter 4: *Modification of SWAT to improve simulation of nitrate-nitrogen removal wetlands* discusses an important water quality improvement strategy, constructed wetlands, and improves a widely-used watershed model to better reflect hydrology and $\text{NO}_3\text{-N}$ removal in wetlands. Ramifications of tile-drained watershed simulations on predicted wetland performance is also evaluated. Chapter 5 summarizes the key findings of Chapters 2 through 4, discusses implications of key findings, and makes recommendations for continued efforts to improve watershed-scale simulation of hydrology and nutrient transport in tile-drained landscapes.

1.4 Research Hypotheses and Objectives

Development of modeling tools capable of simulating small, tile-drained catchments typical of agricultural drainage districts is needed for water quality planning and cost-effective nutrient reduction. The overall goal of this research is to improve understanding and prediction of hydrology and $\text{NO}_3\text{-N}$ transport in tile-drained watersheds and wetlands of the Corn Belt region, specifically north-central Iowa. To achieve this goal, the following hypotheses and objectives are presented for each chapter of the dissertation.

1.4.1 Chapter 2: Nitrate-nitrogen export: magnitude and patterns from drainage districts to downstream river basins.

HYPOTHESES:

- $\text{NO}_3\text{-N}$ losses from drainage district-scale catchments, typically between 200 and 3,000 hectares in size, are critical source-areas for $\text{NO}_3\text{-N}$ exports from larger basins.
- Trends and patterns in streamflow and $\text{NO}_3\text{-N}$ export from larger river basins (i.e., the Boone River) reflect those observed from small, tile-drained catchments in smaller, headwater streams (i.e., Lyons Creek).

OBJECTIVES:

- Quantify water yields, $\text{NO}_3\text{-N}$ concentrations, and $\text{NO}_3\text{-N}$ yields over a 5-yr period from three tile-drained catchments typical of drainage districts in north-central Iowa
- Assess spatial, temporal, and precipitation-driven patterns in hydrology and $\text{NO}_3\text{-N}$ transport
- Discuss implications for watershed management and water quality improvement in these landscapes.

1.4.2 Chapter 3: Simulating short-term fluctuations in subsurface flow and nitrate-nitrogen in small, tile-drained watersheds using SWAT.

HYPOTHESES:

- The SWAT model's ability to simulate pathway-specific flow components and short-term fluctuation of NO₃-N transport is not thoroughly tested and documented in the literature despite its widespread use.
- Watershed models used to predict effects of BMP implementation require more thorough performance assessment, including evaluation of pathway-specific components and intermediate nutrient processes/fluxes.
- These intermediate processes should be reported as standard procedure in watershed modeling studies, and improved parameterization methods and model algorithms may be required to improve model performance.

OBJECTIVES:

- Develop and calibrate SWAT models for small, tile-drained watersheds.
- Evaluate model performance for pathway-specific flows and NO₃-N simulation at monthly and daily intervals.
- Document important intermediate model processes for assessment of model performance and make recommendations for model parameterization.

1.4.3 Chapter 4: Modification of SWAT to improve simulation of nitrate-nitrogen removal wetlands.

HYPOTHESES:

- Simulation of wetlands using SWAT is largely untested and undocumented in the literature.
- Current wetland algorithms in the SWAT model can be modified to better represent hydrology and NO₃-N removal in water quality wetlands.
- Parameterization of modified wetland algorithms using monitoring results from Iowa CREP wetlands can better inform simulation of wetlands that lack detailed monitoring data.
- Reliable simulation of some nutrient reduction BMPs may be limited by the accuracy of short-term simulations of nutrient concentrations.

OBJECTIVES:

- Modify existing algorithms in SWAT by adapting proven CREP wetland models.
- Compare model performance using original SWAT algorithms and modified wetland equations to simulate two Iowa CREP wetlands.
- Evaluate the ramifications of watershed and tile simulations errors on prediction of NO₃-N in Iowa CREP wetlands.

1.5 References

- Alexander, R. B., R. A. Smith, G. E. Schwarz, E. W. Boyer, J. V. Nolan, and J. W. Brakebill. 2008. Differences in phosphorus and nitrogen delivery to the gulf of Mexico from the Mississippi river basin. *Environmental Science & Technology*. 42 (3): 822-830.
- Baker, D. B., R. Confesor, D. E. Ewing, L. T. Johnson, J. W. Kramer, and B. J. Merryfield. 2014. Phosphorus loading to Lake Erie from the Maumee, Sandusky and Cuyahoga

- rivers: The importance of bioavailability. *J. Great Lakes Res.* 40:502-517.
<http://dx.doi.org/10.1016/j.jglr.2014.05.001>
- Bishop, R. A., and A. G. van der Valk. 1982. Wetlands. pp. 208-229. In T.C. Cooper (ed.) *Iowa's Natural Heritage*. Iowa Natural Heritage Foundation and Iowa Academy of Science. Des Moines, Iowa, USA.
- Cambardella, C. A., Moorman, T. B., Parkin, T. B., Karlen, D. L., Novak, J. M., Turco, R. F., & Konopka, A. E. 1994. Field-scale variability of soil properties in central Iowa soils. *Soil Sci. Soc. Amer. J.* 58(5):1501-1511. doi:10.2136/sssaj1994.03615995005800050033x
- Coelho, B. B., R. Murray, D. Lapen, E. Topp, and A. Bruin. 2012. Phosphorus and sediment loading to surface waters from liquid swine manure application under different drainage and tillage practices. *Agricultural Water Management.* 104: 51-61.
- Crumpton, W. G., G. A. Stenback, B. A. Miller, and M. J. Helmers. 2006. Potential benefits of wetland filters for tile drainage systems: impact on nitrate loads to Mississippi River subbasins. Ames, Iowa. Final report to the U.S. Department of Agriculture (USDA).
- David, M.B., L.E. Drinkwater, and G.F. McIsaac. 2010. Sources of nitrate yield in the Mississippi River basin. *J. Environ. Qual.* 39:1657–1667. doi:10.2134/jeq2010.0115
- El-Sadek, A., J. Feyen, M. Radwan, and D. El Quosy. 2003. Modeling water discharge and nitrate leaching using DRAINMOD-GIS technology at small catchment scale. *Irrigation and Drainage.* 52 (4): 363-381.
- Fipps, G., and R.W. Skaggs. 1991. Simple methods for predicting flow to drains. *J. Irrig. Drain. Eng.* 117(6):881–896. doi:10.1061/(ASCE)0733-9437(1991)117:6(881)
- Gentry, L. E., M. B. David, T. V. Royer, C. A. Mitchell, and K. M. Starks. 2007. Phosphorus transport pathways to streams in tile-drained agricultural watersheds. *J. Environ. Qual.* 36:408–415. doi:10.2134/jeq2006.0098
- Goolsby, D.A., W.A. Battaglin, B.T. Aulenbach, and R.P. Hooper. 2000. Nitrogen flux and sources in the Mississippi River basin. *Sci. Total Environ.* 248:75–86.
 doi:10.1016/S0048-9697(99)00532-X
- Goswami, D., P.K. Kalita, R.A. Cooke, and M.C. Hirschi. 2008. Estimation and analysis of baseflow in drainage channels in two tile-drained watersheds in Illinois. *Trans. ASABE* 51(4):1201–1213. doi:10.13031/2013.25238
- Hatfield, J.L., J.H. Prueger, and D.B. Jaynes. 1998. Environmental impacts of agricultural drainage in the Midwest. In: *Drainage in the 21st century: Food production and the environment*. Proceedings of the 7th Annual Drainage Symposium, Orlando, FL. 8–10 Mar. 1998. ASAE, St. Joseph, MI.
- Johnson, L. T., D. B. Baker, R. Confesor, K. A. Krieger, and R. P. Richards. 2014. Research to help Lake Erie: Proceedings of the “Phosphorus along the land-river-lake continuum” research planning and coordination workshop. *J. Great Lakes Res.* 40:574-577.
<http://dx.doi.org/10.1016/j.jglr.2014.07.001>
- King, K. W., M. R. Williams, and N R. Fausey. 2014. Contributions of systematic tile drainage to watershed-scale phosphorus transport. *J. Environ. Qual.* doi:10.2134/jeq2014.04.0149
- Lemke, A. M., K. G. Kirkham, T. T. Lindenbaum, M. E. Herbert, T. H. Tear, W. L. Perry, and J. R. Herkert. 2011. Evaluating Agricultural Best Management Practices in Tile-Drained Subwatersheds of the Mackinaw River, Illinois. *J. Environ. Qual.* 40(4):1215-1228.
- McCorvie, M.R., and C.L. Lant. 1993. Drainage district formation and the loss of Midwestern wetlands, 1850-1930. *Agric. Hist.* 67(4):13–39.

- Miller, B. A., W. G. Crumpton, and A. G. van der Valk. 2009. Spatial distribution of historical wetland classes on the Des Moines Lobe, Iowa. *Wetlands*. 29(4):1146-1152.
- Schilling, K. E., and M. Helmers. 2008. Effects of subsurface drainage tiles on streamflow in Iowa agricultural watersheds: Exploratory hydrograph analysis. *Hydrological Processes*. 22 (23): 4497-4506.
- Sui, Y., and J. R. Frankenberger. 2008. Nitrate loss from subsurface drains in an agricultural watershed using SWAT2005. *Transactions of the Asabe*. 51 (4): 1263-1272.
- Smith, D. R., K. W. King, L. Johnson, W. Francesconi, P. Richards, D. Baker, and A. N. Sharpley. 2014. Surface runoff and tile drainage transport of phosphorus in the midwestern United States. *J. Environ. Qual.* doi:10.2134/jeq2014.04.0176
- Stenback, G. A., W. G. Crumpton, K. E. Schilling, and M. J. Helmers. 2011. Rating curve estimation of nutrient loads in Iowa rivers. *J. Hydrol.* 396(1-2):158-169.
- Urban, M.A. 2005. An uninhabited waste: Transforming the Grand Prairie in nineteenth century Illinois, USA. *J. Hist. Geogr.* 31:647–665. doi:10.1016/j.jhg.2004.10.001

CHAPTER 2. NITRATE-NITROGEN EXPORT: MAGNITUDE AND PATTERNS FROM DRAINAGE DISTRICTS TO DOWNSTREAM RIVER BASINS

A modified version of this paper is published in the Journal of Environmental Quality¹

Charles D. Ikenberry, Michelle L. Soupir,

Keith E. Schilling, Christopher S. Jones, Anthony Seeman.

2.1 Abstract

Alteration of the prairie pothole ecosystem through installation of subsurface tile drains has enabled the U.S. Corn Belt to become one of the most agriculturally productive areas in the world but has also led to increased nitrogen (N) losses to surface water. The literature contains numerous field plot studies but few in-depth studies of nitrate-nitrogen (NO₃-N) exports from small, tile-drained catchments representative of agricultural drainage districts. The objectives of this study were to quantify hydrology and NO₃-N export patterns from three tile-drained catchments and the downstream river over a 5-yr period, compare results to prior plot-, field-, and watershed-scale studies, and discuss implications for water quality improvement in these landscapes. The tile-drained catchments had an annual average water yield of 247 mm yr⁻¹, a flow-weighted NO₃-N concentration of 17.1 mg L⁻¹, and an average NO₃-N loss of nearly 40 kg ha⁻¹ yr⁻¹. Overall, water yields consistent with prior tile drainage studies in Iowa and the upper Midwest, but associated NO₃-N concentrations and losses were among the highest reported for plot studies and higher than those found in small watersheds.

¹ *J. of Envir. Qual.* 43:2024-2033. doi:10.2134/jeq2014.05.0242

More than 97% of the nitrate export occurs during the highest 50% of flows, at both the small catchment and river basin scale. Findings solidified the importance of working at the drainage district scale to achieve nitrate reductions necessary to meet water quality goals. They also point to the need for implementing strategies that address both hydrology and nitrogen supply in tile-drained landscapes.

Keywords: tile drainage, hydrology, nitrate transport, drainage district, hypoxia

2.2 Introduction

Alteration of the prairie pothole ecosystem of the midwestern United States has enabled the region to become one of the most agriculturally productive areas in the world (McCorvie and Lant, 1993; Urban, 2005). One primary feature of this transformation is increased drainage capacity of poorly drained soils through installation of subsurface tile drains. Widespread agricultural drainage projects were facilitated by the federal Swamp Land Acts enacted in the middle of the 19th century to encourage drainage and development of wetlands for agricultural purposes. Because drainage projects were expensive, states passed legislation that made possible the formation of drainage districts, which provided the financing and organization necessary to install drainage infrastructure across multiple tracts of land. The State of Iowa passed drainage district legislation in 1873, and by 1930, 22% of all farmland in the state was drained and 18% of farmland (over 2.4 million ha) was included in a drainage district (McCorvie and Lant, 1993). Authors of the Iowa Nutrient Reduction Strategy, completed in 2013, estimated that 66.8% of row crop land in the Central Iowa and Minnesota Till Prairies Major Land Resource Area (MLRA) has subsurface tile drainage (Iowa State University, 2013).

Subsurface drainage infrastructure includes privately owned perforated pipes installed in parallel configurations at a field scale. These pipes drain to a system of increasingly larger tiles (subcollectors and collector mains) operated by a drainage district that eventually discharge to ditches or streams. Surface inlets are sometimes placed in poorly drained depressions to drain surface ponding through the tile system. Tile drains enable row crop production and improve crop yields in poorly drained soils by lowering the water table, thereby limiting saturation of the root zone to prevent root aeration stress (Hatfield et al., 1998; Goswami et al., 2008). Drainage also improves trafficability for planting and harvesting equipment (Fipps and Skaggs, 1991). In many areas of the Corn Belt, including north-central Iowa, cultivation of poorly drained soils for corn (*Zea mays* L.) and soybean [*Glycine max* (L.) Merr.] would not be viable if not for the installation of subsurface tile drainage systems.

Unfortunately, artificial subsurface drainage has some unintended and undesirable ecological and environmental consequences. From a water quality perspective, the direct link between subsurface tile drainage and increased transport of nonpoint-source pollution, particularly $\text{NO}_3\text{-N}$, to surface waters is a primary concern (Dinnes et al., 2002). Des Moines Water Works (DMWW) treats and distributes the potable water supply for approximately 500,000 people in the Des Moines, IA, metropolitan area. Due to nitrate levels at the surface water intakes that frequently exceed the maximum contaminant level (MCL), DMWW constructed a nitrate removal system in 1992, which is said to be the largest of its kind in the world (DMWW, 2009). Even with multiple sources of raw water and the nitrate removal system, meeting the drinking water $\text{NO}_3\text{-N}$ MCL of 10 mg L^{-1} at the tap can be difficult when river nitrate concentrations are high. This challenge, combined with large-scale concerns

regarding nitrate transport from the Upper Mississippi River basin (UMRB) to the Gulf of Mexico, has increased the focus on nitrate exports from agricultural drainage districts in north-central Iowa.

In a long-term study (1989–2004) correlating nitrate losses in tile drains to fertilizer application rates, Lawlor et al. (2008) observed average $\text{NO}_3\text{-N}$ yields approaching $40 \text{ kg ha}^{-1} \text{ yr}^{-1}$ and maximum losses over 70 kg ha^{-1} in 0.05-ha research plots near Gilmore City, IA. Average annual losses of 10.3 kg ha^{-1} and flow-weighted concentrations of 16 mg L^{-1} were observed from 1993 to 1998 on field plots near Nashua, IA (Bakhsh et al., 2002). An 11-yr plot-scale study in southern Minnesota revealed average annual flow-weighted concentrations between 12.0 and 13.4 mg L^{-1} and associated losses of 41 and 43 kg ha^{-1} for 0.02-ha plots with conventional tillage and no tillage, respectively (Randall and Iragavarapu, 1995). A 4-yr study in northwest Ohio yielded average annual exports of 15.3 and 27.4 kg ha^{-1} (Logan et al., 1994). Hofmann et al. (2004) measured $\text{NO}_3\text{-N}$ concentrations of 17.7 and 24.3 mg L^{-1} from plots with 20-m and 30-m spacing, respectively, resulting in annual average losses of 26.6 and 22.2 kg ha^{-1} over 6 yr.

In larger field plots between 3.3 and 8.5 ha in east-central Illinois, Kalita et al. (2006) found flow-weighted $\text{NO}_3\text{-N}$ concentrations between 15 and 20 mg L^{-1} and losses between 23 and $33 \text{ kg ha}^{-1} \text{ yr}^{-1}$ from 1991 to 2000. From 1995 to 1997, Gentry et al. (2000) observed concentrations of 10.2 and 13.1 mg L^{-1} , and losses of 41.6 and $32.7 \text{ kg ha}^{-1} \text{ yr}^{-1}$, from 15- and 5-ha field plots in the same region of Illinois. Jaynes et al. (2001) observed $\text{NO}_3\text{-N}$ yields between 13 and $61 \text{ kg ha}^{-1} \text{ yr}^{-1}$ from a 22-ha production field in central Iowa. At large watershed scales in central Iowa, $\text{NO}_3\text{-N}$ yields of 15 to $31 \text{ kg ha}^{-1} \text{ yr}^{-1}$ were estimated for the Des Moines and Raccoon River basins between 1980 and 1996 (Goolsby et al., 2000). A

NO₃-N flux of 7.2 kg ha⁻¹ yr⁻¹ was calculated for the entire UMRB between 1997 and 2006 (David et al., 2010). A trend of decreasing nitrate concentrations and yields in the downstream direction is prevalent in the literature; however, few publications report nitrate yields from small- to mid-sized watersheds.

On the basis of 2 yr (2009 and 2010) of flow and NO₃-N concentration data at tile outlets, NO₃-N yields between 33.8 and 77.0 kg ha⁻¹ yr⁻¹ were estimated for drainage districts in the Lyons Creek watershed, a second-order HUC-12 watershed located in the Boone River basin within the UMRB (Schilling et al., 2012). Relationships between nitrate levels and drainage area were established, but limited years of data prevented a thorough analysis of spatial and temporal patterns in hydrology and nitrate export from these sites over time. Long-term flow and nitrate concentration data (1992–2000) were obtained at two tile outlets and the mouth of the 5,130-ha Walnut Creek watershed, another second-order stream in central Iowa (Jaynes et al., 1999; Tomer et al., 2003). Relationships between flow and nitrate flux were reported, with major findings being that nitrate concentrations and yields were lower at the watershed outlet than at tile outlets and that nitrate concentrations were typically not diluted by high flows except during highly infrequent, flooding conditions. Both studies determined that nitrate concentrations decrease in the downstream direction and highlighted the importance of addressing nitrate loads at the drainage district scale for realization of meaningful reductions in nitrate transport.

Drainage district tile mains draining small catchments (typically between 200 and 1,500 ha) discharge to drainage ditches and small headwater streams in the Des Moines Lobe upstream of the DMWW surface water intakes. Land within drainage districts accounts for 75% of the total drainage area of the Boone River watershed (Figure 2.1). It is recognized

that nitrate losses from drainage districts are critical to nitrate transport at larger scales, but quantification of nitrate exports at this scale is lacking. The objectives of this study were (i) to quantify water yields, nitrate concentrations, and nitrate yields over a 5-yr period from three tile-drained catchments typical of drainage districts in north-central Iowa; (ii) to assess spatial, temporal, and precipitation-driven patterns in hydrology and nitrate transport; and (iii) to discuss implications for watershed management and water quality improvement in these landscapes.

2.3 Materials and Methods

2.3.1 Study area

The study focused on three drainage districts discharging to Lyons Creek, a small headwater stream that flows into the Boone River, a major tributary to the Des Moines River upstream of the DMWW surface water intake (Figure 2.1). The confluence of Lyons Creek with the Boone River is located in Webster City, IA. Precipitation data were obtained from the National Weather Service weather station at Webster City, which is available for download from the Iowa Environmental Mesonet (Iowa State University, 2014). Flow and NO₃-N data were collected at the tile outlet of each drained catchment, with monitoring stations identified as LCR3T, LCR4T, and LCR5T. The catchments are representative of drainage districts in the Des Moines Lobes ecoregion, with similar soils (silty loams in glacial till), topography (flat to rolling with pothole depressions), land cover (predominately corn and soybean), and subsurface tile drainage infrastructure (Table 2.1). Drainage in Lyons Creek includes surface inlets in some depressions and ditches (Schilling et al., 2012, 2013), which introduces some runoff into the tile drain system.

Table 2.1 Watershed characteristics for the Lyons Creek drainage districts.

Characteristic	LCR3T	LCR4T	LCR5T
Drainage area, DA (ha)	309		227
Row crop (% of DA)	93	92	90
Poor drainage (% of DA) ^[a]	79	75	76
Slope classification (% of DA)			
0-2% slope	46	44	42
2-5% slope	51	49	53
5-9% slope	3	7	6

^[a] Row crop areas with slopes < 5% and soils classified as somewhat poor to poorly-drained.

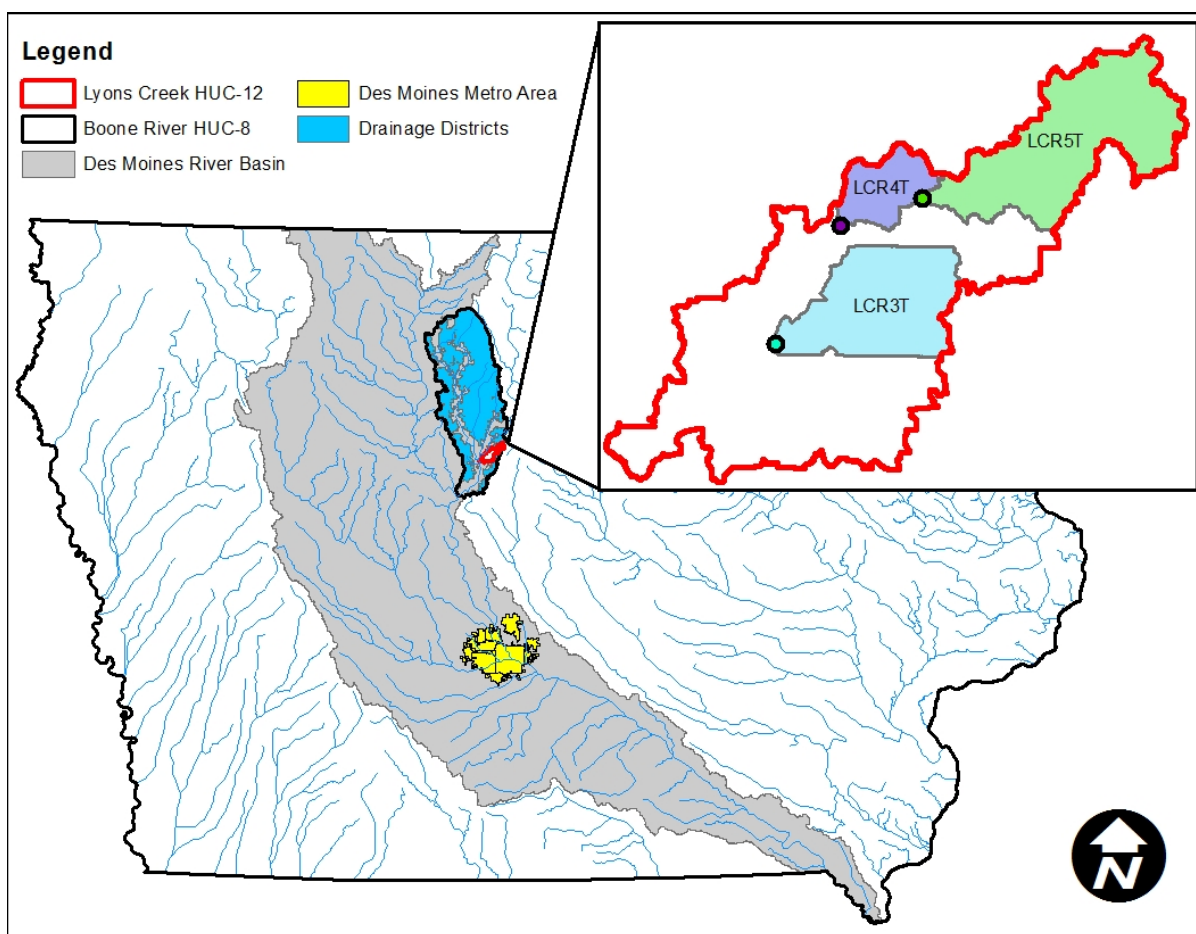


Figure 2.1 Map of the Boone River and Lyons Creek watersheds. The Boone River watershed is a HUC-8 that lies within the Des Moines River basin upstream of Des Moines. Blue-shaded areas represent agricultural land in drainage districts that rely on subsurface tile drainage systems. The Lyons Creek Huc-12 watershed is outlined in red in the insert. Tile-drained catchments and tile outlet locations for LCR3T, LCR4T, and LCR5T are shown in the insert.

The monitored catchments encompass working-scale farms across multiple landowners, and a full accounting of agronomic practices (e.g., tillage and fertilizer application rates) is not available, unlike controlled, plot-scale studies. Catchments were delineated using a 3-m horizontal resolution digital elevation model (DEM) that was developed using Light Detection and Ranging (LiDAR) data (Iowa Department of Natural Resources, 2013b). The DEM required hydraulic reinforcement to account for culverts and bridges under roadways, as well as known locations of tile collector mains. Resulting drainage areas were 747 ha for LCR3T, 260 ha for LCR4T, and 1091 ha for LCR5T. Flow and nitrate concentration data were also obtained for the Boone River, a fifth-order stream and HUC-8 watershed that drains 2,350 km² of the predominantly row-cropped agricultural land on the Des Moines Lobe.

2.3.2 Data collection and analysis

Tile discharge was measured using ISCO 2150 area-velocity flow modules. The sensors were placed in the tiles 2 m from the outlet and secured using expansion rings. The area-velocity modules include a pressure transducer to measure water depth, and they emit ultrasonic sound waves to measure water velocity. Measurements were recorded and stored at 5-min intervals but reduced to daily average discharge rates. Daily stream flow in the Boone River was obtained from the USGS gaging station (ID = 05481000) near Webster City, IA, approximately 7 km downstream from the mouth of Lyons Creek.

Grab samples were collected at biweekly intervals from LCR3T, LCR4T, LCR5T, and the Boone River monitoring station from 2009 through 2013, with more frequent tile sampling during times of elevated flows. Samples were transferred from a dipper apparatus to a 500-mL polyethylene terephthalate bottle, stored on ice, and transported to the laboratory

for analysis on the day of collection. NO₃-N concentration, in milligrams per liter, was quantified using USEPA Method 300.0 (Pfaff, 1993), with quality control procedures including blanks, spikes, replicates, and known-concentration samples. Additional grab samples were collected from the Boone River site by the Iowa Department of Natural Resources (DNR) and obtained from the DNR's STORET (Iowa Department of Natural Resources, 2013a) database. During storm events, automated ISCO samplers (Teledyne ISCO Inc.) collected multiple samples at 1-h intervals from the tile outlets. These samples were collected in separate bottles and analyzed separately to assess possible distinctions in nitrate concentrations at different points on the storm event hydrograph. Little variation was observed between nitrate concentrations analyzed during the same storm event; therefore, daily average NO₃-N concentrations were calculated from event samples for the purposes of this study. Concentrations were estimated for days on which no samples were collected by interpolating between measured concentrations from adjacent sample collection days.

Daily NO₃-N loads (kg d⁻¹) from the Lyons Creek catchments (LCR3T, LCR4T, and LCR5T) and the Boone River were calculated by multiplying daily discharge and NO₃-N concentration. Load duration curves (LDCs) were developed using daily discharge and measured (but not interpolated) nitrate concentrations. Daily discharges and nitrate loads at each monitoring location were converted to water yields (mm) and NO₃-N yields (kg ha⁻¹ d⁻¹). Precipitation, water yield, and NO₃-N losses were also averaged by year and by month across the entire study period to assess temporal and seasonal patterns.

2.4 Results

2.4.1 Hydrology

Average annual precipitation in the Lyons Creek watershed during the 5-yr study period was 853 mm, 3.8% less than the 30-yr (1984–2013) average of 887 mm yr⁻¹. The highest annual rainfall total occurred in 2010, with 1315 mm of precipitation (Table 2.2). Below-normal precipitation occurred in 2011, 2012, and 2013, but the timing of precipitation was notably different, with spring 2013 being exceptionally wet and the latter half of 2013 being exceptionally dry (Figure 2.2a).

Site-specific, annual water yields from the tile outlets ranged from 24 mm at LCR3T in 2012 to 693 mm at LCR4T in 2010, and averaged 248 mm. The corresponding ratio of annual water yield to precipitation, termed drainage ratio (DR), ranged between 3.7 and 52.7% and averaged 29.1% across all three catchments (Table 2.2). Despite similar annual precipitation from 2011 to 2013, water yields in 2012 were only 14 and 12% of water yields in 2011 and 2013, respectively (Table 2.2).

Table 2.2 Annual average data summary for tile-drained catchments and Boone River.

Year	Tile drain averages†					Boone River		
	Prec.‡ mm	WY‡ mm	DR‡ %	FWC‡ mg L ⁻¹	NO ₃ -N yield kg ha ⁻¹	WY mm	FWC mg L ⁻¹	NO ₃ -N yield kg ha ⁻¹
2009	938	265	28.3	12.9	34.2	232	8.8	20.4
2010	1315	532	40.4	10.6	56.4	574	8.5	48.6
2011	641	190	29.6	16.7	31.7	203	10.5	21.4
2012	646	27	4.1	20.5	5.5	31	10.6	3.2
2013	727	224	30.8	31.8	71.3	223	19.1	42.6
Mean	853	248	29.11§	17.1¶	39.8	253	10.8¶	27.2

† Average of tile-drained catchments in the Lyons Creek watershed (LCR3T, LCR4T, and LCR5T).

‡ Prec. = precipitation; WY = water yield; DR = drainage ratio; FWC = flow-weighted annual average concentration.

§ Total water yield divided by total precipitation for the 5-yr study period.

¶ Flow-weighted average nitrate concentration for the 5-yr study period.

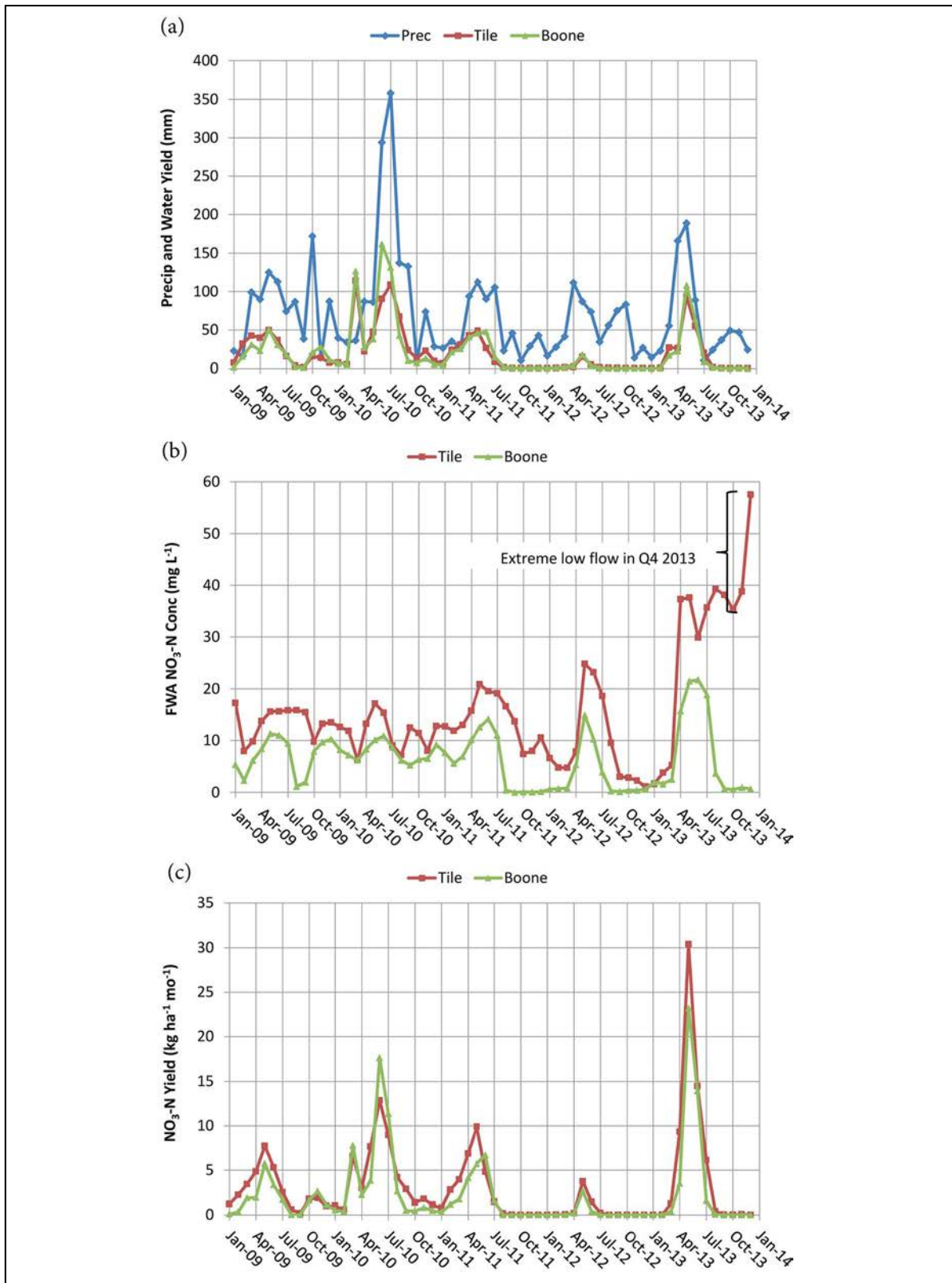


Figure 2.2 Monthly time series plots of (a) precipitation (Precip), water yield from monitored tile outlets, and water yields in the Boone River; (b) flow-weighted average (FWA) $\text{NO}_3\text{-N}$ concentrations in tile flow and the Boone River; and (c) $\text{NO}_3\text{-N}$ yields from the tiles and Boone River. Q4 = fourth quarter of calendar year.

2.4.2 Nitrate concentrations

Sampled $\text{NO}_3\text{-N}$ concentrations from the Lyons Creek tile outlets ranged from 0.1 to 77.4 mg L^{-1} , with 74.2% of discrete samples exceeding the drinking water MCL of 10 mg L^{-1} . Flow-weighted annual concentrations varied from 9.8 mg L^{-1} at LCR3T in 2010 to 38.0 mg L^{-1} at LCR4T in 2013. Concentrations at all three tile outlets were highest in 2013, with maximum concentrations ranging from 47.9 to 77.4 mg L^{-1} in the three drainage districts. Overall, the annual flow-weighted average for all three sites during the 5-yr study period was 17.1 mg L^{-1} . Nitrate-N concentrations in the Boone River, which receives the tile drainage contributions, ranged from non-detectable to 30.0 mg L^{-1} in the spring of 2013, with 24.4% of all samples exceeding 10 mg L^{-1} . Flow-weighted average annual concentrations measured in the Boone River ranged from 8.5 mg L^{-1} in 2010 to 19.1 mg L^{-1} in 2013 and averaged 10.8 mg L^{-1} during the 5-yr study period. Both tile concentrations and those measured in the Boone River exhibited strong seasonality (Figure 2.2b). Average monthly flow-weighted concentrations in drainage districts were highest in May (25.5 mg L^{-1}), June (19.9 mg L^{-1}), and April (18.8 mg L^{-1}). Average monthly flow-weighted concentrations in the Boone River ranged from 10.3 to 15.8 mg L^{-1} from April through June, and 4.4 to 9.4 mg L^{-1} for all other months. It is noteworthy that concentrations remained extremely high in late 2013, even when tile flow was minimal (Figure 2.2b).

2.4.3 Nitrate loads and yields

Nitrate-N exported from the Lyons Creek drainage districts from 2009 to 2013 totaled 384.7 Mg, with 62% of the 5-yr total occurring in 2010 and 2013. Annual average loading was 76.9 Mg yr^{-1} . Nitrate-N transported through the Boone River system averaged 6,407 Mg yr^{-1} and totaled 32,036 Mg, with 67% of the total 5-yr load exported in 2010 and

2013, collectively. Analysis of NO₃-N yields revealed that nitrate losses were highest from LCR4T and lowest from LCR3T, with the exception of the drought year of 2012 when nitrate yield was slightly higher from LCR5T than LCR4T. The 5-yr average NO₃-N yields were 28.9 kg ha⁻¹ yr⁻¹ from LCR3T, 52.2 kg ha⁻¹ yr⁻¹ from LCR4T, and 38.3 kg ha⁻¹ yr⁻¹ from LCR5T. Among all tile outlets, the range in annual NO₃-N yields was quite large (3.2–104.4 kg ha⁻¹ yr⁻¹), and the average annual yield from all three catchments was nearly 40 kg ha⁻¹ yr⁻¹. Seasonal patterns in NO₃-N export from each monitored site were evaluated by calculating monthly yields (Figure 2.2c).

2.4.4 Cumulative analysis of nitrate yields

Cumulative analysis of annual nitrate yields, when plotted with precipitation and water yield, reveals additional insights into temporal and spatial patterns and relationships (Figure 2.3).

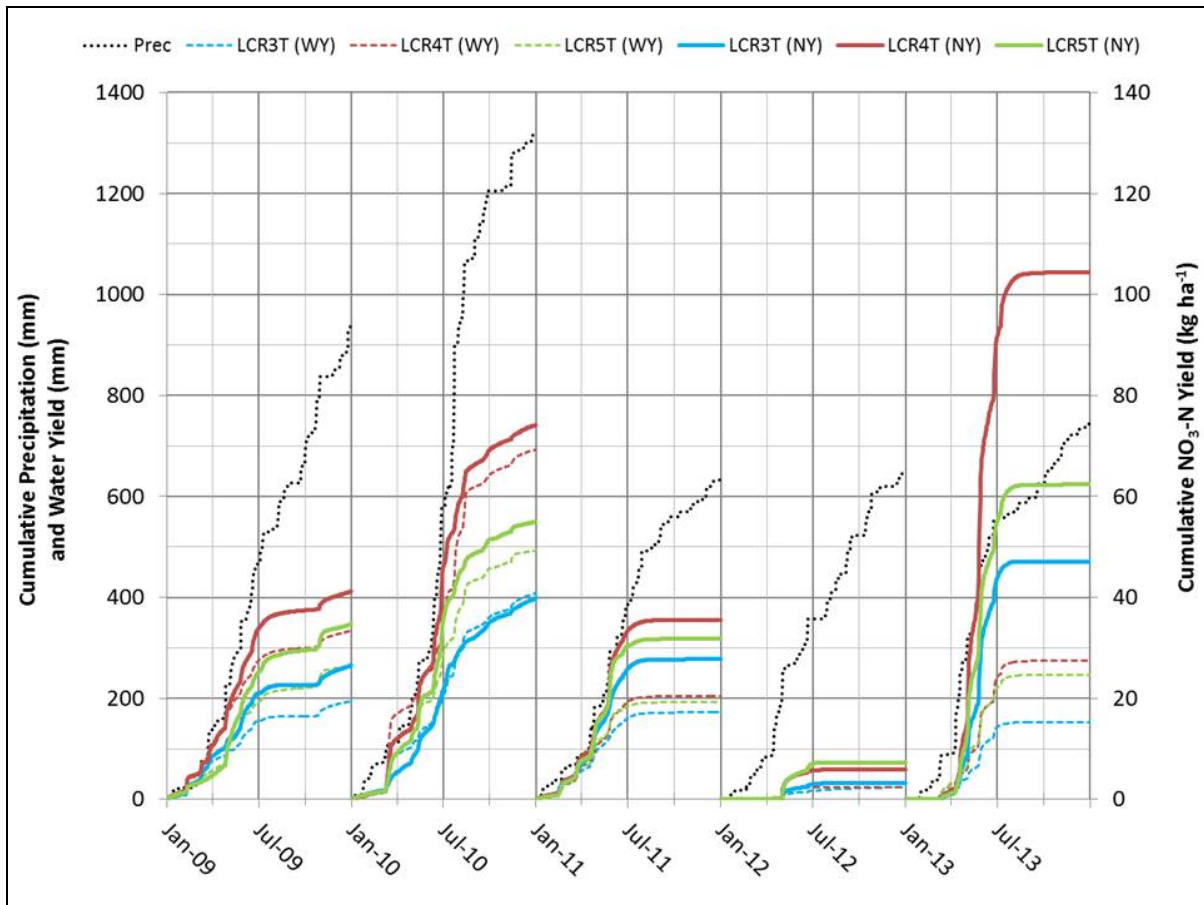


Figure 2.3 Annual cumulative precipitation (prec), water yields (WY), and $\text{NO}_3\text{-N}$ yields (NY) for each drainage district. Black dotted line is precipitation; dashed colored lines represent water yields for each drainage district; and solid colored lines illustrate $\text{NO}_3\text{-N}$ yields.

In most years, water yields increase with precipitation early in the year but level off quickly after 1 July. This pattern did not hold in 2010, when late summer rainfall was extremely high. This pattern also deviated during October 2009 because of sustained, although low, tile flow through the summer followed by heavy rainfall in October of that year. The precipitation patterns in 2011 and 2012 were quite similar, but water yields and $\text{NO}_3\text{-N}$ losses in 2012 were only 14 and 17% of those observed in the prior year, a result of the prolonged dry period that began in 2011. Spring rainfall in 2012 was not enough to overcome moisture and/or groundwater deficits created the prior year. Annual precipitation in 2013 was only

slightly greater than in 2011 and 2012; however, intense spring rains resulted in a steep precipitation curve and an increase in $\text{NO}_3\text{-N}$ yields that exceeded 2012 losses by a factor of 13.

2.4.5 Nitrate and discharge relations

In-stream nitrate loads calculated from observed flows and concentrations were plotted against the flow duration (i.e., the percentage of time a discharge rate is exceeded) at each monitoring site. The resulting LDCs (Figure 2.4) graphically compare in-stream nitrate loads to loads compliant with the drinking water MCL of 10 mg L^{-1} , illustrate temporal loading patterns, and reveal effects of hydrologic conditions on nitrate transport. Seasonality is illustrated with distinct symbols representing observations made within each quarter of the calendar year. Flow conditions were split into five categories: high flow (0–10% exceedance), moist conditions (10–40% exceedance), mid-range conditions (40–60% exceedance), dry conditions (60–90% exceedance), and low flows (90–100% exceedance). Condition boundaries are commonly set at these intervals because it places the midpoint of each condition at the 5th, 25th, 50th, 75th, and 95th percentiles (USEPA, 2007). Note that flow exceedance is the inverse of flow percentile.

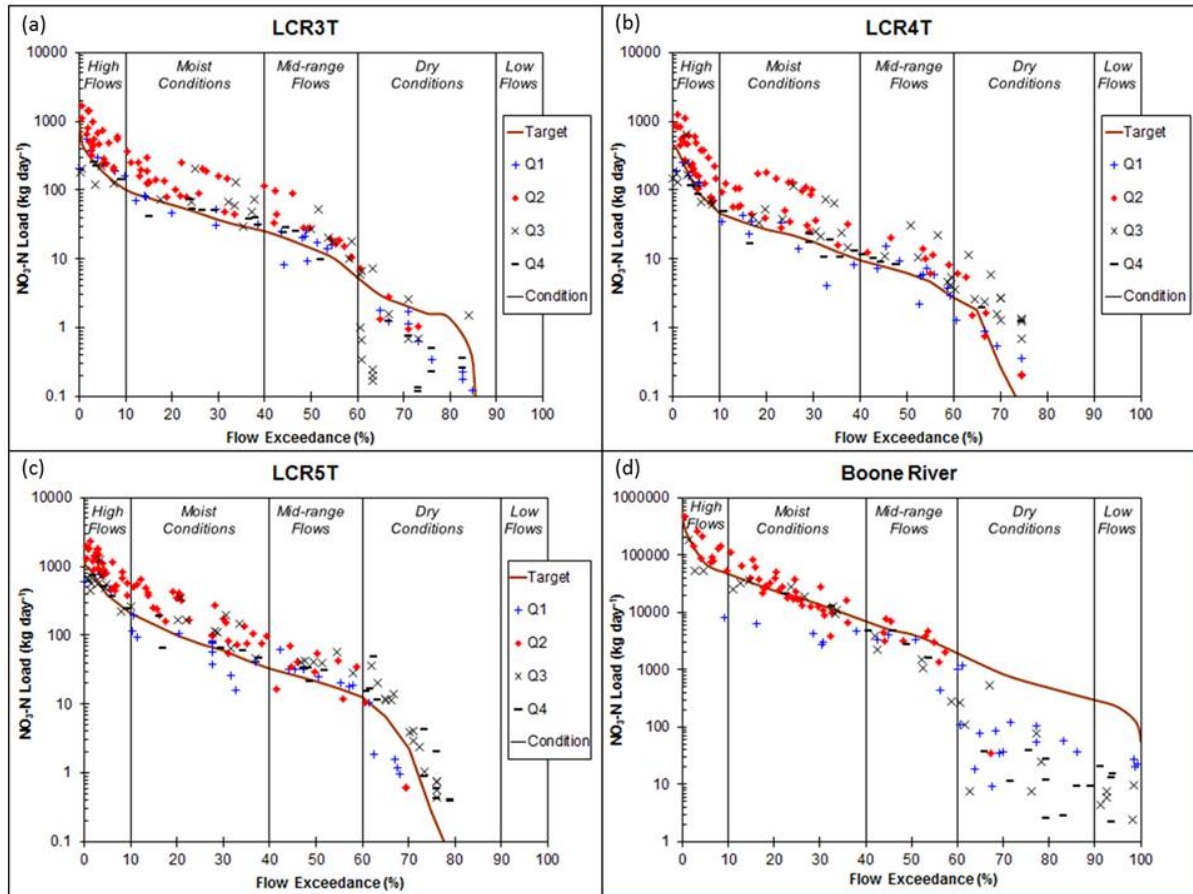


Figure 2.4 Load duration curves for (a) LCR3T, (b) LCR4T, (c) LCR5T, and (d) the Boone River. The curved line represents the $\text{NO}_3\text{-N}$ load that would result from the observed flow distribution and $\text{NO}_3\text{-N}$ concentrations equal to the drinking water maximum contaminant level of 10 mg L^{-1} . Blue “+” symbols represent observations in the first quarter (Q1) of the calendar year. Red diamonds are observations from the second quarter (Q2), black “X” symbols are from the third quarter (Q3), and bold, black dashes are from the fourth quarter (Q4).

The LDCs reveal $\text{NO}_3\text{-N}$ concentrations exceeding the drinking water MCL of 10 mg L^{-1} the vast majority of time that flow was measurable at all three tile outlets. At LCR3T, unlike the other tile outlets, concentrations decreased markedly at flows that were exceeded 60% of the time (i.e., the 40th percentile flow and lower). Loads exceeding the MCL equivalent load in the Boone River were limited to mid-range and higher flow conditions,

with no concentrations exceeding the MCL during dry and low-flow conditions. Yet even in the Boone, the MCL was exceeded more often than not during the highest 40% of flows. Nitrate–N levels at all four sites tend to exceed the MCL by the widest margins in the second quarter of the calendar year. Concentrations above the MCL commonly occur in the third quarter at the tile outlets, but not in the Boone River.

The flow duration or flow-percentile concept is also useful for evaluating the importance of flow conditions to total nitrate exports over the 5-yr period. More than half the total nitrate exported from the tile outlets and through the Boone River occurs during the highest 10% of daily discharges, represented by the 90th percentile flow (Table 2.3). The importance of the upper 25% and upper 50% of flows is also significant, with 82.7% (tile outlets) and 88.6% (Boone River) of nitrate exports occurring at or above the 75th percentile flow and nearly all nitrate (97.1 and 98.8%) exported during the upper half of daily flows. It is noteworthy that nitrate exports closely mirror water yields on a percentile basis.

Table 2.3 Percentage of total water yield and nitrate exported during various discharge conditions.

Location		% of yield/export†		
		Q ≥ 90th percentile	Q ≥ 75th percentile	Q ≥ 50th percentile
Tile outlets‡	Water	61.0	82.8	97.0
	Nitrate-N	56.1	82.7	97.1
Boone River	Water	59.4	84.0	96.9
	Nitrate-N	62.0	88.6	98.8

† Q = daily flow.

‡ Summarizes three tile-drained catchments in the Lyons Creek watershed (LCR3T, LCR4T, and LCR5T).

2.5 Discussion

2.5.1 Hydrologic patterns and relationships

The tile-drained catchments monitored in the Lyons Creek watershed had an average annual water yield of 247 mm yr⁻¹ and DR of 29.1%. During development of the Iowa

Nutrient Reduction Strategy, a water yield of 263 mm yr⁻¹ was estimated for the entire Des Moines Lobe (Iowa State University, 2013). Lawlor et al. (2008) observed an annual average DR of 29% from tile-drained plots near Gilmore City between 1994 and 2004, and Thorp et al. (2007) measured an annual average DR of 24% for a plot-scale study near Story City from 1996 to 2005. Similar water yields and DRs have been observed in plot studies in east-central Illinois (Kalita et al., 2006), southern Minnesota (Randall and Iragavarapu, 1995), west-central Indiana (Hofmann et al., 2004), and northwest Ohio (Logan et al., 1994). Overall, based on 5-yr average values, water yields observed from the tile-drained catchments in Lyons Creek were consistent with prior tile drainage studies in Iowa and other tile-drained areas of the midwestern United States.

On an annual basis, water yields varied substantially within the Lyons Creek watershed. Despite similar annual precipitation from 2011 to 2013, water yields and DRs in 2012 were, at most, 14% of those observed in adjacent years. This is most likely due to the timing of precipitation. A prolonged dry period began in 2011, which created a moisture deficit and reduced tile flow in 2012. Summer 2010 was very wet, with 922 mm (70.1% of the annual) of rainfall falling from June to September. Rainfall in 2011 was below normal, and the second half of the year was dry, with only 290 mm of precipitation (27.7% below normal). This produced the large gap between cumulative precipitation and water yields at the beginning of 2012 (Figure 2.3), and continued dry weather resulted in very little tile flow that year. In spring 2013, heavy rainfall produced 355 mm (nearly half the annual precipitation) in April and May alone. This produced water yields in the first half of 2013 that were comparable to annual water yields observed in 2009 and 2011.

The timing of precipitation and water yields were not always synchronous (Figure 2.2a). Spikes in monthly precipitation were not always followed by major increases in tile flow, although peaks normally coincided when the timing and amount of precipitation was sufficient to cause subsurface tile flow. Both time series (Figure 2.2a) and cumulative analysis (Figure 2.3) illustrate that monthly precipitation typically peaks in June and decreases after 1 July, whereas water yields are very low after 1 July in most years. Jaynes et al. (2001) observed a similar temporal trend and relationship in a 22-ha field-scale study of tile drainage from 1996 to 1999. Increased evapotranspiration and decreased precipitation are both responsible for this seasonal pattern in tile flow. Flow in the Boone River followed the same pattern as water yield from the tile outlets (Figure 2.2a), indicating the importance of tile flow and drainage district hydrology to river basin hydrology. The average annual water yield of 253 mm in the Boone River is within 4% of the 1998 to 2003 average annual water yields in three large river basins in a heavily tile-drained region of Illinois (Royer et al., 2006).

2.5.2 Tile nitrate concentrations: magnitude and implications

Although water yields from the Lyons Creek tile outlets were consistent with prior studies at various scales, $\text{NO}_3\text{-N}$ concentrations observed in this study were higher than those typically observed in the literature. Lawlor et al. (2008) observed flow-weighted annual $\text{NO}_3\text{-N}$ concentrations ranging from 3.9 to 28.7 mg L^{-1} in tile flow beneath corn and soybean rotation field plots receiving 45 and 252 kg ha^{-1} of N fertilizer (in corn years only), respectively. Plots receiving 168 kg ha^{-1} of N application had annual average flow-weighted concentrations of 14.9 mg L^{-1} , while plots receiving 252 kg N ha^{-1} had an annual average flow-weighted mean concentration of 23.3 mg L^{-1} . Bakhsh et al. (2002) observed 6-yr

average flow-weighted NO₃-N concentrations between 8.3 and 11.7 mg L⁻¹ from 0.4-ha plots near Nashua, IA. Randall and Iragavarapu (1995) measured average flow-weighted NO₃-N concentrations between 12.0 and 13.4 mg L⁻¹ from continuous corn plots receiving 200 kg ha⁻¹ yr⁻¹ of fertilizer N in southern Minnesota.

At a larger scale, Tomer et al. (2003) documented 1992 to 2000 annual flow-weighted NO₃-N concentrations ranging between non-detectable and 23.5 mg L⁻¹ from two tiled catchments in the Walnut Creek watershed in central Iowa, with average annual flow-weighted means of 11.3 and 13.4 mg L⁻¹. Lyons Creek drainage districts in this study had higher maximum annual flow-weighted concentrations (38.0 mg L⁻¹ at LCR4T in 2013) and an average annual flow-weighted concentration (17.1 mg L⁻¹) between those observed in the highest two fertilizer rates of the Lawlor field plot study and notably higher than in concentrations observed at the field plots near Nashua or the Walnut Creek catchments.

Based on controlled variations in fertilizer application rate (kg-N ha⁻¹) and resulting subsurface tile NO₃-N concentrations (mg L⁻¹), Lawlor et al. (2008) developed a relationship between the two variables, as follows:

$$\text{NO}_3\text{-N Concentration} = 5.72 + 1.33 * \exp [0.0104 \times (\text{N-application rate})] \quad (1)$$

This relationship was compared with data collected from other tile-drained sites in Iowa and Minnesota as part of the science assessment of the Iowa Nutrient Reduction Strategy.

Although the relationship does not account for differences in precipitation and other site-specific factors, it was found to be useful across sites with similar soil, land use, and drainage characteristics (Iowa State University, 2013). Applying the equation to the average flow-

weighted $\text{NO}_3\text{-N}$ concentration in the Lyons Creek tile outlets (17.1 mg L^{-1}) implies an average N fertilizer rate of 206 kg ha^{-1} for corn in a corn–soybean rotation in the Lyons Creek catchments. This is slightly higher than the Des Moines Lobe average rate of 192 kg ha^{-1} estimated in the Iowa Nutrient Reduction Strategy (Iowa State University, 2013). There is certainly variation in this relationship, and applying it across sites and scales should be done cautiously. The analysis in the Iowa Nutrient Reduction Strategy indicates that application rates as low as $150 \text{ kg N ha}^{-1} \text{ yr}^{-1}$ have been associated with $\text{NO}_3\text{-N}$ concentrations of 17 mg L^{-1} in some studies.

Because nitrate concentrations typically decrease with increasing drainage area in this study and others (Schilling et al., 2012; Tomer et al., 2003), this analysis may underestimate application rates in the Lyons Creek catchments, as it was developed at the plot, rather than catchment scale. If the relationship developed by Lawlor et al. (2008) holds true at the drainage district scale, it points to the limitations of decreasing in-stream nitrate concentrations solely by reducing fertilizer application. To meet a flow-weighted $\text{NO}_3\text{-N}$ concentration of 10 mg L^{-1} , application rates to corn in a corn-soybean rotation could not exceed 113 kg N ha^{-1} , far lower than what is customary on the Des Moines Lobe. Only two sites for which this relationship was evaluated in the Iowa Nutrient Reduction Strategy had flow-weighted concentrations less than the MCL, and the associated application rates were less than 70 kg N ha^{-1} .

2.5.3 Nitrate losses: magnitude and context

Despite hydrology that was consistent with previous tile drain studies, $\text{NO}_3\text{-N}$ yields (i.e., losses) from the Lyons Creek catchments between 2009 and 2013 were higher most reported in literature. Tomer et al. (2003) observed losses approaching 60 kg ha^{-1} from one of

the tiled catchments in Walnut Creek in 1993, a year with extreme flood flow, but losses of $20 \text{ kg ha}^{-1} \text{ yr}^{-1}$ were more typical. Similar maximum and typical losses were reported from a 22-ha field site in central Iowa (Jaynes et al., 2001). Research plots receiving N application rates of 168 and 252 kg ha^{-1} had average $\text{NO}_3\text{-N}$ losses of 39 and 63 kg ha^{-1} from 2001 to 2004, respectively, with a maximum loss of 86 kg ha^{-1} from high application rate plots in 2001 (Lawlor et al., 2008). In contrast, annual $\text{NO}_3\text{-N}$ losses from the Lyons Creek catchments ranged from 3.2 kg ha^{-1} at LCR3T in 2012 to 104.4 kg ha^{-1} at LCR4T in 2013. The annual average loss from of all three catchments was extremely high in both 2010 (56.4 kg ha^{-1}) and 2013 (71.3 kg ha^{-1}). The 5-yr average loss of 39.8 kg ha^{-1} from all three Lyons Creek drainage district tiles is consistent with plot-scale studies with high losses, including Lawlor et al. (2008), Randall and Iragavarapu (1995), and Gentry et al. (2000), but much higher than field- and catchment-scale losses reported by Jaynes et al. (2001) and Tomer et al. (2003). Even excluding the extreme year of 2013 from the Lyons Creek analysis, the 4-yr average annual $\text{NO}_3\text{-N}$ loss of $31.9 \text{ kg ha}^{-1} \text{ yr}^{-1}$ would still exceed most literature values, even at small-plot scales. This magnitude of nitrate loss, relative to water yields, implies a high N supply, possibly due to fertilizer application (rate and/or timing), manure application, high soil mineralization rates, or other natural and agronomic factors. Nitrate exports in the Boone River were more typical of those observed in other studies of tile-drained watersheds in the Upper Midwest (Royer et al., 2006; Goolsby et al., 2000).

2.5.4 Scaling drainage district losses to river basin exports

The monitored catchments in Lyons Creek occupy less than 1% of the Boone River watershed, and nitrate exports from the catchments equated to less than 1.2% of loads discharged from the Boone River. However, drainage districts similar to those monitored in

Lyons Creek dominate the landscape (Schilling et al., 2013) and comprise 75% of the total land area in the Boone River watershed. Scaling up average annual $\text{NO}_3\text{-N}$ yields from the Lyons Creek catchments suggests that drainage districts could easily account for all of the total nitrate export in the Boone River from 2009 to 2013 (Figure 2.5a). Scaled-up drainage district contributions were higher than actual Boone River loads in every year except 2010, which was by far the wettest year. On a monthly basis, the highest-scaled drainage districts loads, relative to Boone River loads, occurred in September. This is indicative of warm-water, low-flow conditions when removal mechanisms (e.g., denitrification and biological uptake) are highest (Bernot et al., 2006; Royer et al., 2004) and nitrate concentrations are lowest. Potential contributions during the high export season (March–July) varied between 77.2% in June and 157.1% in April (Figure 2.5b) but averaged over 100%. Scaling up losses in this manner is a simplification of the link between nitrate exports from small upland catchments to downstream river basins. In-stream processes and lag time affect this relationship, but this analysis affirms findings by others that in tile-drained landscapes, drainage districts dominate nitrate transport in downstream rivers and are the scale at which improvement strategies should be focused.

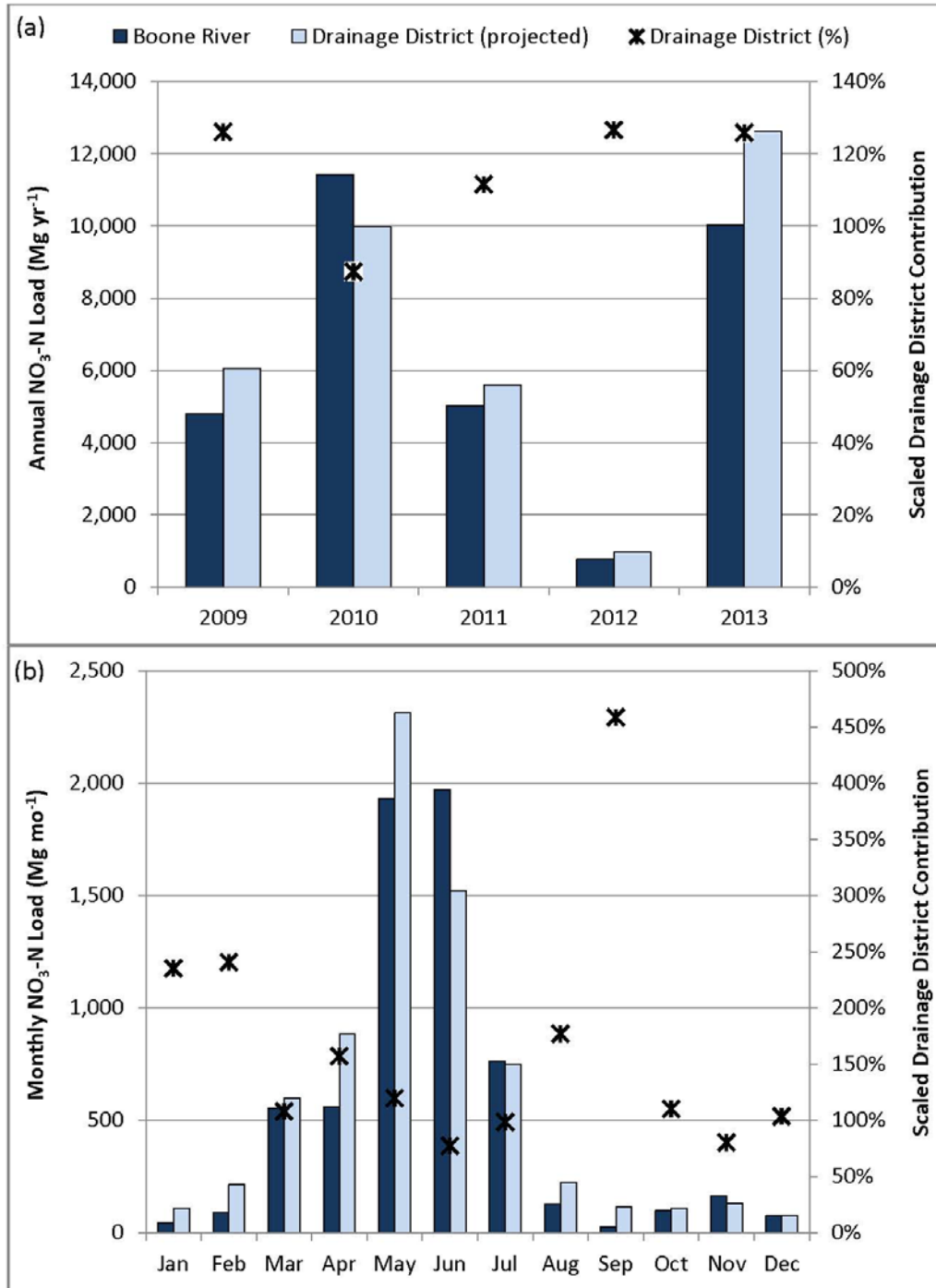


Figure 2.5 Average (a) annual and (b) monthly $\text{NO}_3\text{-N}$ loads in the Boone River with the potential contributions from drainage districts. Black asterisks represent the potential drainage district contributions (percentage) after scaling up the average nitrate loss from Lyons Creek drainage districts across the entire area of land lying within drainage districts in the Boone River watershed.

The degree of subsurface drainage, indicated by DR and water yield, appears to be the primary driver of nitrate export from the Lyons Creek catchments and nitrate transport in the Boone River. In all years, the catchment with the largest DR also had the largest nitrate yield. Furthermore, annual nitrate losses were higher in years with higher DRs (Table 2.2). Cumulative annual nitrate yields follow similar patterns as water yields (Figure 2.3), and monthly time series plots generally show coincident peaks of flow and nitrate yields (Figure 2.2). Summing exports by corresponding flow percentile revealed that 56.1% of nitrate exports from the tiled catchments and 62.0% of exports in the Boone River occur during the upper 10% of daily flows, and 97.1% of nitrate from the small catchments and 98.8% of Boone River export occur during the upper 50% of daily flows. These relationships are nearly identical to those observed in three riverine watersheds draining hundreds of square kilometers of tile-drained agricultural land in Illinois (Royer et al., 2006). It appears that in tile-drained landscapes, the lower half of daily flows have almost no impact on nitrate export, and relationships between flow and nitrate transport are quite similar across spatial scales in the midwestern Corn Belt area of the Prairie Pothole Region. Load duration curves (Figure 2.4) also illustrate that nitrate levels are generally higher during high flow conditions. This is particularly true at larger scales, as shown in the Boone River data. To achieve $\text{NO}_3\text{-N}$ concentrations less than 10 mg L^{-1} at all times, loads would need to be reduced by 8.5% during moist conditions and by 34.9% during high flow conditions in the Boone River. In addition to underlining the importance of strategies that reduce nitrate transport during wet conditions and elevated flows, these findings also suggest that nitrate concentrations are not generally diluted by high flows, with the exception of infrequent, extreme flood events.

Despite the dominant influence of hydrology and transport limitations on nitrate loss, nitrate yields are not always explained solely by the corresponding water yields. The nitrogen supply in these landscapes also plays an important role in nitrate loss, as demonstrated by Lawlor et al. (2008) in the case of fertilizer application rates. In Lyons Creek catchments, cumulative nitrate yields tracked water yields closely in most years (Figure 2.3). However, the rapid increase in nitrate losses from 2012 to 2013 was greater than prior years' relationships with tile hydrology would suggest. This is most likely due to the interrelated factors of drought and poor crop yields in 2012, which would both contribute to higher-than-normal residual nitrate in the soil (Lucey and Goolsby 1993).

Based on countywide yield estimates from 2011 (11.3 Mg ha⁻¹) and 2012 (8.7 Mg ha⁻¹) and assuming a dry-basis N content of 1.2% (IPNI, 2012; Ciampitti and Vyn, 2012), it was estimated that 27 kg ha⁻¹ less N was exported during corn harvest in 2012 than 2011. Countywide soybean yields (3.4 Mg ha⁻¹ in 2011 and 3.0 Mg ha⁻¹ in 2012) would result in 26 kg ha⁻¹ less N removed via harvest, assuming a dry-basis N content of 6.2% (IPNI, 2012; Ciampitti and Vyn, 2012). This potential carryover N is less than, but comparable in magnitude to annual NO₃-N losses via subsurface drainage. The heavy spring rains of 2013 flushed the residual nitrate from the soil, in addition to concurrent N inputs that typically contribute to annual nitrate leaching, leading to tile losses in 2013 that were significantly larger than would be expected based solely on annual water yield. While the estimate is coarse, and site-specific data may vary, the relative impact is consistent with previously demonstrated relationships between nitrate concentration and prior year flows in the Raccoon River of central Iowa (Lucey and Goolsby, 1993) and several large tributaries to the

Mississippi River (Murphy et al., 2013), and with agronomic studies of carryover soil nitrate following drought years (Sawyer, 2013).

2.6 Conclusions

Although annual precipitation and water yields from three tile-drained catchments in the Lyons Creek watershed were consistent with historical data and other tile drain studies, $\text{NO}_3\text{-N}$ concentrations and yields are among the highest reported in the literature. Typically, more drainage (as indicated by either water yield or DR) results in higher $\text{NO}_3\text{-N}$ losses when examining both annual and intercatchment variability. Relationships between flow percentile and nitrate export were virtually identical across scales. Nitrate–N exported from the Boone River was consistent with other studies of rivers in the upper Midwest, despite higher losses from the Lyons Creek tile drains. High $\text{NO}_3\text{-N}$ losses from these drainage districts relative to other small watershed-scale studies, and the overwhelming impact that drainage district exports have on the timing and magnitude of river-basin exports, confirm the importance of working at this scale to attain water quality goals downstream. Although nitrate exports from the catchments were primarily hydrology-driven, larger-than-expected $\text{NO}_3\text{-N}$ losses from tile outlets in Lyons Creek suggest that the nitrogen supply may be higher in this system than in most, whether from natural or agronomic influences. These findings confirm that strategies that address both hydrology and nitrogen supply will be necessary for meeting water quality objectives in tile-drained landscapes.

2.7 Acknowledgements

The material presented here is based on work supported by Agriculture’s Clean Water Alliance, with funding made possible by the McKnight Foundation. Any opinions, findings, and conclusions or recommendations expressed in this material are those of the authors and

do not necessarily reflect the views of the ACWA or the McKnight Foundation. The authors would also like to thank the Iowa Department of Natural Resources for collecting and reporting flow and nitrate data in the Boone River.

2.8 References

- Bakhsh, A., R.S. Kanwar, R.B. Bailey, C.A. Cambardella, D.L. Karlen, and T.S. Colvin. 2002. Cropping system effects on NO₃-N loss with subsurface drainage water. *Trans. ASABE* 45(6):1789–1797.
- Bernot, M.J., J.L. Tank, T.V. Royer, and M.B. David. 2006. Nutrient uptake in streams draining agricultural catchments of the midwestern United States. *Freshwater Biol.* 51:499–509. doi:10.1111/j.1365-2427.2006.01508.x
- Ciampitti, I.A., and T.J. Vyn. 2012. Physiological perspectives of changes over time in maize yield dependency on nitrogen uptake and associated nitrogen efficiencies: A review. *Field Crops Res.* 133:48–67. doi:10.1016/j.fcr.2012.03.008
- David, M.B., L.E. Drinkwater, and G.F. McIsaac. 2010. Sources of nitrate yield in the Mississippi River basin. *J. Environ. Qual.* 39:1657–1667. doi:10.2134/jeq2010.0115
- Des Moines Water Works (DMWW). 2009. Fact sheet: Nitrate removal facility. <http://www.dmww.com/upl/documents/water-quality/lab-reports/fact-sheets/nitrate-removal-facility.pdf> (accessed Feb. 2014).
- Dinnes, D.L., D.L. Karlen, D.B. Jaynes, T.C. Kaspar, J.L. Hatfield, T.S. Colvin, and C.A. Cambardella. 2002. Nitrogen management strategies to reduce nitrate leaching in tile-drained midwestern soils. *Agron. J.* 94:153–171. doi:10.2134/agronj2002.0153
- Fipps, G., and R.W. Skaggs. 1991. Simple methods for predicting flow to drains. *J. Irrig. Drain. Eng.* 117(6):881–896. doi:10.1061/(ASCE)0733-9437(1991)117:6(881)
- Gentry, L.E., M.B. David, F.E.K.M. Smith-Starks, and D.A. Kovacic. 2000. Nitrogen fertilizer and herbicide transport from tile drained fields. *J. Environ. Qual.* 29:232–240. doi:10.2134/jeq2000.00472425002900010030x
- Goolsby, D.A., W.A. Battaglin, B.T. Aulenbach, and R.P. Hooper. 2000. Nitrogen flux and sources in the Mississippi River basin. *Sci. Total Environ.* 248:75–86. doi:10.1016/S0048-9697(99)00532-X
- Goswami, D., P.K. Kalita, R.A. Cooke, and M.C. Hirschi. 2008. Estimation and analysis of baseflow in drainage channels in two tile-drained watersheds in Illinois. *Trans. ASABE* 51(4):1201–1213. doi:10.13031/2013.25238
- Hatfield, J.L., J.H. Prueger, and D.B. Jaynes. 1998. Environmental impacts of agricultural drainage in the Midwest. In: *Drainage in the 21st century: Food production and the environment*. Proceedings of the 7th Annual Drainage Symposium, Orlando, FL. 8–10 Mar. 1998. ASAE, St. Joseph, MI.
- Hofmann, B.S., S.M. Brouder, and R.F. Turco. 2004. Tile spacing impacts on Zea mays L. yield and drainage water nitrate load. *Ecol. Eng.* 23:251–267. doi:10.1016/j.ecoleng.2004.09.008
- IPNI. 2012. A nutrient use information system (NuGIS) for the U.S. Norcross, Georgia. International Plant Nutrition Institute. 12 Jan.2012. www.ipni.net/nugis.

- Iowa Department of Natural Resources. 2013a. Iowa STORET/WQX water quality database. <https://programs.iowadnr.gov/iastoret/> (accessed Feb. 2014).
- Iowa Department of Natural Resources. 2013b. Natural resources geographic information system library. Iowa Geological and Water Survey, Iowa City. <https://programs.iowadnr.gov/nrgislibx/> (accessed 24 June 2013).
- Iowa State University. 2013. Iowa nutrient reduction strategy. <http://www.nutrientstrategy.iastate.edu> (accessed 20 Feb. 2014).
- Iowa State University. 2014. Iowa environmental mesonet. <http://mesonet.agron.iastate.edu/> (accessed March 2014).
- Jaynes, D.B., T.S. Colvin, D.L. Karlen, C.A. Cambardella, and D.W. Meek. 2001. Nitrate loss in subsurface drainage as affected by nitrogen fertilizer rate. *J. Environ. Qual.* 30:1305–1314. doi:10.2134/jeq2001.3041305x
- Jaynes, D.B., J.L. Hatfield, and D.W. Meek. 1999. Water quality in Walnut Creek watershed: Herbicides and nitrate in surface waters. *J. Environ. Qual.* 28:45–59. doi:10.2134/jeq1999.00472425002800010005x
- Kalita, P.K., A.S. Algoazany, J.K. Mitchell, R.A.C. Cooke, and M.C. Hirshi. 2006. Subsurface water quality from a flat, subsurface drained watershed in Illinois, USA. *Agric. Ecosyst. Environ.* 115:183–193.
- Lawlor, P.A., M.J. Helmers, J.L. Baker, S.W. Melvin, and D.W. Lemke. 2008. Nitrogen application rate effect on nitrate-nitrogen concentration and loss in subsurface drainage for a corn-soybean rotation. *Trans. ASABE* 51(1):83–94. doi:10.13031/2013.24229
- Logan, T.J., D.J. Eckert, and D.G. Beak. 1994. Tillage, crop, and climatic effects on runoff and tile drainage losses of nitrate and four herbicides. *Soil Tillage Res.* 30:75–103. doi:10.1016/0167-1987(94)90151-1
- Lucey, K.J., and D.A. Goolsby. 1993. Effects of climatic variations over 11 years on nitrate-nitrogen concentrations in the Raccoon River, Iowa. *J. Environ. Qual.* 22:38–46. doi:10.2134/jeq1993.00472425002200010005x
- McCorvie, M.R., and C.L. Lant. 1993. Drainage district formation and the loss of Midwestern wetlands, 1850-1930. *Agric. Hist.* 67(4):13–39.
- Murphy, J.C., R.M. Hirsch, and L.A. Sprague. 2013. Antecedent flow conditions and nitrate concentrations in the Mississippi River Basin. *Hydrol. Earth Syst. Sci. Discuss.* 10:11451–11484. doi:10.5194/hessd-10-11451-2013
- Pfaff, J.D. 1993. Method 300.0: Determination of inorganic ions by ion chromatography. USEPA Environ. Monit. Sys. Lab. Cincinnati, OH.
- Randall, G.W., and T.K. Iragavarapu. 1995. Impact of long-term tillage systems for continuous corn on nitrate leaching to tile drainage. *J. Environ. Qual.* 24:360–366. doi:10.2134/jeq1995.00472425002400020020x
- Royer, T.V., M.B. David, and L.E. Gentry. 2006. Timing of riverine export of nitrate and phosphorus from agricultural watersheds in Illinois: Implications for reducing nutrient loading to the Mississippi River. *Environ. Sci. Technol.* 40:4126–4131. doi:10.1021/es052573n
- Royer, T.V., J.L. Tank, and M.B. David. 2004. Transport and fate of nitrate in headwater agricultural streams in Illinois. *J. Environ. Qual.* 33:1296–1304. doi:10.2134/jeq2004.1296

- Sawyer, J. 2013. Soil profile nitrate in corn fields following the 2012 drought. Iowa State University Extension. <http://www.extension.iastate.edu/CropNews/2013/0221sawyer.htm> (accessed 1 Apr. 2014).
- Schilling, K.E., C.S. Jones, and A. Seeman. 2013. How paired is paired? Comparing nitrate concentrations in three Iowa drainage districts. *J. Environ. Qual.* 42:1412–1421. doi:10.2134/jeq2013.03.0085
- Schilling, K.E., C.S. Jones, A. Seeman, E. Bader, and J. Filipiak. 2012. Nitrate-nitrogen patterns in engineered catchments in the upper Mississippi River basin. *Ecol. Eng.* 42:1–9. doi:10.1016/j.ecoleng.2012.01.026
- Thorp, K.R., R.W. Malone, and D.B. Jaynes. 2007. Simulating long-term effects of nitrogen fertilizer application rates on corn yield and nitrogen dynamics. *Trans. ASABE* 50(4):1287–1303. doi:10.13031/2013.23640
- Tomer, M.D., D.W. Meek, D.B. Jaynes, and J.L. Hatfield. 2003. Evaluation of nitrate nitrogen fluxes from a tile-drained watershed in central Iowa. *J. Environ. Qual.* 32:642–653. doi:10.2134/jeq2003.6420
- Urban, M.A. 2005. An uninhabited waste: Transforming the Grand Prairie in nineteenth century Illinois, USA. *J. Hist. Geogr.* 31:647–665. doi:10.1016/j.jhg.2004.10.001
- USEPA. 2007. An approach for using load duration curves in the development of TMDLs. EPA 841-B-07-006. USEPA, Washington, DC.

CHAPTER 3. SIMULATING SHORT-TERM FLUCTUATIONS IN SUBSURFACE FLOW AND NITRATE-NITROGEN IN SMALL, TILE-DRAINED WATERSHEDS USING SWAT

3.1 Abstract

Artificial subsurface drainage significantly alters hydrologic and nutrient pathways and processes in tile-drained landscapes. Reliable prediction of hydrology and nutrient transport at the watershed scale is needed for effective watershed planning and implementation of water quality BMPs. The Soil and Water Assessment Tool (SWAT) has been widely utilized in tile-drained landscapes, but few applications have thoroughly evaluated the model's ability to simulate pathway-specific components or short-term fluctuations in small watersheds. The objectives of this study were to develop and calibrate SWAT models for small, tile-drained watersheds, evaluate model performance for pathway-specific flow and nitrate-nitrogen ($\text{NO}_3\text{-N}$) simulation at monthly and daily intervals, and document important intermediate processes and N-fluxes.

Model calibration and evaluation revealed that it is possible to meet generally accepted performance criteria for simulation of monthly total flow (WYLD), subsurface flow (SSF), and $\text{NO}_3\text{-N}$ loads. Nash-Sutcliffe Efficiency (NSE) values for the KS and AL watersheds were 0.79 and 0.71, respectively, for monthly WYLD; 0.55 and 0.66 for monthly SSF; and 0.72 and 0.60 for monthly $\text{NO}_3\text{-N}$ load (using the modified $\text{NO}_3\text{-N}$ lagging algorithms). Simulation of daily surface runoff (SURQ), SSF, and $\text{NO}_3\text{-N}$ concentration were generally not satisfactory ($\text{NSE} < 0.50$) with the exception of daily SURQ in the KS watershed, for which NSE was 0.55 and percent bias (PBIAS) was -10.0%.

Keywords: tile drainage, hydrology, nitrate transport, drainage district, SWAT

3.2 Introduction

Artificial subsurface drainage (i.e., tile drainage) allows row crop production and improves crop yields in poorly-drained soils by lowering the water table to limit saturation of the root zone and prevent root aeration stress (Hatfield et al., 1998), and by increasing planting and harvest windows during spring and fall, respectively. Streamflow and nutrient transport is significantly impacted by subsurface drainage because tile drains alter the pathways and processes that govern hydrology and nutrient cycling (Schilling and Helmers, 2008a). The distribution of water balance components; runoff, lateral flow, shallow groundwater flow, and aquifer recharge; differ in tiled versus non-tiled watersheds (Goswami et al., 2008; Sui and Frankenberger, 2008). The presence of tile drainage also impacts water quality processes such as sheet and rill erosion, nutrient mineralization and denitrification, and nitrate-nitrogen ($\text{NO}_3\text{-N}$) leaching (Dinnes et al., 2002; El-Sadek et al., 2002; Lemke et al., 2011; Coelho et al., 2012). Proper identification and quantification of these pathways and processes is critically important for reliable prediction of nonpoint source pollutant loads (Goolsby et al., 2000) and quantifying nutrient transport to downstream waterbodies (e.g., the Mississippi River and Gulf of Mexico (Alexander et al., 2008; David et al., 2010; Stenback et al., 2011)). Additionally, design and simulation of best management practices and strategies to mitigate negative effects of tile drainage require thorough understanding of the underlying hydrologic and water quality processes (Rozemeijer et al., 2010; Yen et al., 2014).

The need to predict tile drain hydrology and simulate drainage led to the development of DRAINMOD, a field-scale model upon which many subsurface drainage simulations are based (Skaggs, 1980). DRAINMOD has been used to predict tile flow, water table depth, nitrate loss, and crop yields in artificially-drained row crop fields (El-Sadek et al., 2001; El-

Sadek et al., 2002; Wang et al., 2006; Youssef et al., 2006). Another field-scale model, the Root Zone Water Quality Model (RZWQM), has been used to develop long-term simulations of drainage water management on tile flow and $\text{NO}_3\text{-N}$ transport in tile-drained field plots in the midwestern United States (Thorp et al., 2008; Thorpe et al., 2009; Qi et al., 2012). Attempts to extend these field-scale algorithms to watershed-scale models have shown promise for prediction of hydrology and $\text{NO}_3\text{-N}$ transport (Fernandez et al., 2005; Singh et al., 2007; Sui and Frankenberger, 2008; Ale et al., 2012). However, these models lack the ability to simulate other features of agricultural landscapes, including sources of nutrients not associated with tile drainage. Accurate simulation of tile drainage within the framework of a more comprehensive, versatile, and widely-used watershed model would provide watershed managers and policy makers with a much-needed tool for evaluation of tile drainage within the context of land use change, best management practices (BMPs), and drainage water management scenarios (Kladivko et al., 2004; Bracmort et al., 2006; Sui and Frankenberger, 2008; Ale et al., 2012).

Many commonly used watershed-scale models, such as Hydrologic Simulation Program-FORTRAN (HSPF), Water Erosion Prediction Project (WEPP), and the Watershed Assessment Model (WAM), do not contain algorithms that explicitly account for artificial subsurface drainage (Migliaccio and Srivastava, 2007) and are limited in their ability to simulate other important aspects of an agricultural landscape, such as crop growth, fertilizer and manure application, and agricultural water quality BMPs. Several watershed-scale models are available that do directly simulate subsurface tile drainage, such as MIKE-SHE and HydroGeoSphere. These models are fully-distributed, mechanistic models with detailed input requirements. They are capable of a more discrete and accurate spatial representation

of the landscape, provided that highly resolute input data are available and the added model complexity can justify more onerous development and parameterization requirements. The soil-N cycle is not currently well-represented in MIKE-SHE (Jaber and Shukla, 2012), which is critical for NO₃-N fate and transport modeling. Further, there are few applications of complex models such as MIKE-SHE and HydroGeoSphere in tile-drained landscapes, which increases the difficulty of model parameterization.

The Soil and Water Assessment Tool (SWAT) model is a well-established and widely utilized model for simulation of hydrology and pollutant transport in predominantly agricultural watersheds. The model explicitly accounts for both tile drainage and soil nutrient cycling and is under continuous development/improvement by USDA-ARS. Gassman et al. (2007) prepared an exhaustive literature review summarizing over 250 publications based on a wide range of SWAT applications. Previous SWAT applications include development of Total Maximum Daily Loads (TMDLs) (Du et al., 2005; Borah et al., 2006), assessment of agricultural BMPs (Bracmort et al., 2006; Van Liew et al., 2007; Chaubey et al., 2010), evaluation of land use scenarios (Jha et al., 2010) and simulation of large-scale river basins to study impacts of phenomena such as climate change (Stone et al., 2001; Records et al., 2014), gulf hypoxia (Rabotyagov et al., 2010), sediment management (Betrie et al., 2011), impacts of alternative energy crops (Babcock et al., 2007; Baskaran et al., 2010), and surface water availability (Schuol et al., 2008). Recognizing its extensive use, Arnold et al. (2012) published guidance on the use, calibration, and validation of SWAT models and detailed performance measures and evaluation criteria were set forth by Moriasi et al. (2015a).

Reliable models for simulating hydrology and nutrient transport in these landscapes at small watershed scales is critically needed but particularly challenging. Calibration of SWAT and other watershed models often relies heavily on iterative adjustment of a large number of parameters during calibration. Calibration is typically performed to minimize differences between predicted and observed flow and/or pollutant loads at large spatial and temporal scales. This can lead to the problem of non-unique solutions, sometimes called equifinality, where many possible combinations of model inputs yield similar model performance statistics, making it difficult to discriminate between seemingly equally good simulations (Yen et al, 2014; Moriasi et al, 2015b). A second problem frequently associated with this limited type of calibration process is that optimized parameter values are frequently not constrained within accepted ranges (Malone et al., 2015). Additionally, while simulation criteria for non-pathway specific variables such as stream flow or nutrient loads may appear reasonable, underlying simulation of surface runoff (SURQ) and subsurface flow (SSF), nutrient transport, and N-dynamics (e.g., denitrification and soil-N levels) may be misrepresented (Yen et al, 2014; Arnold et al, 2015). These challenges can limit the model's utility for accurately forecasting flow and nutrient transport across spatial scales, through varying weather patterns, with land use changes, and with implementation of water quality improvement strategies.

Because of its utility for simulating agricultural processes and practices, explicit tile-drain algorithms, broad application history, and continuous support and improvement by USDA, this study takes a closer look at the use of SWAT for simulating hydrology and $\text{NO}_3\text{-N}$ transport in small, tile-drained watersheds typical of agricultural drainage districts in north-central Iowa. The goals of this study are to evaluate and improve simulation of flow

and $\text{NO}_3\text{-N}$ and to provide deeper insights into pathway-specific and short-term model performance. Specific objectives were to (i) develop and calibrate SWAT models for small, tile-drained watersheds, (ii) evaluate model performance for pathway-specific flow and $\text{NO}_3\text{-N}$ simulation at monthly and daily intervals, and (iii) document important intermediate processes and N-fluxes.

3.3 Materials and Methods

3.3.1 Study area

The two watersheds simulated in this study each drain to Conservation Reserve Enhancement Program (CREP) located in the Des Moines Lobe ecoregion in north-central Iowa. The 309-ha KS Wetland watershed is located in Story County, Iowa, at the headwaters of a first-order tributary to Squaw Creek, a HUC-12 watershed in the Skunk River basin. The AL Wetland watershed has a drainage area of 227 ha, and is located in Kossuth County approximately 120 km northwest of the KS Wetland site (Figure 3.1). The AL Wetland watershed drains to a first-order stream that enters Black Cat Creek, a HUC-12 that discharges to the Des Moines River. Watershed characteristics for both wetlands are reported in Table 3.1. All soils in the watersheds are classified as somewhat poorly-drained to very poorly-drained, with the exception of Clarion soils, which are moderately well-drained. Therefore, HRUs with Clarion soils were not parameterized with tile drainage, but all other HRUs include tile drain parameters.

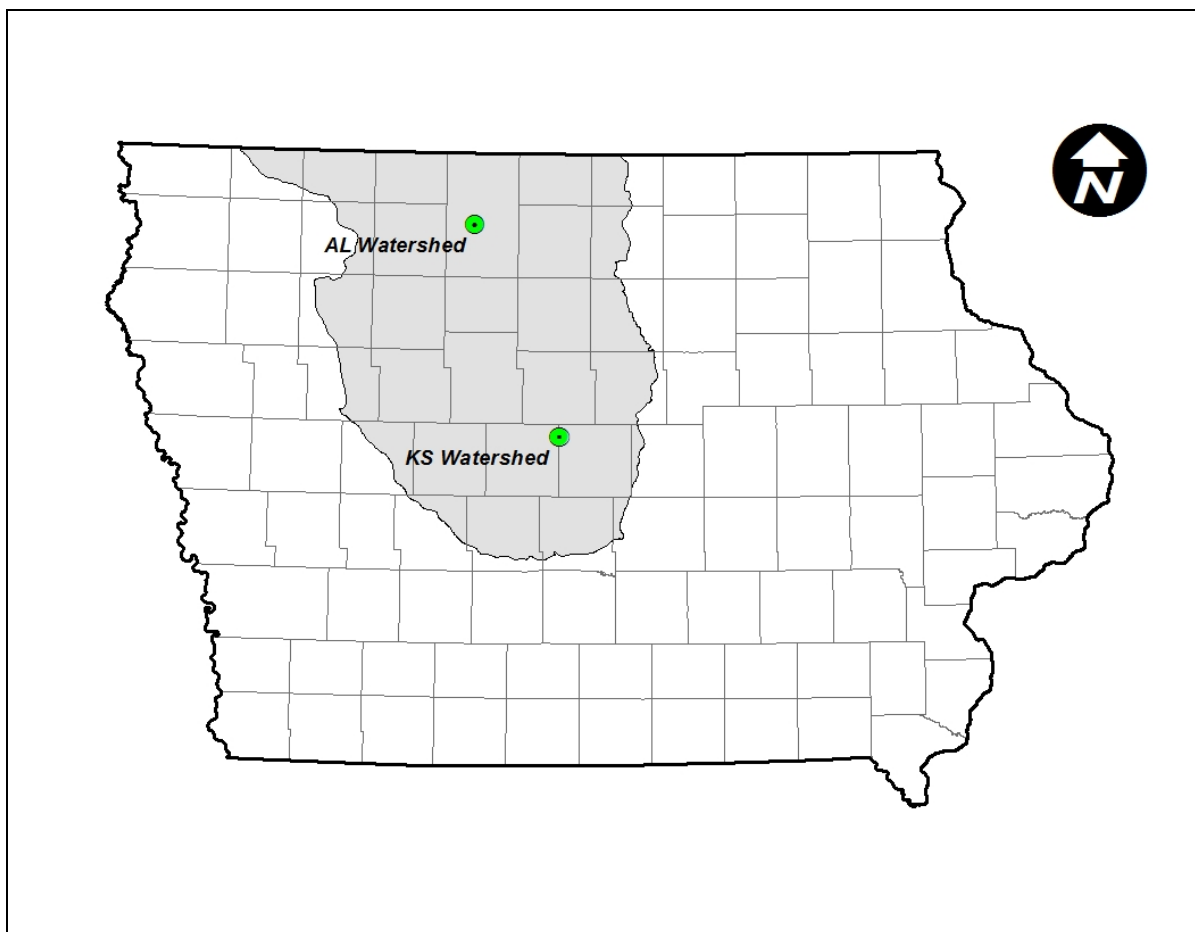


Figure 3.1 Location of CREP wetland watersheds simulated in this study. The shaded region is the Des Moines Lobe ecoregion.

Table 3.1 Watershed characteristics of simulated sites.

Characteristic	KS Wetland	AL Wetland
Drainage area, DA (ha)	309	227
Row crop (% of DA)	93	80
Continuous corn (% of row crop)	35	14
Poor drainage (% of DA) ^[a]	62	77
Annual rainfall (mm) ^[b]	1,081	906
Annual water yield (mm) ^[c]	395	279

^[a] Row crop areas with slopes < 5% and soils classified as somewhat poor to poorly-drained.

^[b] Average annual rainfall during model simulation period (2008-2011 for KS Wetland, 2007-2010 for AL Wetland).

^[c] Average annual water yield during model simulation period.

Flow in both watersheds is predominantly subsurface (tile) flow, with some surface runoff reaching the wetlands during storm events. Flows were measured using Doppler area-velocity meters, which record water depth and velocity on a continuous basis during ice-free conditions (typically late March through November). Flow rates were calculated using these data and a rating curve established for each site using manually measured flow rates. $\text{NO}_3\text{-N}$ concentrations entering and leaving the wetland were measured using automated samplers that collected daily composite samples during the flow-monitoring season. Grab samples were collected approximately weekly at the inflow and outflow locations, and from the wetland itself during periods of zero discharge. Flow was separated into pathway-specific components of SURQ and SSF using an end-member mixing analysis similar to one described by Schilling and Helmers (2008b). The monitoring strategy was designed and implemented as part of the CREP wetland monitoring described by Crumpton et al. (2006). This study utilized four years of data at each site: 2008-2011 for the KS watershed, and 2007-2010 for the AL watershed.

3.3.2 SWAT Model development

Watershed delineations were based on the Light Detection and Ranging (LiDAR) data developed for the State of Iowa in 2010. The Iowa Department of Natural Resources – GIS Section aggregated local LiDAR data to a resolution of one square meter, and hydraulically reinforced the data to incorporate culverts and bridges that convey water through embankments (e.g., roadways). Both watersheds have low topographic relief, with most slopes between zero and two percent and many enclosed depressions.

Sources of climatic data include the National Climatic Data Center Weather Data Library database (NCDC, 2011) and the National Weather Service (NWS) COOP data

available through the Iowa Environmental Mesonet (Iowa State University, 2014). Weather station data included daily rainfall and maximum and minimum daily temperature. The closest weather station to the KS Wetland is located in Ames, Iowa, and data from the weather station in Algona, Iowa, was used for model input in the AL Wetland watershed. Solar radiation, wind speed, and relative humidity were simulated by the weather generator within SWAT.

The USDA National Agricultural Statistics Service (NASS) cropland data layer (CDL) for the years 2005 through 2010 was obtained and used to assess land use and crop rotations. The 2010 NASS land cover was verified by windshield surveys conducted in early spring, 2011. Soils data are from the Soil Survey Geographic Data (SSURGO) database developed by NRCS. Based on the area of land with soils being somewhat poorly, poorly, or very poorly drained, it is estimated that 62% of the KS watershed is tile-drained (Table 3.1). Hydrologic soil group B/D is dominant, with class B applied to HRUs with tile drainage. Soil data include three or four soil layers, depending on soil type, with layer-specific values for bulk density, saturated hydraulic conductivity, and percent sand/silt/clay. Soils in the KS Wetland watershed include Canisteo, Clarion, Harps, Nicollet, and Webster. Clarion and Webster soils together comprise 67% of the watershed. The AL watershed is more intensely drained, with 77% of soils being at least somewhat poorly drained. Soil classifications include Canisteo, Clarion, Nicollet, Okoboji, Storden, and Webster, with 90% of the watershed consisting of Canisteo, Nicollet, or Clarion soils.

SWAT applications typically simulate a large watershed comprised of many subbasins, the size and number of which is determined by setting a stream threshold area and placement of desired subbasin outlets during model delineation. Because this case study was

undertaken to improve tile flow predictions at the drainage-district scale, the watershed models each have only one subbasin. Subbasins in SWAT are divided into hydrologic response units (HRUs) that have unique combinations of land use, soil type, and slope classification. Although HRUs represent real-world locations, they are not spatially contiguous and are lumped at the subbasin level within the SWAT framework. Water and pollutants generated in each HRU are aggregated at the subbasin outlet before being routed in the reach network of the SWAT model.

During HRU development, threshold values were used to filter areas of land use, soil, and slope of negligible size. Both watershed models included thresholds of 3 percent for land use, 5 percent for soil type, and 5 percent for slope classification. As a result, land uses that comprise less than 3 percent of a subbasin are removed and the area is redistributed to the relative percentages of the remaining (non-filtered) land uses in each subbasin. Similarly, soils comprising less than 5 percent of any land uses are filtered, as well as slopes that make up less than 5 percent of any soil group. The filtering process resulted in 17 individual HRUs in the KS Wetland watershed with an average area of 18.2 ha. The AL watershed model was filtered to 26 HRUs with an average size of 8.7 ha. This level of resolution was selected to balance spatial detail and resolution with computational efficiency required for simulation of larger watersheds using SWAT.

3.3.3 Crop rotation and fertilizer application

The majority of row crop production consists of two-year rotations of corn (*Zea mays* L.) and soybeans [*Glycine max* (L.) Merr.], with some continuous corn. Continuous corn was indicated by corn planted in two or more successive growing seasons per historical land use data. Planting and harvest of crops was assumed to occur on May 1 and September 30,

respectively. Seventy-five percent of fertilizer-N was applied in the spring prior to planting corn, with the remaining 25% applied in the fall after soybeans. Fertilizer types consisted of anhydrous ammonia, constituting half of applied-N, urea ammonium nitrate (UAN), and diammonium phosphate (DAP). Table 3.2 lists simulated application rates for each watershed, which are consistent with rates reported in the Iowa Nutrient Reduction Strategy (Iowa State University, 2013).

Table 3.2 Simulated fertilizer-N application.

Crop Rotation	Watershed		Units
	KS	AL	
Corn years of corn-soybean rotations	170	184	kg-N ha ⁻¹
Each year of continuous corn	225	240	kg-N ha ⁻¹

3.3.4 Hydrologic parameterization and calibration

Input parameterization was guided by recommended ranges reported in previous SWAT applications (Douglas-Mankin, 2010; Arnold et al, 2012), with particular focus on efforts in tile-drained landscapes in the Upper Midwest of the United States (Green et al., 2006; Sui and Frankenberger, 2008; Gassman et al., 2009; Moriasi et al., 2012; Moriasi et al., 2013; Yen et al., 2014). Selection of tile-drain related parameters was also informed by previous application of the DRAINMOD and RZWQM models to tile-drained field plots in Central Iowa (Thorpe et al, 2007; Thorpe et al, 2009). Adjustment of objectively derived inputs, such as soil parameters, curve numbers (CN2), and tile drain characteristics, was minimized. Instead, parameter adjustment focused on variables for which physical data is lacking and uncertainty is high. Only four years of observed data is available for calibration in each watershed. The purpose of this study was to evaluate model behavior and performance, rather than use the model for watershed planning. Therefore, neither spatial nor temporal validation was performed.

Table 3.3 is a comprehensive list of input parameters that were adjusted during hydrologic calibration and evaluation. Various combinations of hydrologic parameter adjustments were made using both manual calibration and the Sufi2 algorithm within the SWAT-CUP software program (Abbaspour, 2011). Simulations were executed using SWAT Version 2012, Revision 634, which was obtained from USDA-ARS on November 20, 2014. All parameters shown in Table 3.3 were iteratively adjusted in at least one calibration attempt, but numeric values are reported only for variables utilized in the final hydrologic calibration, which provided the best model performance for each watershed. Performance was assessed using graphical output and performance criteria established by Moriasi et al, (2015a) for Nash-Sutcliffe Efficiency (NSE) and percent bias (PBIAS) (Table 3.4).

Calibration and assessment focused on simulation of daily SURQ, total flow (WYLD), and SSF. SSF is the sum of tile flow, lateral flow, and groundwater flow, with tile flow being the largest component in most tile-drained watersheds. Maximizing model agreement with observed data required calibration parameters unique to each watershed. Additionally, some parameters that were utilized in both watersheds had different calibrated values. SWAT adjusts input CN2 values on a daily basis as a function of either soil moisture or plant evapotranspiration (ET). Both methods have been utilized in previous SWAT applications in tile-drained watersheds, therefore both were evaluated in this study to determine if one provides better hydrologic simulations. For both watersheds, better agreement between measured and predicted hydrologic output was obtained using the Plant ET method. Similarly, model runs using the more recently-incorporated DRAINMOD-based tile equations (Moriasi et al., 2012; Moriasi et al, 2013) provided more accurate hydrologic predictions in both watersheds than the older TDRAIN-based algorithms. Therefore, the

Plant ET curve number method and the DRAINMOD-based tile equations were used in final calibration.

Table 3.3 Hydrologic input parameters considered during model calibration and assessment.

Parameter ID	Description	Default Value	Units	Calibrated Values	
				KS ^[a]	AL ^[b]
ICN	Daily curve number calculation method (0 = Soil Moisture, 1 = Plant ET)	0	--	1	1
CNCOEF	Plant ET curve number coefficient	1.00	--	0.85	0.50
R2ADJ	Retention parameter adjustment for low-gradient, poorly-drained soils	1.00	--	n/a ^[c]	n/a ^[c]
SURLAG	Surface runoff lag coefficient	4.00	--	1.08	0.27
TIMP	Snow pack temperature lag factor	1.00	--	0.77	1.00 ^[d]
GW_DELAY	Lag time between water that exits soil profile and enters shallow aquifer	31.0	d	76.8	50.6
GW_REVAP	Groundwater revap coefficient	0.02	--	0.02 ^[d]	0.02 ^[d]
GWQMN	Threshold depth of water in shallow aquifer for required return flow to occur	1000	mm	987	1535
REVAPMN	Threshold depth of water in shallow aquifer for revap to occur	750	mm	1131	750 ^[d]
ALPHA_BF	Baseflow recession constant	0.048	d ⁻¹	0.70	0.048 ^[d]
ESCO	Soil evaporation compensation factor	0.95	--	0.95	-- ^[c]
EPCO	Plant uptake compensation factor	1.00	--	0.96	-- ^[c]
DDRAIN	Depth to tile drains	1200 ^[f]	mm	1446 ^[e]	1012 ^[e]
DEP_IMP	Depth to restrictive layer	2100 ^[f]	mm	1657 ^[e]	1954 ^[e]
RE	Effective radius of tile drains	50	mm	13 ^[f]	13 ^[f]
DRAIN_CO	Drainage coefficient	10	mm d ⁻¹	24.1	10
LATKSATF	Multiplier for lateral saturated hydraulic conductivity	1.00	--	0.55	0.75
SDRAIN	Distance/spacing between tile drains/laterals (mm)	15000	mm	27928	23583
TDRAIN	Time required to drain soil above tiles to field capacity	0	hr	-- ^[c]	-- ^[c]

^[a]KS wetland watershed parameter values (final calibration)

^[b]AL wetland watershed parameter values (final calibration)

^[c]Parameter evaluated but not applicable to (i.e., not used) in final calibration

^[d]Parameter evaluated but default value used in final calibration

^[e]DDRAIN and DEP_IMP input only in HRUs with subsurface tile drains

^[f]Value based on physical data and best available guidance

Table 3.4 Performance evaluation criteria^[a].

Statistic	Output	Time Scale ^[b]	Performance Criteria			
			Very Good	Good	Satisfactory	Not Satisfactory
NSE ^[c]	Flow	D-M-A	NSE > 0.80	0.70 < NSE ≤ 0.80	0.50 < NSE ≤ 0.70	NSE ≤ 0.50
	NO ₃ -N	M	NSE > 0.65	0.50 < NSE ≤ 0.65	0.35 < NSE ≤ 0.50	NSE ≤ 0.35
PB ^[d]	Flow	D-M-A	PB < ±5	±5 < PB ≤ ±10	±10 < PB ≤ ±15	PB ≥ ±15
	NO ₃ -N	D-M-A	PB < ±15	±15 < PB ≤ ±20	±20 < PB ≤ ±30	PB ≥ ±30

^[a] Adapted from Moriasi et al. (2015a)

^[b] D = daily, M = monthly, A = annual

^[c] NSE = Nash-Sutcliffe efficiency

^[d] PB = PBIAS = percent bias (%)

3.3.5 Nitrogen input parameterization

After hydrologic simulations were calibrated and assessed, NO₃-N-related variables reported in the top portion of Table 3.5 were adjusted during calibration to observed daily NO₃-N concentrations. Hydrologic and NO₃-N calibrations were performed separately to avoid counter-acting parameter adjustments and provide more independent measures of model performance. The calibrated concentration represents the composite concentration of all flow pathways because pathway specific concentrations are not currently output in a manner convenient for calibration. Calibration and assessment focused on the daily concentrations rather than monthly loads commonly reported in the SWAT literature. This provides additional insights to the suitability of the model for simulation of water quality BMPs and for assessment of water quality standards, which are concentration-based. Furthermore, simultaneous calibration of flows and loads can mask performance deficiencies. For example, NO₃-N concentrations could potentially be calibrated upwards during periods of flow underestimation in order to improve load predictions, but the appearance of improvement would be artificial and may worsen model performance and limit the model's utility for its intended use.

After evaluating simulation of daily NO₃-N concentrations using existing algorithms in SWAT, a revised executable version of SWAT (a modified version of Revision 636 obtained from USDA-ARS on January 20, 2016) was utilized to try and improve model performance. Hydrologic algorithms were not modified from Revision 634 and 636. Code revisions included the addition of several NO₃-N parameters relating to soil profile-N and NO₃-N transport via tile drains. New parameters were incorporated into the plant nutrient uptake algorithms (nup.f source code) and tile-NO₃ transport algorithms (nlch.f source code). The parameter names, descriptions, and calibrated values, are listed in the lower section of Table 3.5, along with calibrated values of NO₃-N-related parameters.

Table 3.5 Nitrogen-related parameters considered during model calibration and assessment.

Parameter ID	Description	Default Value	Units ^[a]	Calibrated Values	
				KS ^[b]	AL ^[c]
NO₃-N simulation using existing soil and tile NO₃-N algorithms					
NPENCO	Nitrate percolation coefficient	0.20	--	0.20 ^[d]	0.20 ^[d]
ANION_EXCL	Fraction of porosity (void space) from which anions are excluded	0.50	fraction	0.11	0.27
CDN	Denitrification exponential rate coefficient	1.40	--	1.26	1.24
SDNCO	Denitrification threshold water content	1.10	fraction	1.18	1.19
NO₃-N simulation using modified algorithms with lagging parameters					
N_REDUCE	New NO ₃ -N plant uptake reduction factor	300	--	300 ^[d]	300 ^[d]
N_LAG	New dimensionless lag coefficient for tile NO ₃ -N concentration	0.25	--	0.25 ^[d]	0.25 ^[d]
N_LN	New dimensionless exponent for NO ₃ -N lagging function	2.0	--	1.5	1.5
N_LNCO	New dimensionless coefficient for NO ₃ -N lagging function	2.0	--	1.5	1.5
NO₃-N simulation using modified algorithms with lagging parameters (above) and re-calibration					
ANION_EXCL	Fraction of porosity (void space) from which anions are excluded	0.50	fraction	0.40	0.50
CDN	Denitrification exponential rate coefficient	1.40	--	0.46	0.21
SDNCO	Denitrification threshold water content	1.10	fraction	1.29	1.27

^[a]Units are dimensionless except ANION_EXCL (fraction of porosity) and SDNCO (fraction of field capacity)

^[b]KS wetland watershed parameter values (final calibration)

^[c]AL wetland watershed parameter values (final calibration)

^[d]Parameter evaluated but default value was used in final calibration

3.4 Results and Discussion

3.4.1 Evaluation of hydrologic simulation

Calibrating to pathway-specific flow components WYLD, SURQ, and SSF, proved more difficult than calibrating only to total flow. All NSE and PBIAS values for both daily and monthly WYLD meet the evaluation criteria of satisfactory or better, as set forth by Moriasi et al. (2015a) (Table 3.6). NSE values for daily SSF were not satisfactory for either watershed, although PBIAS is very good in the KS model and satisfactory for AL. Simulation of SURQ is not satisfactory at either time step for the AL model. Average runoff in the AL watershed was only 30 mm yr⁻¹ from 2007-2010, and SWAT was unable to replicate these extremely low runoff conditions. The overall water balance of both models matched observed data reasonably well. Observed SSF in the KS watershed accounted for 75% of the measured flow, with simulated SSF equal to 73% of total WYLD. Observed SSF in the AL watershed comprised 89% of total flow, whereas simulated SSF made up 85% of the simulated WYLD. Simulations of monthly WYLD were good for both watersheds.

Table 3.6 Performance statistics for pathway-specific flow components.

	Daily		Monthly	
	NSE ^[a]	PBIAS ^[b]	NSE ^[a]	PBIAS ^[b]
KS Watershed				
WYLD	0.68 [S]	-2.7 [VG]	0.79 [G]	-5.0 [G]
SURQ	0.55 [S]	-10.0 [S]	0.87 [VG]	-11.1 [S]
SSF	0.36 [NS]	-0.3 [VG]	0.55 [S]	-2.9 [VG]
AL Watershed				
WYLD	0.51 [S]	9.2 [G]	0.71 [G]	9.2 [G]
SURQ	-0.25 [NS]	-21.5 [NS]	0.10 [NS]	-21.5 [NS]
SSF	0.46 [NS]	12.9 [S]	0.66 [S]	12.9 [S]

^[a] Nash-Sutcliffe efficiency.

^[b] Percent bias (negative indicates over-estimation)

^[a,b] VG=very good, G=good, S=satisfactory, NS=not satisfactory (Moriasi et al., 2015a)

Time series plots illustrate the challenges of accurately simulating daily SSF in SWAT. The model captures the general trends/directions in SSF, but consistently underestimates peak flows and fails to reflect hydrograph recession in both the KS (Figure 3.2) and AL (Figure 3.3) watersheds. Several instances of large disagreement between observed and simulated SSF likely stem from significant differences between local and weather station precipitation due to the distance of weather stations from the watersheds. Other factors may include the influence of surface intakes, which is not captured in the model, uncertainty regarding characteristics of the local tile drainage infrastructure, and the lumped nature of HRUs, which does not allow mechanistic routing of subsurface flow through the watersheds.

These results were not spatially or temporally validated due to limited years of data and the exploratory nature of this analysis. Variation in hydrologic behavior between the two watersheds is largely unexplained by known inputs (i.e., soil, climate, etc.), which are similar for both watersheds. Distinct hydrologic behavior and differences in calibrated parameters between watersheds indicate that spatial validation would be difficult to achieve. This suggests that SWAT models applied and calibrated to large watersheds in tile-drained landscapes will not accurately simulate pathway-specific flows at the drainage district scale. Additionally, model performance will vary substantially between drainage-district scale watersheds. The degree of variation in observed WYLD and $\text{NO}_3\text{-N}$ between drainage districts in this study was consistent with patterns observed in adjacent drainage districts within the same HUC-12 watershed in Hamilton County, Iowa (Ikenberry et al., 2014).

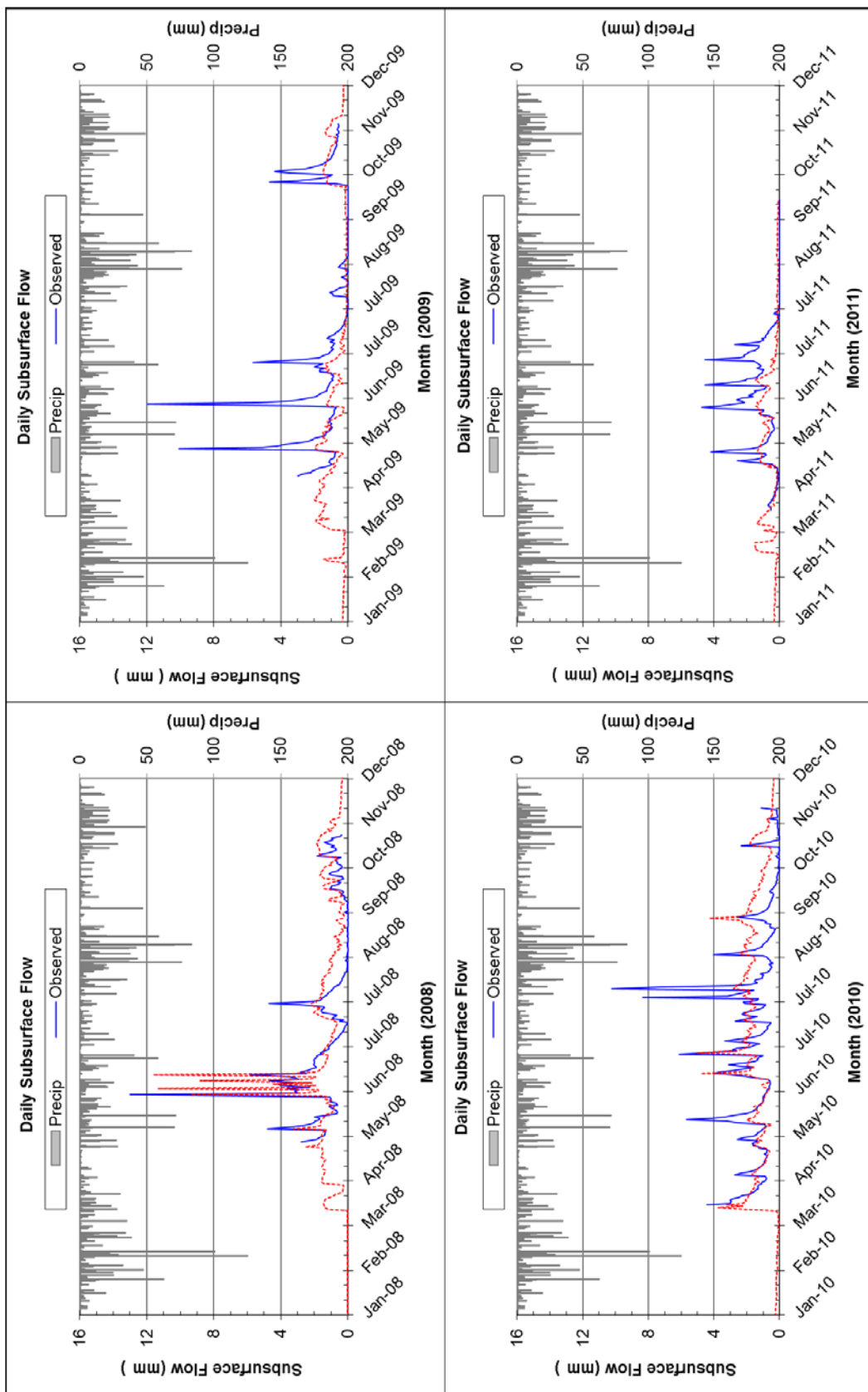


Figure 3.2 Daily time series SSF for the KS watershed. Blue line is observed SSF, red dashed line is simulated SSF, and precipitation is shown in gray bars at the top of the y-axis.

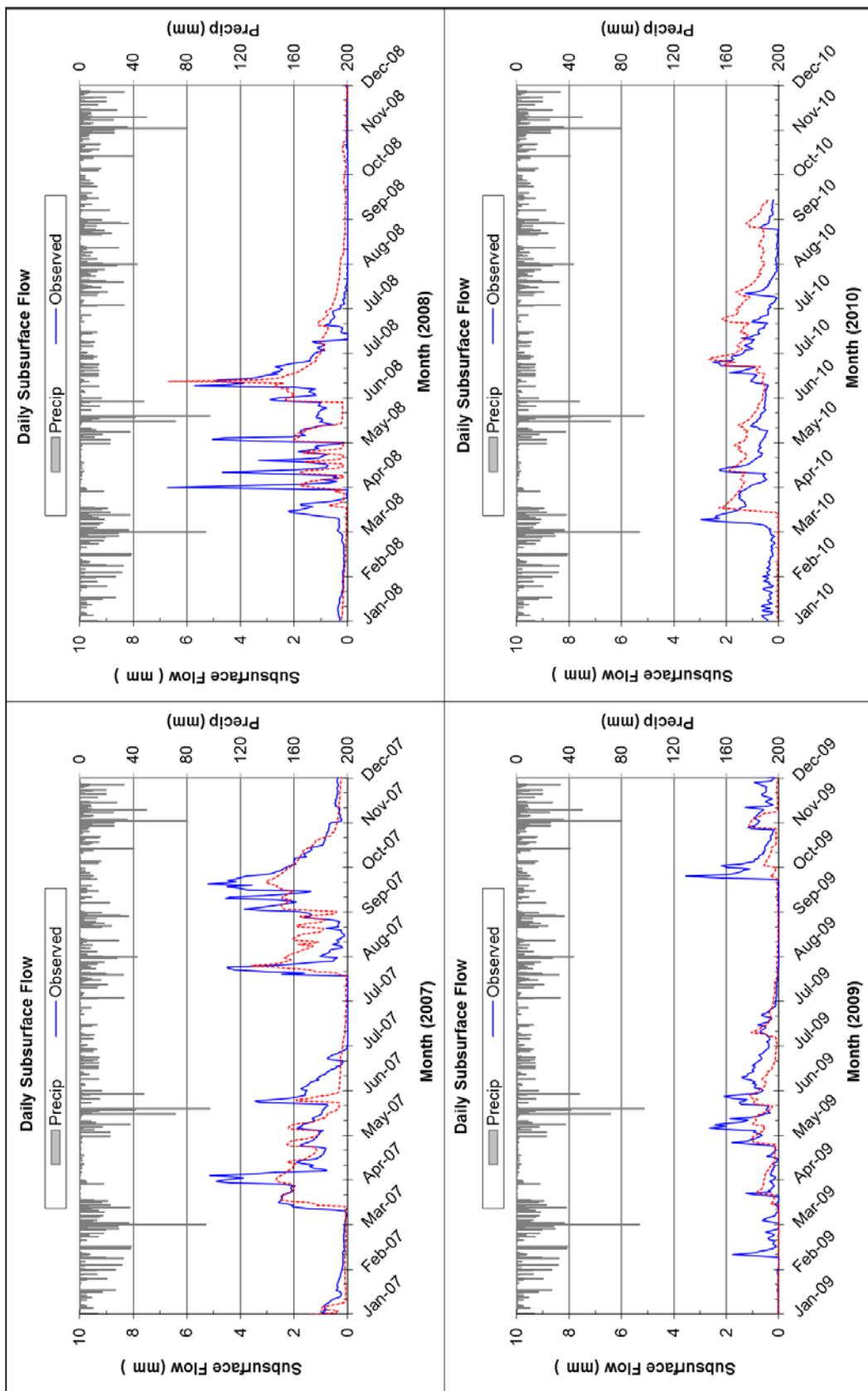


Figure 3.3 Daily time series SSF for the AL watershed. Blue line is observed SSF, red dashed line is simulated SSF, and precipitation is shown in gray bars at the top of the y-axis.

3.4.2 Evaluation of $\text{NO}_3\text{-N}$ simulation

Simulation of $\text{NO}_3\text{-N}$ concentration was more problematic than prediction of daily flow components, with concentrations falling steeply in June/July and remaining near zero through the end of the growing season in both KS (Figure 3.4) and AL (Figure 3.5) models. Simulated $\text{NO}_3\text{-N}$ is depleted from the soil too quickly, possibly due to misrepresentation of soil-N cycle and/or $\text{NO}_3\text{-N}$ transport algorithms. Prior to depletion of soil-N, simulated concentration varied with flow, showing more short-term fluctuation than observed concentration. Additionally, there are several instances of sharp increases in simulated concentration concurrent with declines in observed concentration. This occurs in June 2008 in the KS watershed and AL watershed, and again in July 2010 for AL, at times when both SSF and SURQ increase. Evaluation of pathway-specific flows and $\text{NO}_3\text{-N}$ concentrations revealed that the discrepancy stems from over-estimation of SSF $\text{NO}_3\text{-N}$ concentrations at these times. Although model performance for $\text{NO}_3\text{-N}$ concentration was not satisfactory (Table 3.7), the proportion of $\text{NO}_3\text{-N}$ carried by SSF relative to SURQ was as expected, with SSF concentrations consistently far exceeding runoff concentrations. Simulated flow-weighted average (FWA) $\text{NO}_3\text{-N}$ concentrations in SURQ were less than 1 mg L^{-1} for both watersheds, while FWA $\text{NO}_3\text{-N}$ concentrations in SSF were over 10 mg L^{-1} .

Table 3.7 Performance statistics for initial daily $\text{NO}_3\text{-N}$ concentration calibration.

Watershed	Daily Concentration		Daily Load		Monthly Load	
	NSE ^[a]	PBIAS ^[b]	NSE ^[a]	PBIAS ^[b]	NSE ^[a]	PBIAS ^[b]
KS	-1.90	50.6	-0.06	32.8	0.37 [S]	41.4
AL	-2.70	71.7	-0.15	53.7	0.14	53.6

^[a] Nash-Sutcliffe efficiency.

^[b] Percent bias (negative indicates over-estimation)

^[a,b] All performance criteria are not satisfactory (NS) per Moriasi et al., (2015a) unless otherwise indicated.

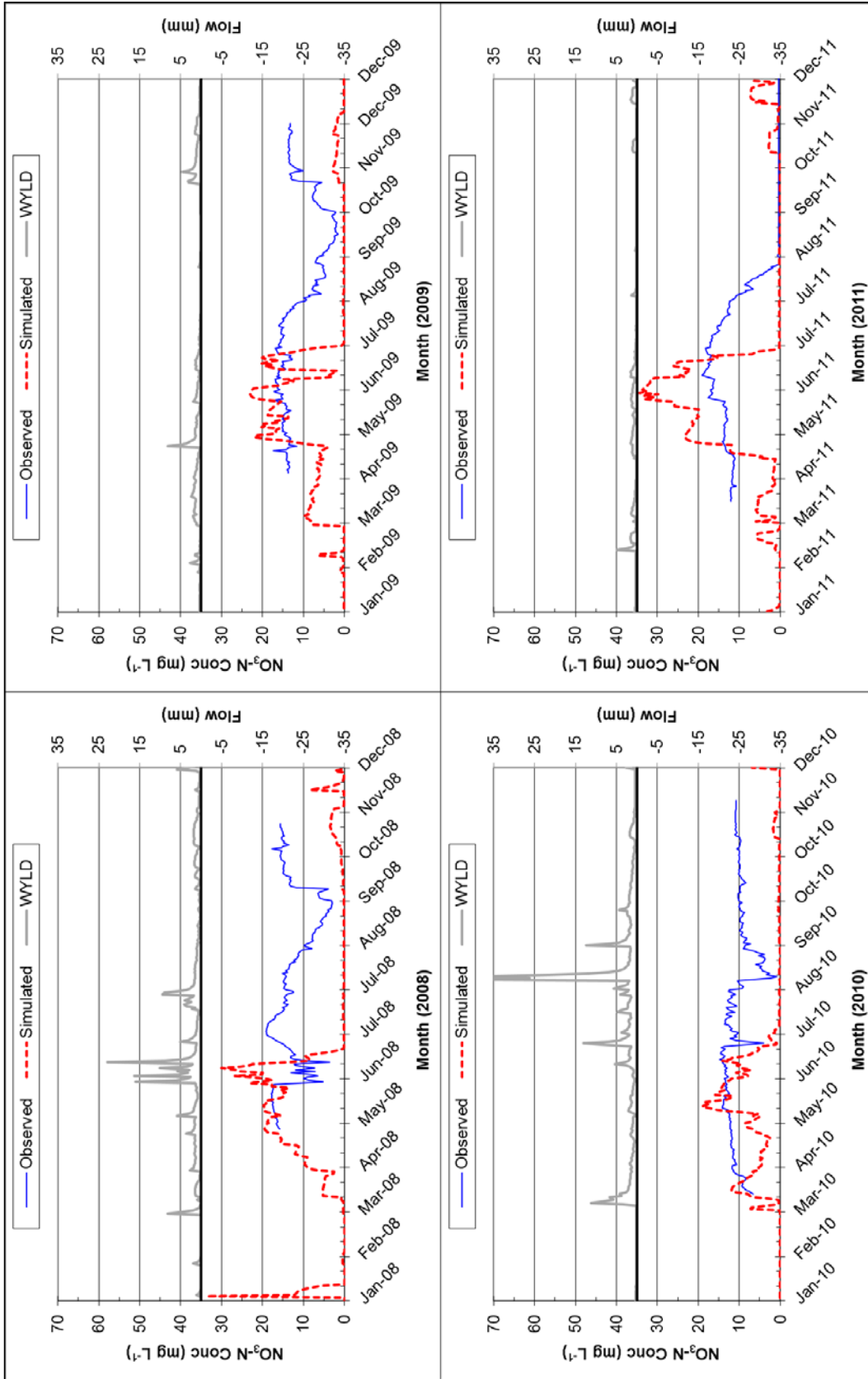


Figure 3.4 Daily time series $\text{NO}_3\text{-N}$ concentration for the KS watershed. Blue line is observed, red dashed line is simulated, with simulated WYLD shown in gray.

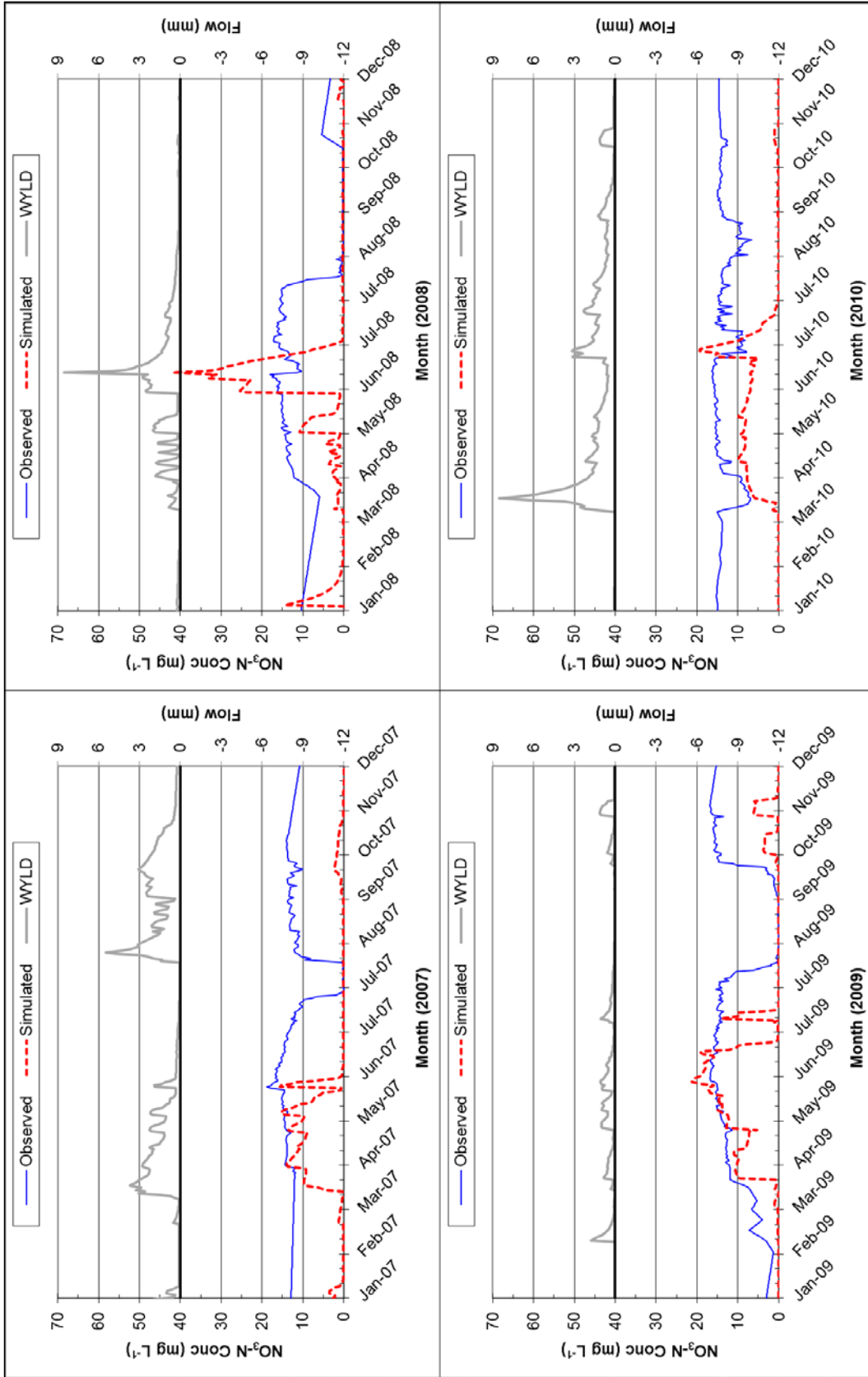


Figure 3.5 Daily time series $\text{NO}_3\text{-N}$ concentration for the AL watershed. Blue line is observed, red dashed line is simulated, with simulated WYLD shown in gray.

Simulated soil-NO₃ concentrations for a several soils in corn-soybean rotations are plotted for the KS (Figure 3.6) and AL (Figure 3.7) models, along with measured data for similar soils in Central Iowa (Cambardella et al., 1999). The trend for simulated soil-NO₃ is similar to the measured pattern with an important deviation: simulated soil-NO₃ is fully depleted by mid-summer in both corn and soybean years, whereas measured mid-summer residual levels off at 30-40 kg-NO₃ ha⁻¹ in corn years and remains steady at approximately 45 kg-NO₃ ha⁻¹ in soybean years. The increase in soil-NO₃ from fertilizer application is reflected by the models, as is post-harvest mineralization of organic-N to NO₃-N. Soil-NO₃ levels are much lower in the Canisteo soil than the Webster or Clarion soils in the KS watershed, but this difference is not observed in the AL model.

Modeled corn yields for the 4-year simulations were 8,713 kg ha⁻¹ (139 bu ac⁻¹) in the KS watershed and 10,335 kg ha⁻¹ (164 bu ac⁻¹) in the AL watershed, which are about 16% and 10% lower than reported county-wide yield data, respectively (ISU, 2015). The fact that simulated yields are higher in the AL watershed than KS is geographically consistent with the county-wide yield data. Simulated depletion of soil-NO₃ levels to zero in the middle of the growing season is responsible for lower than expected corn yields, indicated by the number of N-stress days reported in model output. This depletion occurs even in dry years and in years in which simulated denitrification is zero. Additional causes of this error may be related to crop growth processes such as N uptake and N use efficiency, as plant growth parameters for corn in the SWAT plant database are likely outdated and do not reflect current crop genetics.

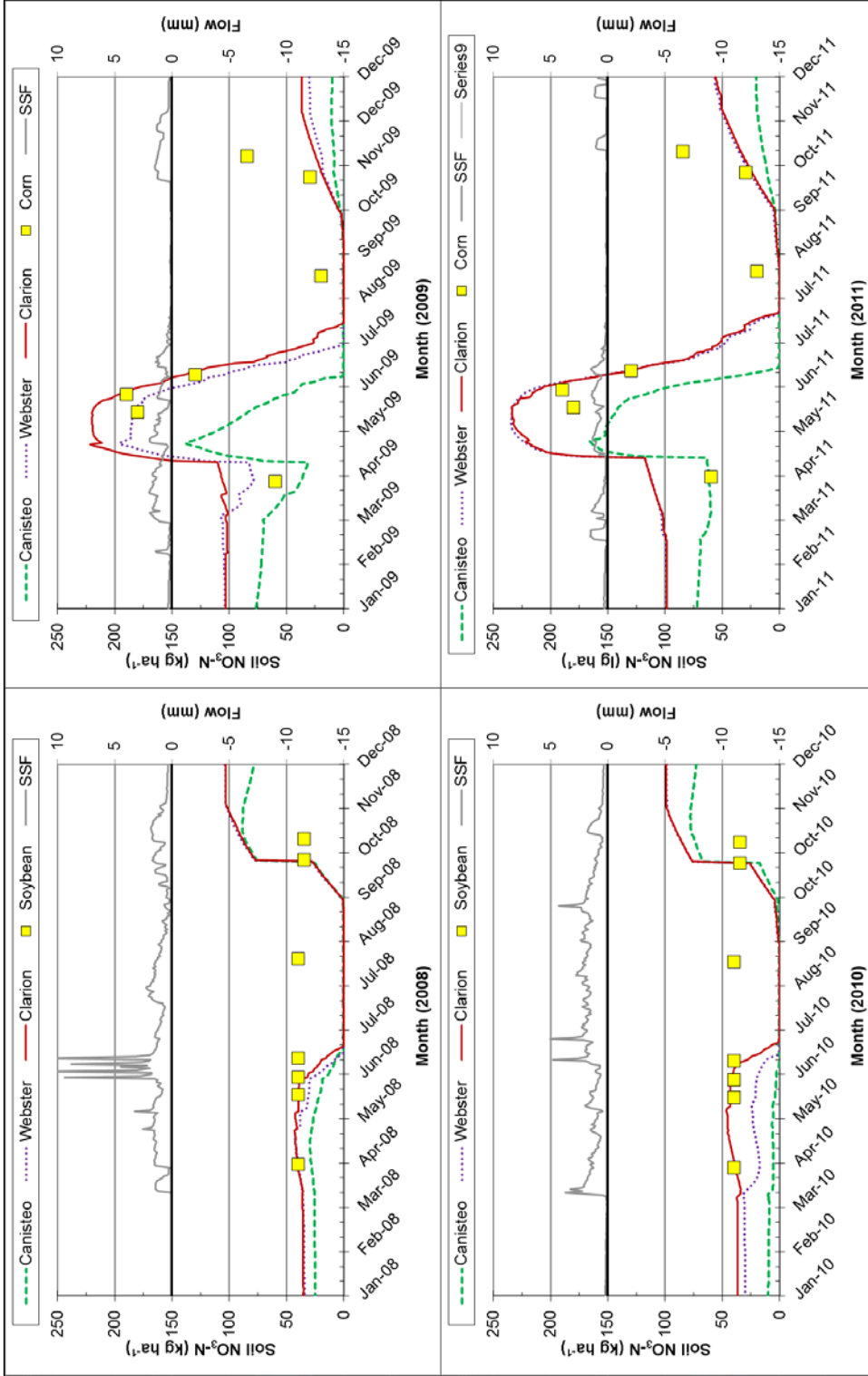


Figure 3.6 Simulated soil profile NO₃-N for corn-soybean rotations in the KS watershed. Dashed green line is soil-NO₃-N for Canisteo soil, dotted purple line is for Webster, and solid brown line is for Clarion. Simulated SSF is shown in gray on the top portion of each graph. Yellow squares are data measured in similar Central Iowa soils from Cambardella et al., (1999).

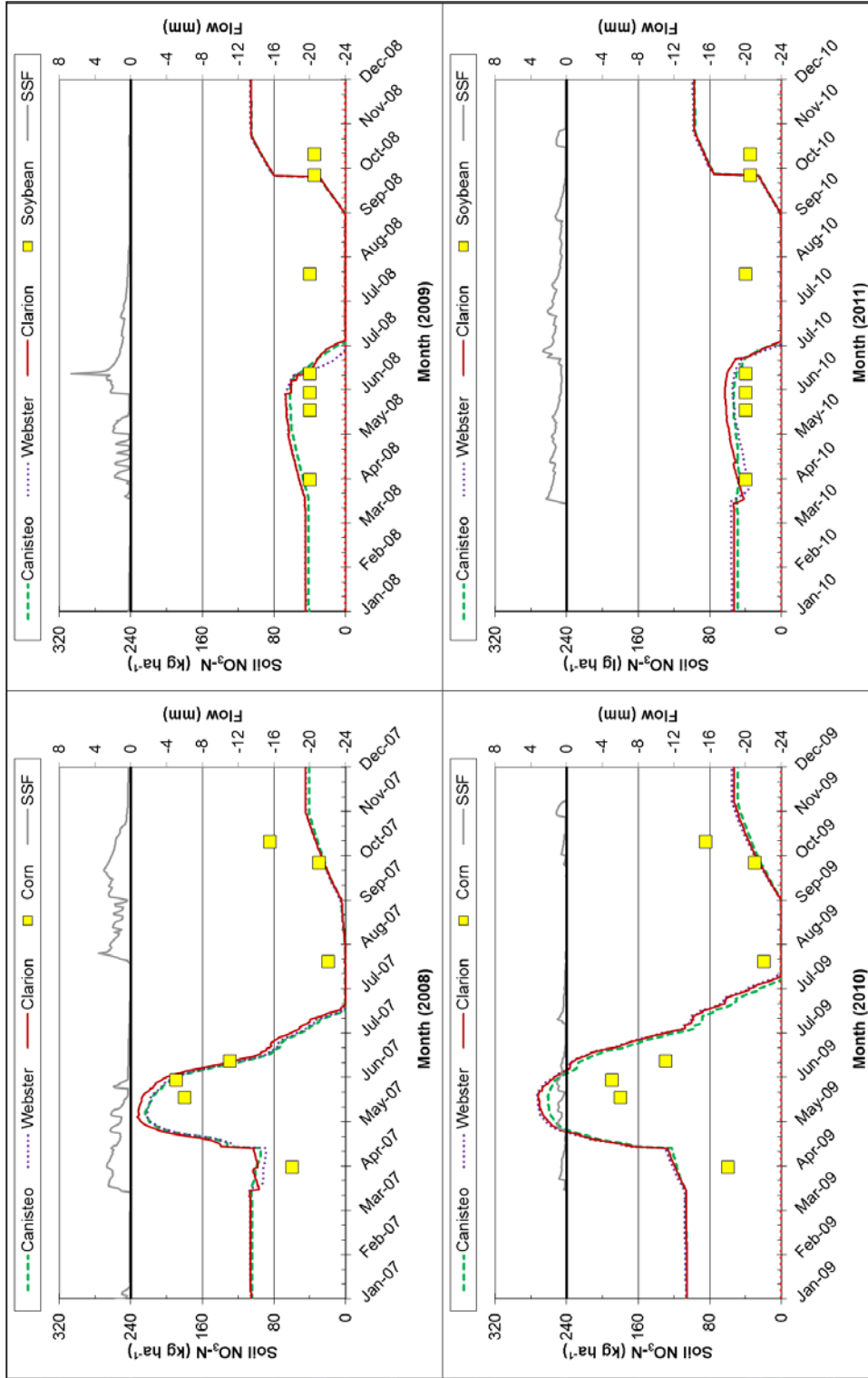


Figure 3.7 Simulated soil profile $\text{NO}_3\text{-N}$ for corn-soybean rotations in the AL watershed. Dashed green line is soil- $\text{NO}_3\text{-N}$ for Canisteo soil, dotted purple line is for Webster, and solid brown is for Clarion. Simulated SSF is shown in gray on the top portion of each graph. Yellow squares are data measured in similar Central Iowa soils from Cambardella et al., (1999).

Simulated soil-N dynamics are reported in Table 3.8. Magnitude of simulated fluxes were generally within ranges reported in regional guidance and literature data, but fluxes are highly variable and our ability to estimate N-fixation and denitrification are limited (Christianson et al., 2012). In Webster soil HRUs, average simulated denitrification was 28 kg-N ha⁻¹ yr⁻¹ for the KS model and 20-N kg ha⁻¹ yr⁻¹ for AL.

Table 3.8 Simulated soil-N dynamics for Webster and Clarion soil HRUs after calibration using existing NO₃-N algorithms.

	Soil/ Crop	^[a] Positive Fluxes (kg-N ha ⁻¹)				^[b] Negative Fluxes (kg-N ha ⁻¹)				
		Appl ^[c]	Atmos	Fix	Min	Denit	Uptake	Runoff	SSF	Seep
KS	Webster/									
2008	Soy	49	13	276	113	27	313	<1	22	0
2009	Corn	122	9	0	109	55	205	<1	29	0
2010	Soy	49	13	227	101	28	271	<1	6	0
2011	Corn	122	8	0	134	0	239	<1	39	0
	Clarion/									
2008	Soy	49	13	269	106	0	313	1	<1	36
2009	Corn	122	9	0	107	0	232	<1	<1	47
2010	Soy	49	13	211	101	0	271	1	<1	22
2011	Corn	122	8	0	127	0	242	<1	<1	29
AL	Webster/									
2007	Corn	135	10	0	121	12	254	<1	34	0
2008	Soy	49	8	293	131	31	338	<1	27	0
2009	Corn	135	8	0	155	0	302	<1	15	0
2010	Soy	49	9	232	134	36	301	<1	20	0
	Clarion/									
2007	Corn	135	10	0	116	0	260	<1	<1	33
2008	Soy	49	8	274	126	0	337	<1	<1	35
2009	Corn	135	8	0	146	0	298	<1	<1	12
2010	Soy	49	9	226	125	0	301	<1	<1	39

^[a] Inputs: Appl = fertilizer-N, Atmos = rainfall-N, Fix = N-fixation, Min = mineralization of organic-N

^[b] Outputs: Denit = denitrification, uptake = plant uptake, Runoff and SSF = N lost to surface water, Seep = N lost to deep aquifer via seepage.

^[c] Fertilizer application occurs in fall after soybean harvest and in spring in corn years.

David et al. (2009) simulated denitrification rates ranging from 3.8 to 21 kg-N ha⁻¹ yr⁻¹ using a variety of models to estimate denitrification rates in a tile-drained corn and soybean rotation in Illinois. In well-drained Clarion soils in the KS and AL models, the simulated denitrification rate was zero and large magnitudes of NO₃-N were lost to deep seepage because of the absence of a restrictive soil layer. N-fixation by soybeans was somewhat

higher than reported in other studies in Iowa (Jaynes et al., 2001; Christianson et al., 2012), and N-uptake was near or above the high end of rates estimated for high yielding corn crops in Iowa (ISU, 2006).

3.4.3 Simulation with modified $\text{NO}_3\text{-N}$ algorithms

Due to problems simulating $\text{NO}_3\text{-N}$ concentrations modifications were made to the SWAT source code to improve $\text{NO}_3\text{-N}$ loss from the soil profile. The modifications included additional lagging parameters for $\text{NO}_3\text{-N}$ in tile drainage. The ANION_EXCL, CDN, and SDNCO parameters were left unchanged. The NSE values for daily concentration and loads were improved using the modified lagging parameters; however values were still not satisfactory and PBIAS was not improved (Table 3.9).

Simulated SSF concentrations did not drop as sharply in mid-summer months as with the original equations, peak concentrations were decreased (Figure 3.8 and Figure 3.9). Visual assessment suggests that the lagging parameters improved the pattern of $\text{NO}_3\text{-N}$ concentrations over time, but overall concentrations were still under-predicted and daily fluctuation of simulated concentrations exceeds fluctuation in the observed data.

Table 3.9 Performance statistics for modified algorithm daily $\text{NO}_3\text{-N}$ concentration.

Watershed	Daily Concentration		Daily Load		Monthly Load	
	NSE ^[a]	PBIAS ^[b]	NSE ^[a]	PBIAS ^[b]	NSE ^[a]	PBIAS ^[b]
KS	-0.75 [NS]	51.5 [VG]	0.34 [NS]	44.28 [NS]	0.29 [NS]	54.0 [NS]
AL	-1.86 [NS]	67.9 [NS]	0.28 [NS]	58.6 [NS]	0.28 [NS]	58.6 [NS]

^[a] Nash-Sutcliffe efficiency.

^[b] Percent bias (negative indicates over-estimation)

^[a,b] VG=very good, G=good, S=satisfactory, NS=not satisfactory (Moriassi et al., 2015a)

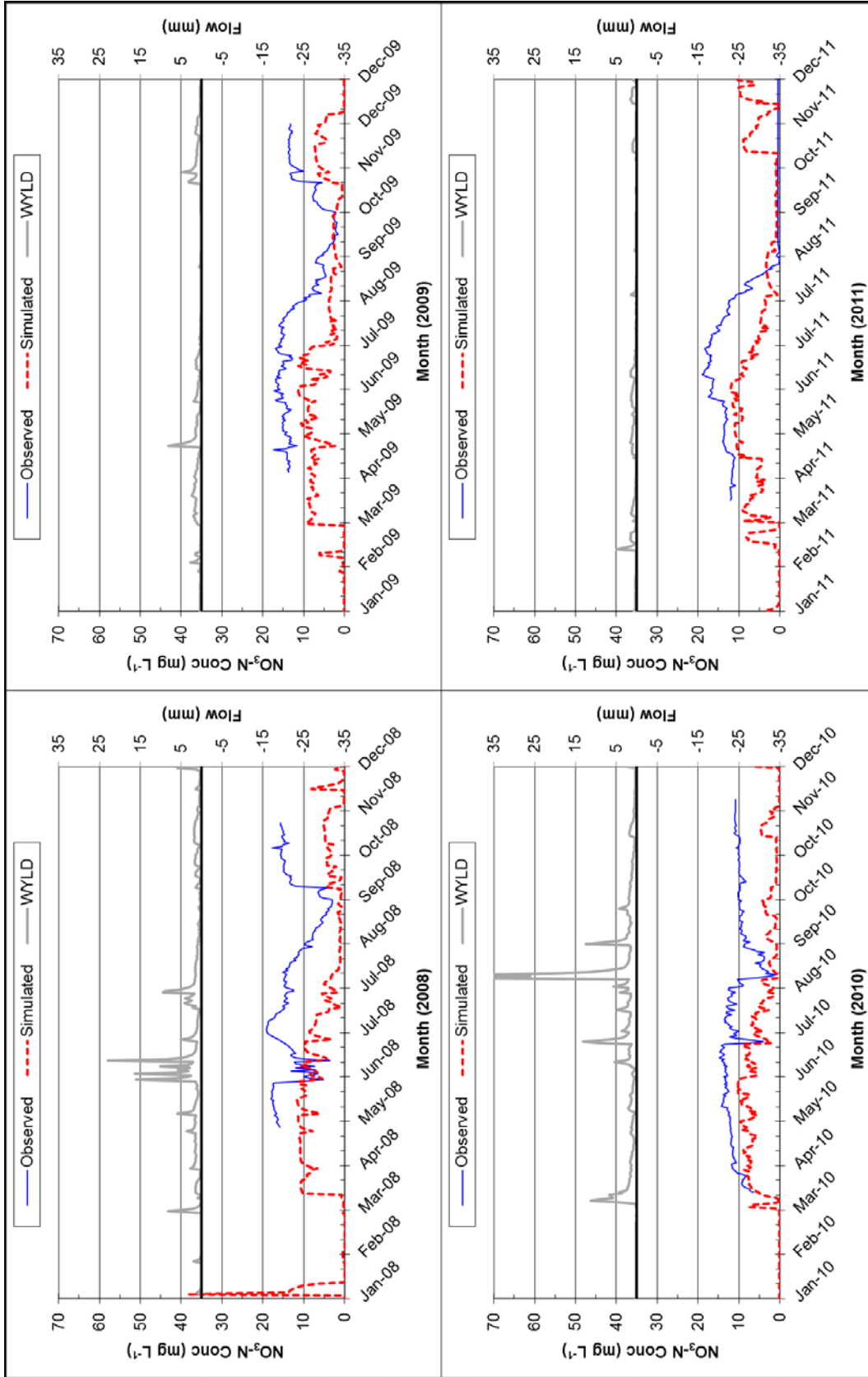


Figure 3.8 Daily time series $\text{NO}_3\text{-N}$ concentration for the KS watershed using modified algorithms. Blue line is observed, red dashed line is simulated, with simulated WYLD shown in gray.

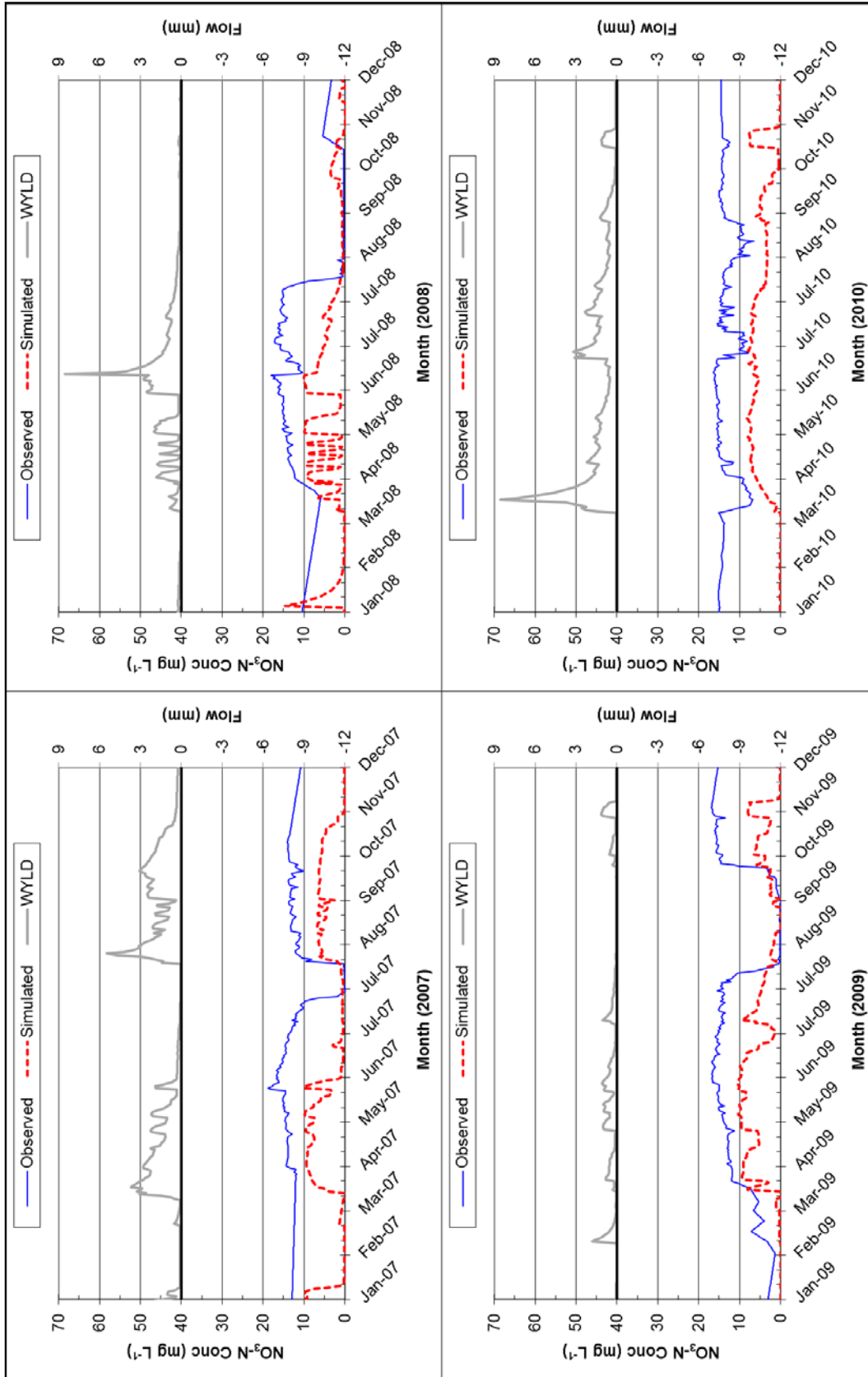


Figure 3.9 Daily time series $\text{NO}_3\text{-N}$ concentration for the AL watershed using modified algorithms. Blue line is observed, red dashed line is simulated, with simulated WYLD shown in gray.

Patterns in soil-NO₃ concentrations were not significantly altered by the modifications (Figure 3.10 and Figure 3.11). Although the basis for the modifications is not well established and problems simulating fate and transport remain, results obtained using the lagging parameters provide insight to the possible causes of error and needed improvements in the simulation of NO₃-N transport in tile-drained watersheds. The lagging parameters increased denitrification (Table 3.10), likely due to increased time NO₃-N remained in the soil profile. Interestingly, NO₃-N losses in SSF increased in some years and decreased in others (Table 3.10). After evaluation of model performance using the modified algorithms, one additional simulation was performed using the lagging parameters and recalibrating the models by adjusting other NO₃-N related variables (ANION_EXCL, CDN, and SDNCO).

Table 3.10 Simulated soil-N dynamics for Webster and Clarion soil HRUs using modified soil NO₃-N algorithms.

	Soil/ Crop	^[a] Positive Fluxes (kg-N ha ⁻¹)				^[b] Negative Fluxes (kg-N ha ⁻¹)				
		Appl ^[c]	Atmos	Fix	Min	Denit	Uptake	Runoff	SSF	Seep
KS	Webster/									
2008	Soy	49	13	304	132	63	313	<1	34	0
2009	Corn	122	9	0	108	72	197	<1	26	0
2010	Soy	49	13	264	101	52	271	<1	21	0
2011	Corn	122	8	0	135	0	255	<1	19	0
	Clarion/									
2008	Soy	49	13	292	106	0	313	1	<1	56
2009	Corn	122	9	0	104	0	223	<1	<1	57
2010	Soy	49	13	243	100	0	271	1	<1	50
2011	Corn	122	8	0	120	0	228	<1	<1	38
AL	Webster/									
2007	Corn	135	10	0	125	18	262	<1	35	0
2008	Soy	49	8	311	136	51	337	<1	21	0
2009	Corn	135	8	0	159	0	311	<1	5	0
2010	Soy	49	9	266	140	69	301	<1	27	0
	Clarion/									
2007	Corn	135	10	0	113	0	252	<1	<1	54
2008	Soy	49	8	296	124	0	338	<1	<1	40
2009	Corn	135	8	0	146	0	298	<1	<1	16
2010	Soy	49	9	251	127	0	301	<1	<1	59

^[a] Inputs: Appl = fertilizer-N, Atmos = rainfall-N, Fix = N-fixation, Min = mineralization of organic-N

^[b] Outputs: Denit = denitrification, uptake = plant uptake, Runoff and SSF = N lost to surface water, Seep = N lost to deep aquifer via seepage.

^[c] Fertilizer application occurs in fall after soybean harvest and in spring in corn years.

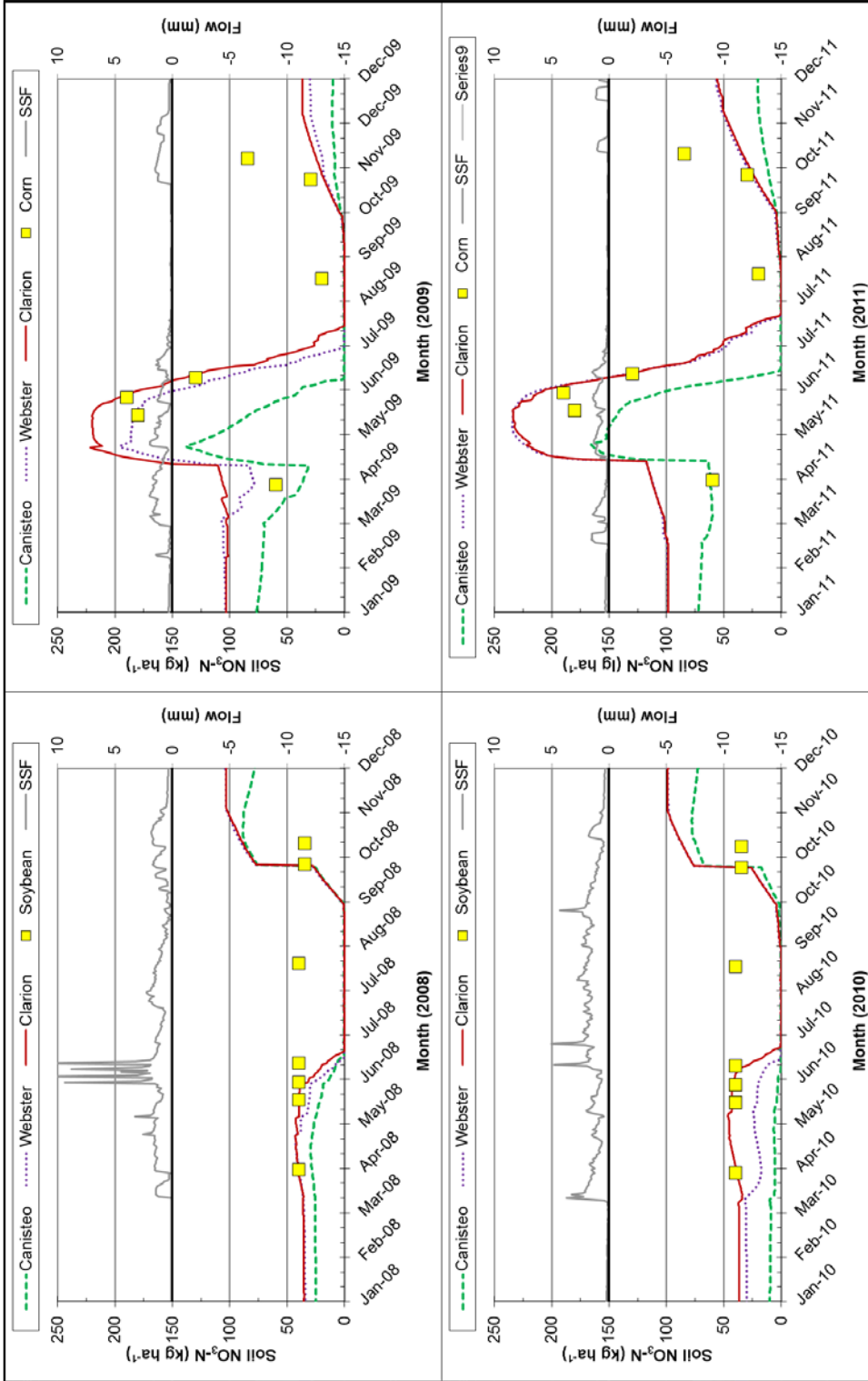


Figure 3.10 Simulated soil profile $\text{NO}_3\text{-N}$ for corn-soybean rotations in the KS watershed with modified soil- NO_3 algorithms. Dashed green line is soil- $\text{NO}_3\text{-N}$ for Canisteo soil, dotted purple line is for Webster, and solid brown is for Clarion. Simulated SSF is shown in gray on the top portion of each graph. Yellow squares are data measured in similar Central Iowa soils from Cambardella et al., (1999).

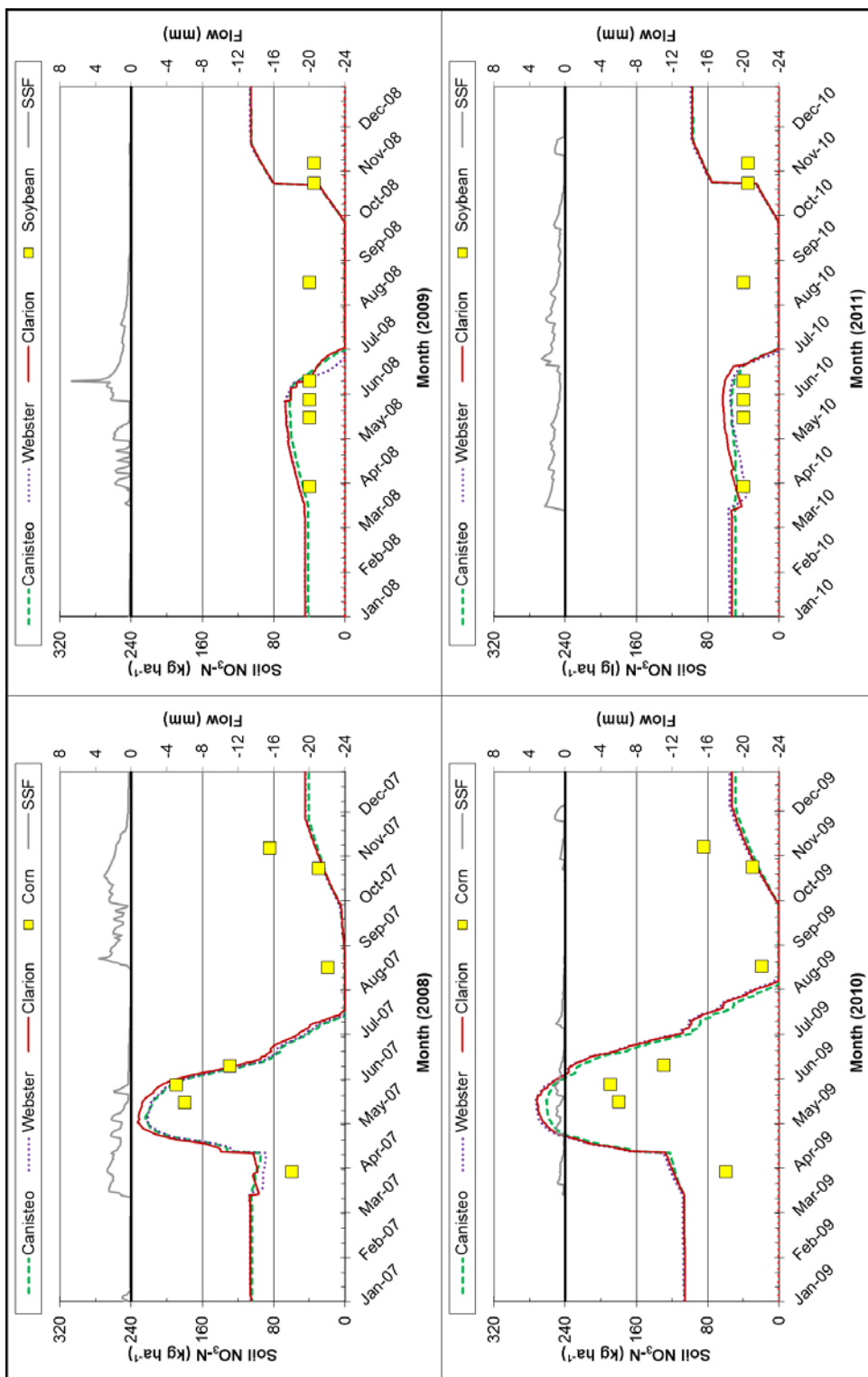


Figure 3.11 Simulated soil profile $\text{NO}_3\text{-N}$ for corn-soybean rotations in the AL watershed using modified soil- NO_3 algorithms. Dashed green line is soil- $\text{NO}_3\text{-N}$ for Canisteo soil, dotted purple line is for Webster, and solid brown is for Clarion. Simulated SSF is shown in gray on the top portion of each graph. Yellow squares are data measured in similar Central Iowa soils from Cambardella et al., (1999).

3.4.4 *Re-calibration with modified NO₃-N algorithms*

Due to problems simulating NO₃-N concentrations that remained after modification of lagging parameters, the models were re-calibrated. After calibration, the modifications provide better agreement between simulated and observed NO₃-N concentrations, as seen in Figure 3.12 for the KS watershed and Figure 3.13 for the AL watershed, but there remained periods of significant divergence between simulated and observed NO₃-N concentrations.

Model performance statistics were improved significantly by slowing down the release of NO₃-N from the soil profile, as can be seen by comparing Table 3.11 with Table 3.9 and Table 3.7. With modification and re-calibration, NSE remained unsatisfactory for daily concentrations, but were satisfactory for daily loads in both models. PBIAS was very good for the KS model but not satisfactory for AL. Simulated concentrations did not drop as sharply in mid-summer months as with the original equations, but short-term fluctuation continued to exceed fluctuations in observed concentration. Despite challenges in simulating daily concentrations and loads, monthly statistics are categorized as “good” or better for all performance criteria except PBIAS in the AL model (Moriassi et al., 2015a). Calibrating solely to monthly WYLD and loads (rather than to pathway-specific flows and NO₃-N concentrations) may result in higher performance criteria for monthly statistics than obtained in this study. However, this methodology would provide no insight to pathway-specific components and short-term fluctuations. Furthermore, it may provide a false sense of security with respect to model performance and suitability for its intended use.

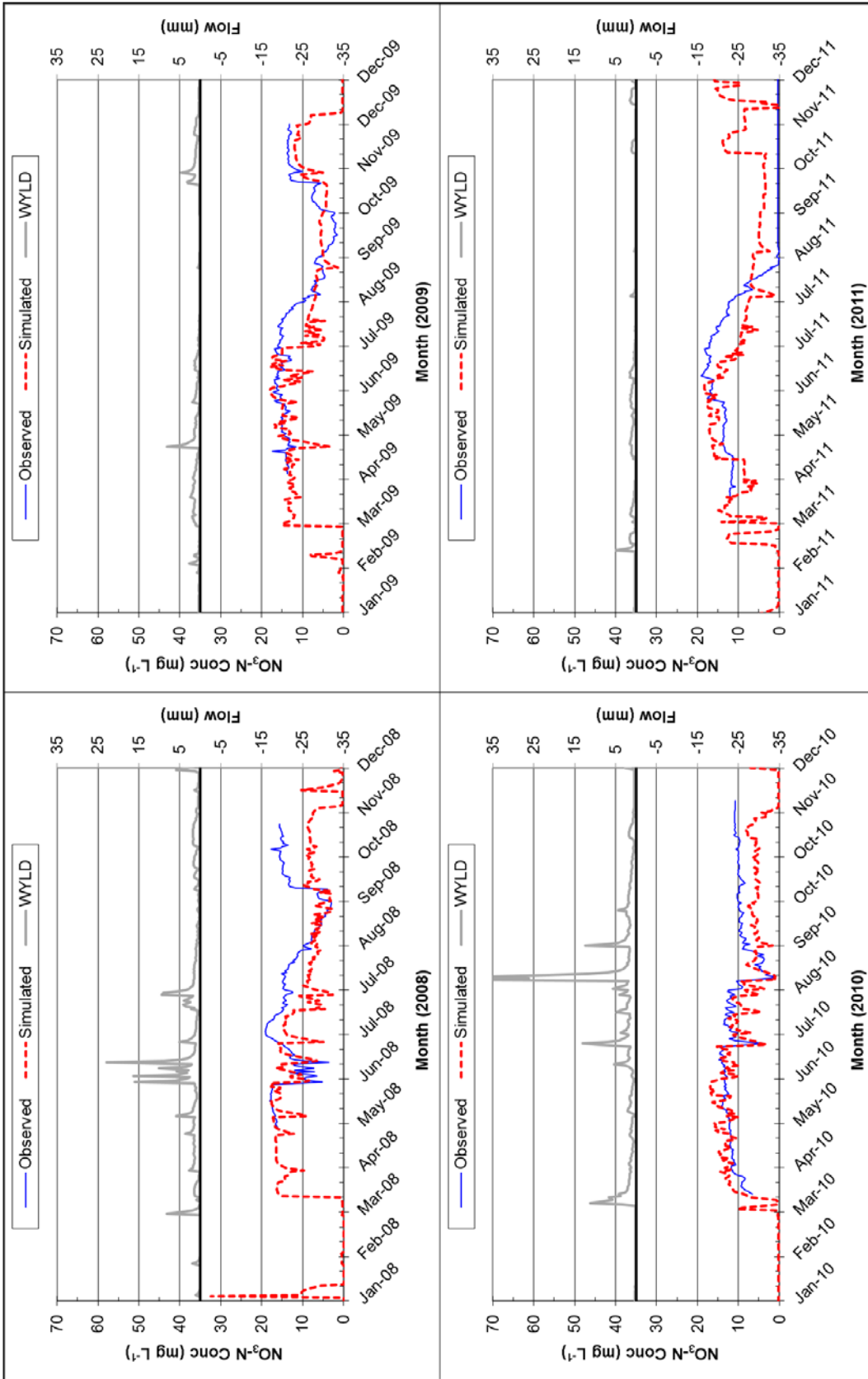


Figure 3.12 Re-calibrated daily time series NO_3-N concentration for the KS watershed using modified algorithms. Blue line is observed, red dashed line is simulated, with simulated WYLD shown in gray.

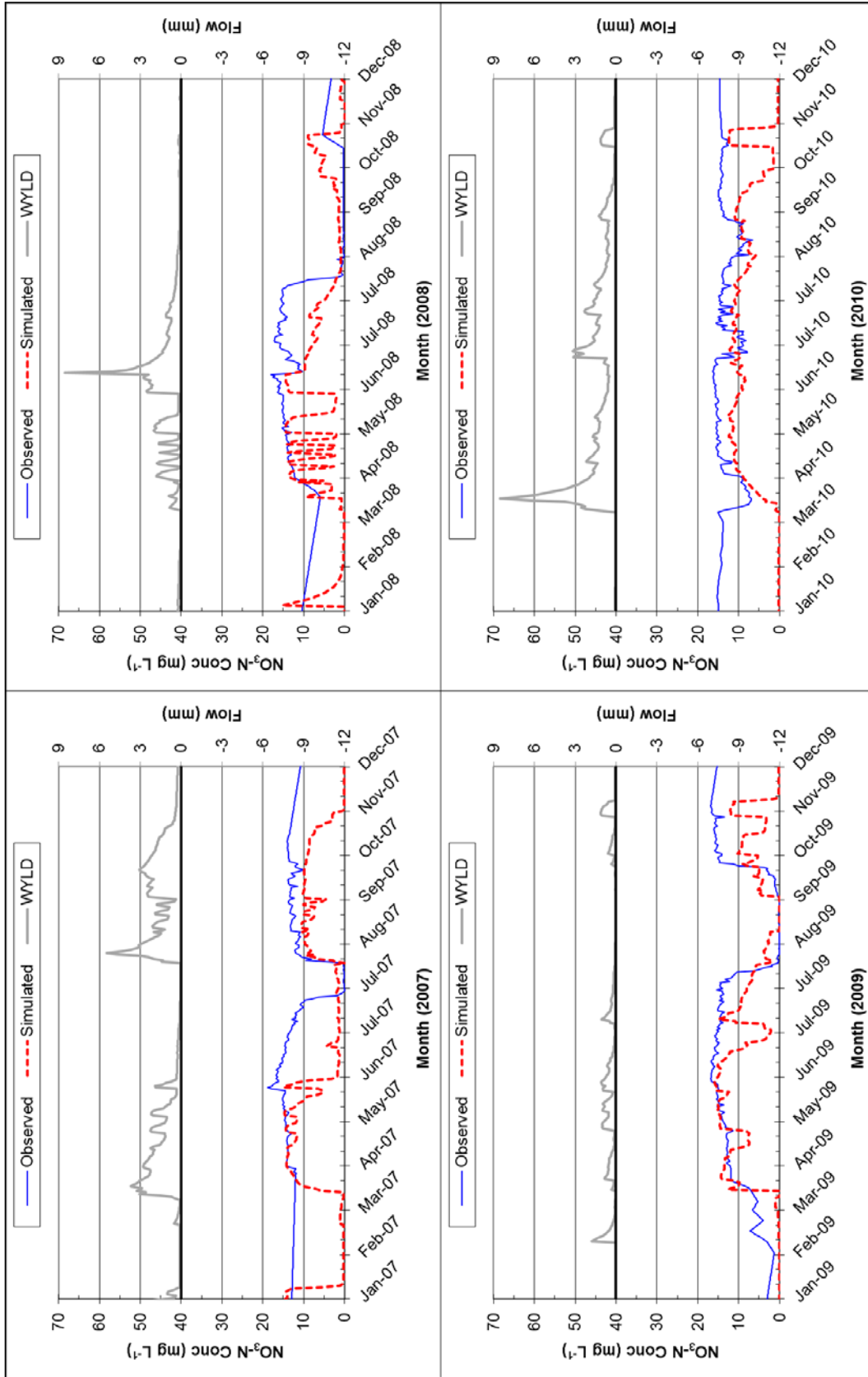


Figure 3.13 Re-calibrated daily time series $\text{NO}_3\text{-N}$ concentration for the AL watershed using modified algorithms. Blue line is observed, red dashed line is simulated, with simulated WYLD shown in gray.

Table 3.11 Performance statistics for modified daily NO₃-N concentration re-calibration.

Watershed	Daily Concentration		Daily Load		Monthly Load	
	NSE ^[a]	PBIAS ^[b]	NSE ^[a]	PBIAS ^[b]	NSE ^[a]	PBIAS ^[b]
KS	0.20 [NS]	8.9 [VG]	0.41 [S]	2.5 [VG]	0.72 [VG]	17.3 [G]
AL	-1.12 [NS]	48.1 [NS]	0.45 [S]	34.8 [NS]	0.60 [G]	34.8 [NS]

^[a] Nash-Sutcliffe efficiency.

^[b] Percent bias (negative indicates over-estimation)

^[a,b] VG=very good, G=good, S=satisfactory, NS=not satisfactory (Moriassi et al., 2015a)

Soil-NO₃ levels resulting from the re-calibrated, modified algorithms were evaluated in similar fashion to the previous simulations. Simulated soil-NO₃ was more representative of Central Iowa soil data (Cambardella et al., 1999), and NO₃ levels were not fully depleted during summer months in either the KS model (Figure 3.14) or the AL model (Figure 3.15). Simulations using the calibrated, modified algorithms eliminated denitrification in these HRUs, which is not realistic and resulted in much higher NO₃-N losses via seepage and deep seepage (Table 3.12). While these modifications and subsequent calibration improved predictions of NO₃-N concentrations and loads compared with the original algorithms, the basis for the modifications is not well established and problems simulating fate and transport remain. Nevertheless, the modifications provide insight to the possible causes of error and may form the basis for needed improvements in the simulation of NO₃-N transport in tile-drained watersheds.

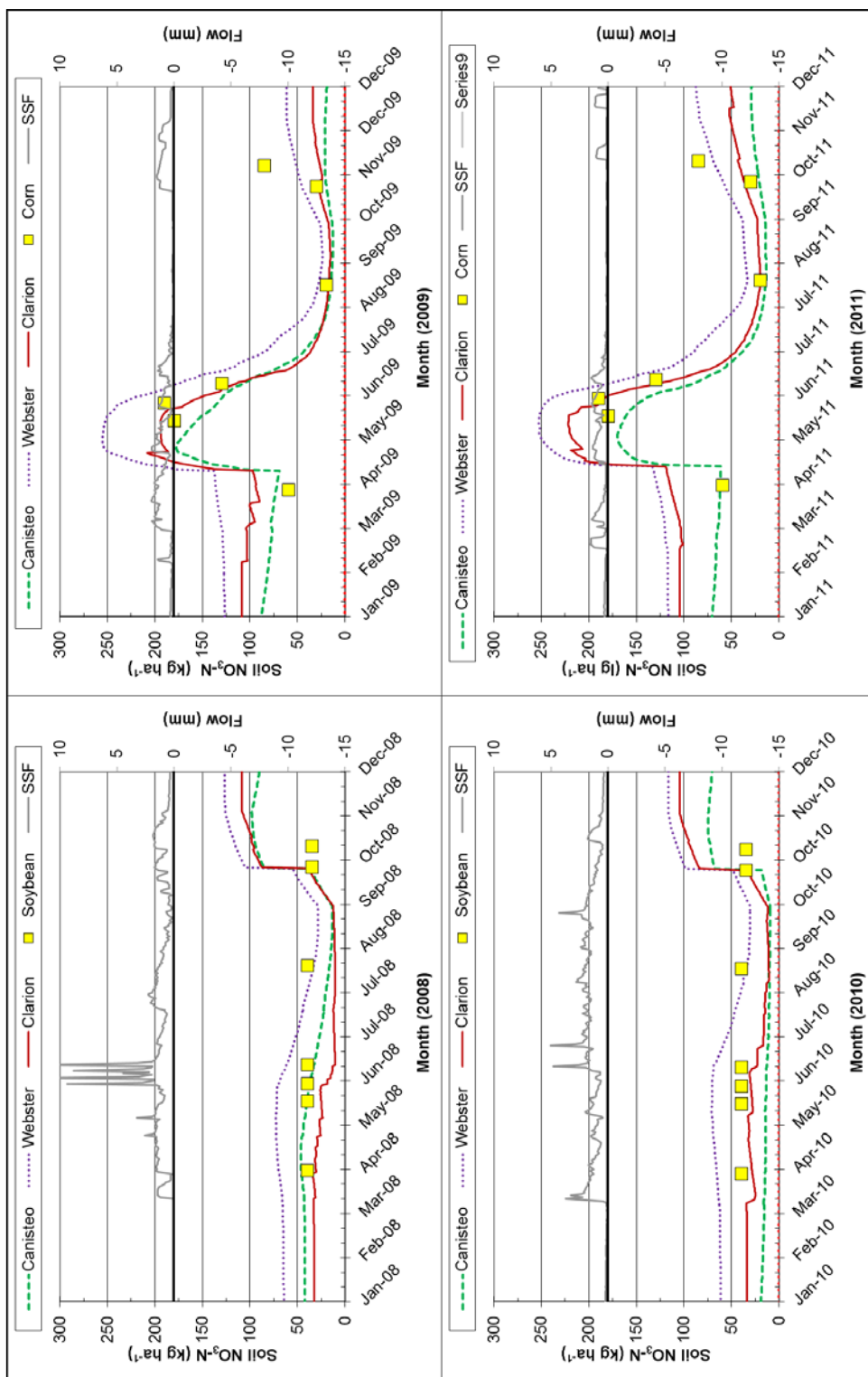


Figure 3.14 Simulated soil profile $\text{NO}_3\text{-N}$ for corn-soybean rotations in the KS watershed with modified soil- NO_3 algorithms after re-calibration. Dashed green line is soil- $\text{NO}_3\text{-N}$ for Canisteo soil, dotted purple line is for Webster, and solid brown is for Clarion. Simulated SSF is shown in gray on the top portion of each graph. Yellow squares are data measured in similar Central Iowa soils from Cambardella et al., (1999).

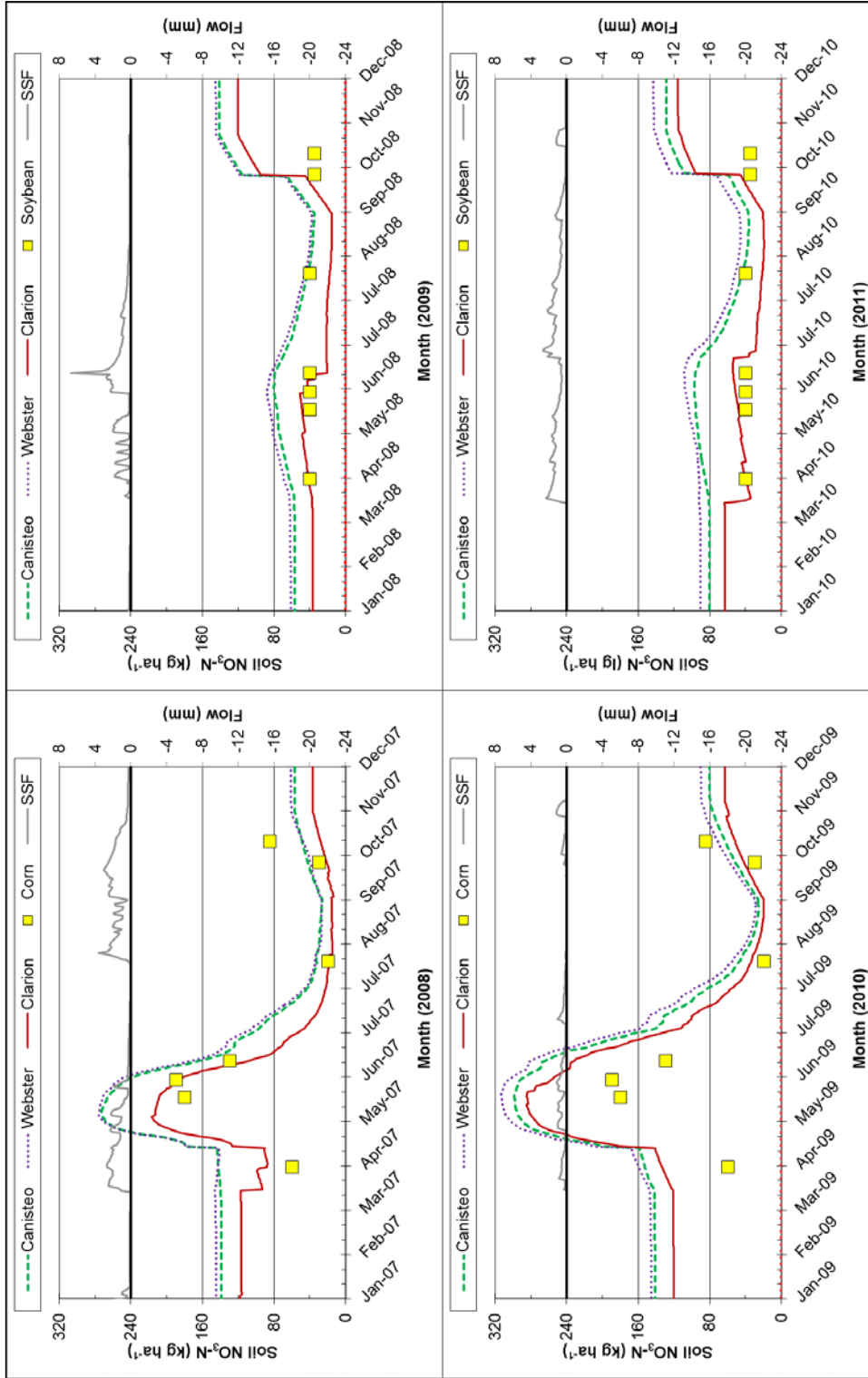


Figure 3.15 Simulated soil profile NO₃-N for corn-soybean rotations in the AL watershed using modified soil-NO₃ algorithms after re-calibration. Dashed green line is soil-NO₃-N for Canisteo soil, dotted purple line is for Webster, and solid brown is for Clarion. Simulated SSF is shown in gray on the top portion of each graph. Yellow squares are data measured in similar Central Iowa soils from Cambardella et al., (1999).

Table 3.12 Simulated soil-N dynamics for Webster and Clarion soil HRUs after re-calibration using modified soil NO₃-N algorithms.

	Soil/ Crop	^[a] Positive Fluxes (kg-N ha ⁻¹)				^[b] Negative Fluxes (kg-N ha ⁻¹)				
		Appl ^[c]	Atmos	Fix	Min	Denit	Uptake	Runoff	SSF	Seep
KS	Webster/									
2008	Soy	49	13	274	129	0	313	<1	67	0
2009	Corn	122	9	0	125	0	251	<1	43	0
2010	Soy	49	13	230	116	0	271	<1	60	0
2011	Corn	122	8	0	137	0	239	<1	29	0
	Clarion/									
2008	Soy	49	13	305	93	0	313	1	<1	53
2009	Corn	122	9	0	93	0	182	<1	<1	93
2010	Soy	49	13	259	89	0	271	1	<1	52
2011	Corn	122	8	0	104	0	194	<1	<1	70
AL	Webster/									
2007	Corn	135	10	0	132	0	277	<1	55	0
2008	Soy	49	8	291	142	0	338	<1	33	0
2009	Corn	135	8	0	165	0	321	<1	8	0
2010	Soy	49	9	224	143	0	301	<1	45	0
	Clarion/									
2007	Corn	135	10	0	101	0	220	<1	<1	83
2008	Soy	49	8	317	111	0	337	<1	<1	43
2009	Corn	135	8	0	138	0	278	<1	<1	30
2010	Soy	49	9	272	118	0	301	<1	<1	73

^[a] Inputs: Appl = fertilizer-N, Atmos = rainfall-N, Fix = N-fixation, Min = mineralization of organic-N

^[b] Outputs: Denit = denitrification, uptake = plant uptake, Runoff and SSF = N lost to surface water, Seep = N lost to deep aquifer via seepage.

^[c] Fertilizer application occurs in fall after soybean harvest and in spring in corn years.

3.5 Conclusions

Model calibration and evaluation revealed that it is possible to meet generally accepted performance criteria (Moriassi et al., 2015a) for simulation of monthly WYLD, SSF, and NO₃-N loads in both case study watersheds. For the KS and AL watersheds, NSE values were 0.79 and 0.71, respectively, for monthly WYLD; 0.55 and 0.66 for monthly SSF; and 0.72 and 0.60 for monthly NO₃-N load (using the modified NO₃-N lagging algorithms). However, calibration efforts were extensive and detailed monitoring data allowing such efforts are not typically available. Simulation of daily SURQ and SSF proved more challenging and were generally not satisfactory (NSE < 0.50) with the exception of daily SURQ in the KS watershed, for which NSE was 0.55 and PBIAS was -10.0%. Simulation of daily NO₃-N concentration was not satisfactory even after modifying NO₃-N algorithms to

lag flushing from the soil profile, with the KS watershed NSE of 0.20 and AL watershed NSE value of -1.12, indicating that simulation in the AL model was less accurate than simply using the daily average concentration.

Differences in hydrology and $\text{NO}_3\text{-N}$ transport between watersheds were not reflected by the model, as evidenced by distinct calibration parameters and parameter values. This suggests that parameterization may not transferable across watersheds with similar characteristics, and also that models calibrated at larger scales may not accurately reflect hydrology and nutrient transport at small watershed (e.g., drainage district) scales, as noted by Baffaut et al. (2015) in an overview of spatial and temporal considerations in watershed modeling. These limitations are especially important in cases where the model is intended to help locate, design, and/or estimate $\text{NO}_3\text{-N}$ removal capabilities of water quality BMPs.

Investigation of internal N dynamics and transport processes reveal that SWAT has the capability to estimate N fixation, N mineralization, plant uptake, and denitrification with some success. When calibrated to $\text{NO}_3\text{-N}$ concentration in flow, the model tracks soil- NO_3 levels reasonably well over time, but over-estimates depletion from the soil during summer months. Attempts to correct this depletion resulted in the complete elimination of denitrification in several HRUs in corn-soybean rotations, which is also not realistic.

Analysis of soil-N dynamics revealed that simulated mineralization and plant uptake rates are generally reasonable compared to literature values; however, these fluxes are highly variable in space and time and heavily influence $\text{NO}_3\text{-N}$ transport via tile drainage. Soil-N fluxes should therefore be evaluated and reported as standard practice when applying the SWAT model for simulation of $\text{NO}_3\text{-N}$ transport. This confirms recommendations by Arnold et al. (2015) on the incorporation of “soft” data into model calibration and suggestions by Saraswat

et al. (2015) for proper watershed model documentation and reporting. Better parameterization methods and supporting data for model inputs related to these processes are needed, and if possible, related inputs and soil-N fluxes should be constrained within reasonable ranges. Interdisciplinary studies involving agronomists and soil scientists would be helpful for model development and application, as improvements to soil-N algorithms may be needed to improve NO₃-N simulation.

3.6 Acknowledgements

This study was made possible through funding by EPA's Initiative Enhancing State and Tribal Wetland Programs grant program (Grant Agreement Number CD-97723301-0). Flow and water quality monitoring data used for model testing and evaluation were collected as part of the Iowa CREP program, a state, federal, local, and private partnership that helps establish and monitor wetlands for water quality improvement in the tile-drained regions of Iowa. Data compilation and dissemination by Greg Stenback in the Department of Ecology, Evolution, and Organismal Biology (EEOB) at Iowa State University, is greatly appreciated. SWAT model FORTRAN code modification and testing was conducted in collaboration with Jeff Arnold and Nancy Sammons in the Grassland, Soil, and Water Research Laboratory of USDA-ARS in Temple, Texas.

3.7 References

- Abbaspour, K. C. 2011. Swat-Cup2: SWAT Calibration and Uncertainty Programs Manual Version 2. Department of Systems Analysis, Integrated Assessment and Modeling (SIAM). Eawag. Swiss Federal Institute of Aquatic Science and Technology. Duebendorf, Switzerland. 106 p.
- Ale, S., L. C. Bowling, P. R. Owens, S. M. Brouder, and J. R. Frankenberger. 2012. Development and application of a distributed modeling approach to assess the watershed-scale impact of drainage water management. *Agricultural Water Management*. 107: 23-33.

- Alexander, R. B., R. A. Smith, G. E. Schwarz, E. W. Boyer, J. V. Nolan, and J. W. Brakebill. 2008. Differences in phosphorus and nitrogen delivery to the gulf of Mexico from the Mississippi river basin. *Environmental Science & Technology*. 42 (3): 822-830.
- Arnold, J. G., D. N. Moriasi, P. W. Gassman, K. C. Abbaspour, M. J. White, R. Srinivasan, C. Santhi, R. D. Harmel, A. van Griensven, M. W. Van Liew, N. Kannan, and M. K. Jha. 2012. SWAT: Model use, calibration, and validation. *Trans. of the ASABE*. 55(4): 1491-1508.
- Arnold, J. G., M. A. Youssef, H. Yen, M. J. White, A. Y. Sheshukov, A. M. Sadeghi, D. N. Moriasi, J. L. Steiner, D. M. Amatya, R. W. Skaggs, E.B. Haney, J. Jeong, M. Arabi, P. H. Gowda. 2015. Hydrological processes and model representation: Impact of soft data on calibration. *Trans. ASABE*. 58(6):1637-1660. doi:10.13013/trans.58.10726.
- Babcock, B. A., P. W. Gassman, M. Jha, and C. L. King. 2007. Adoption subsidies and environmental impacts of alternative energy crops. Briefing paper 07-BP 50. Center for Agricultural and Rural Development. Iowa State University. Ames, Iowa.
- Baffaut, C., S. M. Dabney, M. D. Smolen, M. A. Youssef, J. V. Bonta, M. L. Chu, J. A. Guzman, V. S. Shedekar, M. K. Jha, and J. G. Arnold. 2015. Hydrologic and water quality modeling: Spatial and temporal considerations. *Trans. ASABE*. 58(6):1661-1680.
- Baskaran, L., H. I. Jager, P. E. Schweizer, and R. Srinivasan. Progress toward evaluating the sustainability of switchgrass as a bioenergy crop using the SWAT model. *Trans. ASABE*. 53(5):1547-1556.
- Betrie, G. D., Y. A. Mohamed, A. van Griensven, and R. Srinivasan. 2011. Sediment management modelling in the Blue Nile Basin using SWAT model. *Hydrol. Earth Syst. Sci.* 15:807-818. Doi:10.5194/hess-15-807-2011.
- Borah, D. K., Yagow, G. Saleh, A., Barnes, P. L., Rosenthal, W., Krug, E. C., & Hauck, L. M. (2006). Sediment and nutrient modeling for TMDL development and implementation. *Trans ASABE*, 49(4):967-986.
- Bracmort, K. S., M. Arabi, J. R. Frankenberger, B. A. Engel, and J. G. Arnold. 2006. Modeling long-term water quality impact of structural BMPs. *Transactions of the Asabe*. 49 (2): 367-374.
- Cambardella, C. A., T. B. Moorman, D. B. Jaynes, J. L. Hatfield, T. B. Parkin, W. W. Simpkins, and D. L. Karlen. 1999. Water quality in Walnut Creek watershed: Nitrate-nitrogen in soils, subsurface drainage water, and shallow groundwater. *J. Environ. Qual.* 28:25-34.
- Chaubey, I., L. Chiang, M. Gitau, and S. Mohamed. 2010. Effectiveness of BMPs in improving water quality in a pasture dominated watershed. *J. Soil Water Conserv.* 65(6):424-437. Doi:10.2489/jswc.65.6.424.
- Christianson, L. M. Castellano, and M. Helmers. 2012. Nitrogen and phosphorus balances in Iowa cropping systems: Sustaining Iowa's soil resource. Iowa State University in collaboration with the Iowa Department of Agriculture and Land Stewardship.
- Coelho, B. B., R. Murray, D. Lapen, E. Topp, and A. Bruin. 2012. Phosphorus and sediment loading to surface waters from liquid swine manure application under different drainage and tillage practices. *Agricultural Water Management*. 104: 51-61.
- Crumpton, W. G., Stenback, G. A., Miller, B. A., and Helmers, M. J. (2006). Potential benefits of wetland filters for tile drainage systems: impact on nitrate loads to

- Mississippi River subbasins. Ames, Iowa. Final report to the U.S. Department of Agriculture (USDA).
- David, M. B., S. J. Del Grosso, X. Hu, E. P. Marshall, G.F. McIsaac, W. J. Parton, C. Tonitto, and M. A. Youssef. 2009. Modeling denitrification in a tile-drained, corn and soybean agroecosystem of Illinois, USA. *Biogeochemistry*. 93:7-30. Doi 10.1007/s10533-008-9273-9.
- David, M.B., L.E. Drinkwater, and G.F. McIsaac. 2010. Sources of nitrate yield in the Mississippi River basin. *J. Environ. Qual.* 39:1657–1667. doi:10.2134/jeq2010.0115
- Dinnes, D.L., D.L. Karlen, D.B. Jaynes, T.C. Kaspar, J.L. Hatfi, T.S. Colvin, and C.A. Cambardella. 2002. Nitrogen management strategies to reduce nitrate leaching in tile-drained midwestern soils. *Agron. J.* 94:153–171. doi:10.2134/agronj2002.0153
- Douglas-Mankin, K. R., Srinivasan, R., & Arnold, J. G. (2010). Soil and water assessment tool (SWAT) model: current developments and applications. *Trans. ASABE.*, 53(5): 1423-1431.
- Du, B., J. G. Arnold, A. Saleh, and D. B. Jaynes. 2005. Development and application of SWAT to landscapes with tiles and potholes. *Transactions of the ASAE*. 48 (3): 1121-1133.
- El-Sadek, A., J. Feyen, and J. Berlamont. 2001. Comparison of models for computing drainage discharge. *Journal of Irrigation and Drainage Engineering-Asce*. 127 (6): 363-369.
- El-Sadek, A., J. Feyen, W. Skaggs, and J. Berlamont. 2002. Economics of nitrate losses from drained agricultural land. *Journal of Environmental Engineering-Asce*. 128 (4): 376-383.
- Fernandez, G. P., G. M. Chescheir, R. W. Skaggs, and D. M. Amatya. 2005. Development and testing of watershed-scale models for poorly drained soils. *Trans. ASABE*. 48(2):639-652).
- Gassman, P. W., M. R. Reyes, C. H. Green, and J. G. Arnold. 2007. The soil and water assessment tool: Historical development, applications, and future research directions. *Transactions of the ASABE*. 50 (4): 1211-1250.
- Gassman, P.W., M. Jha, and S. Mickelson. 2009. Application of the SWAT2005 Alternative Runoff Curve Number Method for the Boone River Watershed in North Central Iowa, United States. Presented at the Soil and Water Assessment Tool-Southeast Asia (SWAT-SEA) Conference, January 7-8, Chiang Mai, Thailand.
- Goolsby, D.A., W.A. Battaglin, B.T. Aulenbach, and R.P. Hooper. 2000. Nitrogen flux and sources in the Mississippi River basin. *Sci. Total Environ.* 248:75–86. doi:10.1016/S0048-9697(99)00532-X
- Goswami, D., P.K. Kalita, R.A. Cooke, and M.C. Hirschi. 2008. Estimation and analysis of baseflow in drainage channels in two tile-drained watersheds in Illinois. *Trans. ASABE* 51(4):1201–1213. doi:10.13031/2013.25238
- Green, C. H., M. D. Tomer, M. Di Luzio, and J. G. Arnold. 2006. Hydrologic evaluation of the soil and water assessment tool for a large tile-drained watershed in Iowa. *Trans. ASABE* 49(2):413-422.
- Hatfield, J.L., J.H. Prueger, and D.B. Jaynes. 1998. Environmental impacts of agricultural drainage in the Midwest. In: *Drainage in the 21st century: Food production and the environment*. Proceedings of the 7th Annual Drainage Symposium, Orlando, FL. 8–10 Mar. 1998. ASAE, St. Joseph, MI.

- Ikenberry, C. D., M. L. Soupir, K. E. Schilling, C. S. Jones, and A. Seeman. 2014. Nitrate-nitrogen exports: Magnitude and patterns from drainage districts to downstream river basins. *J. Environ. Qual.* 43:204-2033. doi:10.2134/jeq2014.05.0242.
- Iowa State University. 2006. Concepts and Rationale for Regional Nitrogen Rate Guidelines for Corn. PM2015.
- Iowa State University. 2013. Iowa nutrient reduction strategy. <http://www.nutrientstrategy.iastate.edu> (accessed 20 Feb. 2014).
- Iowa State University. 2014. Iowa Environmental Mesonet. <http://mesonet.agron.iastate.edu/> (accessed March 2014).
- Iowa State University. 2015. Ag Decision Maker. File A1-12. March 2015. www.extension.iastate.edu/agdm. Accessed 3 Feb. 2016).
- Jaber, F. H., and S. Shukla. 2012. MIKE-SHE: Model use, calibration, and validation. *Trans. ASABE.* 55(4): 1479-1489.
- Jaynes, D. B., T. S. Colvin, D. L. Karlen, C. A. Cambardella, and D. W. Meek. 2001. Nitrate loss in subsurface drainage as affected by nitrogen fertilizer rate. *J. Environ. Qual.* 30:1305-1314.
- Jha, M. K., C. F. Wolter, K. E. Schilling, and P. W. Gassman. 2010. Assessment of Total Maximum Daily Load implementation strategies for nitrate impairment of the Raccoon River, Iowa. *J. Envir. Qual.* 39:1317-1327. doi:10.2134/jeq2009.0392.
- Kladivko, E. J., J. R. Frankenberger, D. B. Jaynes, D. W. Meek, B. J. Jenkinson, and N. R. Fausey. 2004. Nitrate leaching to subsurface drains as affected by drain spacing and changes in crop production system. *Journal of Environmental Quality.* 33(5): 1803-1813.
- Lemke, A. M., K. G. Kirkham, T. T. Lindenbaum, M. E. Herbert, T. H. Tear, W. L. Perry, and J. R. Herkert. 2011. Evaluating Agricultural Best Management Practices in Tile-Drained Subwatersheds of the Mackinaw River, Illinois. *J. Environ. Qual.* 40(4):1215-1228.
- Malone, R. W., G. Yagow, C. Baffaut, M. W. Gitau, Z. Qi, D. M. Amatya, P. B. Parajuli, J. V. Bonta, and T. R. Green. 2015. Parameterization guidelines and considerations for hydrologic models. *Trans. ASABE.* 58(6):1681-1703. doi:10.13031/trans.58.10709.
- Migliaccio, K. W. and P. Srivastav. 2007. Hydrologic components of watershed-scale models. *Trans. ASABE.* 50(5):1695-1703.
- Moriasi, D. N., C. G. Rossi, J. G. Arnold, and M. D. Tomer. 2012. Evaluating hydrology of the Soil and Water Assessment Tool (SWAT) with new tile drain equations. *Jour. Of Soil and Water Cons.* 67(6):513-524.
- Moriasi, D. N., P. H. Gowda, J. G. Arnold, D. J. Mulla, S. Ale, J. L. Steiner, and M. D. Tomer. 2013. Evaluation of the Hooghoudt and Kirkham tile drain equations in the Soil and Water Assessment Tool to simulate tile flow and nitrate-nitrogen. *J. Environ. Qual.* 42:1699-1710
- Moriasi, D. N., M. W. Gitau, N. Pai, and P. Daggupati. 2015a. Hydrologic and water quality models: Performance measures and evaluation criteria. *Trans. of the ASABE* 58(6):1763-1785.
- Moriasi, D. N., R. W. Zeckowski, J. G. Arnold, C. B. Baffaut, R. W. Malone, P. Daggupati, J. A. Guzman, D. Saraswat, Y. Yuan, B. W. Wilson, A. Shirmohammadi, and K. R. Douglas-Mankin. 2015b. Hydrologic and water quality models: Key calibration and validation topics. *Trans. of the ASABE* 58(6): 1609-1618

- Qi, Z., L. Ma, M. J. Helmers, L. R. Ahuja, & R. W. Malone. 2012. Simulating nitrate-nitrogen concentration from a subsurface drainage system in response to nitrogen application rates using RZWQM2. *J. Environ. Qual.* 41:289-295. doi:10.2134/jeq2011.0195
- Rabotyagov, S., T. Campbell, M. Jha, P. W. Gassman, J. Arnold, L. Kurkalova, S. Secchi, H. Feng, and C. L. Kling. 2010. Least-cost control of agricultural nutrient contributions to the Gulf of Mexico hypoxic zone. *Ecological Applications.* 29(6):1542-1555.
- Records, R. M. M. Arabi, S. R. Fassnacht, W. G. Duffy, M. Ahmadi, and K. C. Hegewisch. 2014. Climate change and wetland loss impacts on a western river's water quality. *Hydrol. Earth Syst. Sci.* 18:4509-4527. doi:10.5194/hess-18-4509-2014
- Rozemeijer, J. C., Y. van der Velde, F. C. van Geer, M. F. P. Bierkens, and H. P. Broers. 2010. Direct measurements of the tile drain and groundwater flow route contributions to surface water contamination: From field-scale concentration patterns in groundwater to catchment-scale surface water quality. *Environmental Pollution.* 158 (12):3571-3579.
- Saraswat, D. J. R. Frankenberg, N. Pai, S. Ale, P. Daggupati, K. R. Douglas-Mankin, and M. A. Youssef. 2015. Hydrologic and water quality models: Documentation and reporting procedures for calibration, validation, and use. *Trans. ASABE.* 58(6):1787-1797. doi:10.13031/trans.57.10707.
- Schilling, K. E., and M. Helmers. 2008a. Effects of subsurface drainage tiles on streamflow in Iowa agricultural watersheds: Exploratory hydrograph analysis. *Hydrological Processes.* 22(23):4497-4506.
- Schilling, K. E., and M. Helmers. 2008b. Tile drainage as karst: Conduit flow and diffuse flow in a tile-drained watershed. *Journ. of Hydrol.* 349:291-301. doi:10.1016/j.jhdrol.2007.11.014.
- Schuol, J., K. C. Abbaspour, H. Yang, R. Srinivasan, and A. J. B. Zehnder. 2008. Modeling blue and green water availability in Africa. *Water Resources Research.* 44:1-18. Doi:10.1029/2007WR006609.
- Singh, R., M. J. Helmers, W. G. Crumpton, and D. W. Lemke. 2007. Predicting effects of drainage water management in Iowa's subsurface drained landscapes. *Agr. Water Management.* 92:162-170. Doi:10.1016/j.agwat.2007.06.012.
- Skaggs, R. W. 1980. A WATER MANAGEMENT MODEL FOR ARTIFICIALLY DRAINED SOILS. North Carolina Agricultural Research Service Technical Bulletin. (267): 1-54.
- Stenback, G. A., W. G. Crumpton, K. E. Schilling, and M. J. Helmers. 2011. Rating curve estimation of nutrient loads in Iowa rivers. *J. Hydrol.* 396(1-2):158-169.
- Stone, M. C., R. H. Hotchkiss, C. M. Hubbard, T. A. Fontaine, L. O. Mearns, and J. G. Arnold. 2001. Impacts of climate change on Missouri River basin water yield. *J. AWRA.* 37(5):1119-1129.
- Sui, Y., and J. R. Frankenberger. 2008. Nitrate loss from subsurface drains in an agricultural watershed using SWAT2005. *Trans. of the ASABE.* 51(4):1263-1272.
- Thorp, K.R., R.W. Malone, and D.B. Jaynes. 2007. Simulating long-term effects of nitrogen fertilizer application rates on corn yield and nitrogen dynamics. *Trans. ASABE* 50(4):1287-1303. doi:10.13031/2013.23640

- Thorpe, K. W., D. B. Jaynes, and R. W. Malone. 2008. Simulating long-term performance of drainage water management across the Midwestern United States. *Trans. ASABE* 51(3):961-976.
- Thorp, K. R., M. A. Youssef, D. B. Jaynes, R. W. Malone, and L. Ma. 2009. DRAINMOD-N II: Evaluated for an agricultural system in Iowa and compared to RZWQM-DSSAT. *Trans. of the ASABE*. 52(5):1557-1573.
- Van Liew, M.W. T. L. Veith, D. D. Bosch, and J. G. Arnold. 2007. Suitability of SWAT for the conservation effects assessment project: Comparison on USDA agricultural research service watersheds. *Journ. of Hydrol. Eng.* 12(2)173-189.
doi:10.1061/(ASCE)1084-0699(2007)12:2(173).
- Wang, X., C. T. Mosley, J. R. Frankenberger, and E. J. Kladivko. 2006. Subsurface drain flow and crop yield predictions for different drain spacings using DRAINMOD. *Agricultural Water Management*. 79(2):113-136.
- Yen, H., R. T. Baily, M. Arabi, M. Ahmadi, M. J. White, and J. G. Arnold. 2014. The role of interior watershed processes in improving parameter estimation and performance of watershed models. *Jour. Environ. Qual.* 43(5):1601-1613.
<http://dx.doi.org/10.2134/jeq2013.03.0110>.
- Youssef, M. A., R. W. Skaggs, G. M. Chescheir, and J. W. Gilliam. 2006. Field evaluation of a model for predicting nitrogen losses from drained lands. *Journal of Environmental Quality*. 35(6):2026-2042.

CHAPTER 4. MODIFICATION OF SWAT TO IMPROVE SIMULATION OF NITRATE-NITROGEN REMOVAL WETLANDS

4.1 Abstract

Implementation of subsurface tile drainage infrastructure for cultivation of row crops in poorly-drained areas has resulted in loss of wetland ecosystems and increased transport of nitrate-nitrogen ($\text{NO}_3\text{-N}$) to surface water. The ability to accurately simulate flow and nutrient removal in treatment wetlands within an agricultural watershed model is needed to develop effective plans for meeting nutrient reduction goals associated with protection of drinking water supplies and reduction of the Gulf of Mexico hypoxic zone. The objectives of this study were to modify existing algorithms in the Soil and Water Assessment Tool (SWAT) by adapting proven CREP wetland models, compare model performance using both original SWAT algorithms and modified wetland equations to simulate two Iowa CREP wetlands, and evaluate the ramifications of watershed and tile drain simulation errors on prediction of $\text{NO}_3\text{-N}$ in Iowa CREP wetlands.

The modified equations improved simulation of hydrology and $\text{NO}_3\text{-N}$ in the wetlands, with Nash-Sutcliffe efficiency (NSE) values of 0.88 to 0.99 for daily load predictions, and percent bias (PBIAS) values generally less than 6%. The $\text{NO}_3\text{-N}$ removal rate (NSETLR) is the critical input parameter for $\text{NO}_3\text{-N}$ reduction and strongly influences model performance. The applicability of the modified equations to wetlands without detailed monitoring data was improved over the original SWAT equations due to more objectively-informed parameterization, reduced need for hydrologic calibration, and incorporation of an irreducible nutrient concentration and temperature correction factor. Model improvements

enhance the utility of SWAT for simulating flow and nutrients in wetlands and other impoundments.

Simulation of $\text{NO}_3\text{-N}$ in the KS watershed CREP wetland revealed the impacts of errors in watershed/tile simulation on wetland simulations. While isolating the wetland from the watershed resulted in an NSE of 0.98 and PBIAS of 2.6% for $\text{NO}_3\text{-N}$ load at the wetland outlet, integrating the wetland and watershed simulations decreased the NSE to 0.30 and PBIAS increased to 53.3%, indicating that simulation of wetlands is limited by the ability of the model to reflect short-term fluctuations in $\text{NO}_3\text{-N}$ concentration.

Keywords: wetlands, tile drainage, nitrate transport, hypoxia, SWAT

4.2 Introduction

Alteration of the landscape of the Upper Midwest of the United States has enabled the region to become one of the most agriculturally productive areas in the world (Skaggs et al., 1992; Urban, 2005). This alteration was greatly facilitated by the formation of agricultural drainage districts, which provided the organization and financing necessary to drain wetlands and poorly-drained soils across multiple tracts of land (McCorvie and Lant, 1993). Unfortunately, the benefits of artificial subsurface drainage are accompanied by some unintended and undesirable ecological and environmental consequences. A primary ecological impact of tile drainage on the regional scale has been significant loss of prairie wetlands and associated wildlife habitat in the Corn Belt. Iowa has lost at least 95% of its swamp and wetland areas (Bishop et al., 1982; Miller et al., 2009), with similar losses in Illinois, Indiana, and Ohio (McCorvie and Lant, 1993). Prior to artificial drainage, wetlands comprised nearly half of the land area of the Des Moines Lobes ecoregion (Miller et al., 2009). From a water quality perspective, the direct link between subsurface tile drainage and

increased transport of nitrate-nitrogen ($\text{NO}_3\text{-N}$) to surface waters is a primary concern, both for drinking water supplies and the hypoxic zone in the Gulf of Mexico (Dinnes, 2002; Alexander et al., 2008). Loss of wetlands compounds water quality concerns related to tile drainage, because wetland ecosystems provide removal of nutrients, particularly $\text{NO}_3\text{-N}$, from surface water.

The environmental benefits of wetlands have long-been widely recognized, and the re-establishment of these ecosystems in the landscape has been practiced for decades. The concept of designing and locating wetlands for water quality improvement gained momentum in the 1990s, with efforts to develop guidelines and document the feasibility of constructing wetlands for treatment of stormwater, municipal wastewater, (WPCF, 1990) and agricultural nonpoint source pollution (van der Valk and Jolly, 1992). Kadlec and Knight (1996) compiled results from an already wide body of research to document performance and design guidelines for treatment wetlands. Because of their high capacity for $\text{NO}_3\text{-N}$ removal via denitrification (Ingersoll and Baker, 1998; Xue et al, 1999; Lin et al., 2002), high $\text{NO}_3\text{-N}$ concentrations observed in agricultural subsurface drainage, and aforementioned concerns regarding drinking water supplies and Gulf of Mexico hypoxia, the use of wetlands for treating tile drainage water gained traction (Kovacac et al., 2000; Dinnes et al., 2002).

Crumpton (2001) demonstrated the importance of strategically locating wetlands to maximize interception of tile drainage, thereby increasing $\text{NO}_3\text{-N}$ removal at watershed scales. This concept is foundational to the construction/restoration of wetlands for treating tile drainage as part of the Iowa Conservation Reserve Enhancement Program (CREP). Because the CREP program targets wetland restoration for water quality improvement (particularly $\text{NO}_3\text{-N}$ removal) in tile-drained landscapes, there are several performance-based

eligibility requirements. Potential wetlands must (1) be located below a tile drainage system with an area of at least 200 ha (500 ac), (2) have a wetland pool area that is between 0.5% and 2.0% of the contributing drainage area, (3) have 75% of the pool area be less than 0.9 m (3 ft) deep, and (4) be designed to maintain the drainage rights of landowners in the contributing drainage area (Crumpton et al, 2006). The program includes funding for measuring the performance of CREP wetlands, which is assessed using flow and NO₃-N data collected at the inlet and outlet of a subset of wetlands each year.

The removal of NO₃-N in wetlands is variable and dependent on many factors (Phipps and Crumpton, 1994), such as hydraulic loading rate (HLR), residence time, NO₃-N loading rates, NO₃-N concentration, water temperature, wetland shape (i.e., hydraulic efficiency), carbon concentrations (Ingersoll and Baker, 1998), and extent and density of vegetation (Lin et al., 2002). Percent removal of NO₃-N in CREP wetlands can be predicted using the annual HLR, with mass removal predictions requiring the incorporation of annual flow-weighted average (FWA) NO₃-N concentration (Crumpton et al., 2006; Tomer et al., 2013):

$$\%NR = 103 \times AHL^{-0.33} \quad (1)$$

$$MNR = 10.3 \times AHL^{0.67} \times FWA \quad (2)$$

where

%NR = percent NO₃-N removal (%)

AHL = annual hydraulic loading rate (m yr⁻¹)

MNR = mass removal rate (kg-N ha⁻¹ yr⁻¹)

FWA = flow-weighted average NO₃-N concentration (mg L⁻¹).

These models have been used to estimate average annual removal potential of NO₃-N by wetlands at various scales, from relatively small watersheds (Tomer et al., 2013), potential CREP sites in the Des Moines Lobe ecoregion (Crumpton et al., 2012), and across the Upper Mississippi and Ohio River basins (Crumpton et al., 2006).

Reduction of NO₃-N concentration in wetlands can be predicted at a daily interval using a temperature dependent, first-order process (Kadlec and Knight, 1996; Crumpton et al, 1998; Crumpton, 2001):

$$J = k_{20} \times C \times \theta^{(T-20)} \quad (3)$$

where

J = areal NO₃-N loss rate (g-N m⁻² day⁻¹)

k_{20} = rate coefficient for NO₃-N at 20°C (m day⁻¹)

C = NO₃-N concentration (g m⁻³ = mg L⁻¹)

θ = temperature coefficient

T = water temperature (°C)

This approach, in the context of a mass balance tanks-in-series model, parameterized with flow and NO₃-N concentrations entering a wetland, has been successfully used to simulate the short-term variability of nitrate reduction in Iowa CREP wetlands (Crumpton et al, 2006).

Although NO₃-N removal in wetlands treating tile drainage has been accurately modeled at watershed scales, there is a lack of tools capable of simulating wetlands in conjunction with other water quality improvement practices in tile-drained watersheds. Several common, public-domain watershed models are not currently capable of simulating both tile drainage and NO₃-N removal in wetlands. For example, the Annualized Agricultural Nonpoint Source Pollution Model (AnnAGNPS) contains algorithms for

subsurface tile drainage and for sediment removal in wetlands, but further enhancements are needed to simulate nutrient reductions obtained by wetlands in AnnAGNPS (Bingner and Theurer 2005; Yuan et al, 2011). Another widely-used model, the Hydrologic Simulation Program-Fortran (HSPF), lacks a mechanism for direct simulation of tile drainage (EPA, 1998; Singh et al, 2005) and crop growth (EPA, 1998). The Soil and Water Assessment Tool (SWAT) simulates a variety of agricultural activities and crop growth and also includes specific components for simulation of tile drainage and $\text{NO}_3\text{-N}$ removal in wetlands (Neitsch et al., 2011). While SWAT has been utilized to facilitate design of constructed riverine wetlands (Arnold et al., 2001) and to assess impacts of wetlands on water quality (Records et al., 2014; Kalcic et al., 2015), performance of wetland simulations in SWAT have not been tested and reported against wetland monitoring data.

The ability to reliably simulate tile drainage treatment wetlands integrated with other water quality improvement strategies in an agricultural watershed model would be valuable for watershed planning to meet nutrient reduction goals associated with protection of drinking water supplies and reduction of the Gulf of Mexico hypoxic zone. Thus, the objectives of this study are to (i) modify existing algorithms in SWAT by adapting proven CREP wetland models, (ii) compare model performance using original SWAT algorithms and modified wetland equations to simulate two Iowa CREP wetlands, and (iii) evaluate the ramifications of errors in watershed and tile drain simulation on prediction of $\text{NO}_3\text{-N}$ in Iowa CREP wetlands. Updates to the SWAT algorithms resulting from this work are incorporated into the public domain model maintained and disseminated by USDA-ARS and Texas A&M University.

4.3 Materials and Methods

4.3.1 *The SWAT model*

The SWAT model is a continuous, daily time step model used to simulate hydrology, crop growth, erosion, and pollutant transport in agricultural watersheds (Borah, 2006). SWAT was selected for the simulation of CREP wetlands in this study because it is a public domain model, actively supported by USDA-ARS, and commonly used for simulation of hydrology and pollutant transport in agricultural landscapes around the world. Gassman et al. (2007) and Douglas-Mankin (2010) provided extensive reviews of the SWAT model, including discussions of its development, application history, and evolution. SWAT has been extensively applied in tile-drained watersheds, with varying results. Reliable application of SWAT in tile-drained landscapes is challenging, although progress has been made in recent attempts (Moriassi et al, 2012; Moriassi et al., 2013). SWAT is a semi-distributed model in the sense that it simulates unique combinations of land use, soil type, and slope – called hydrologic response units (HRUs) – that represent actual spatial locations in the landscape. These HRUs and corresponding .hru files form the foundation of a SWAT model, as they represent the landscape areas for which most of the hydrologic and agricultural processes are simulated. However, SWAT is a lumped model in the sense that simulated outputs from individual HRUs are aggregated at the subbasin level without regard to their connectivity to each other or position in the landscape (i.e., upland, lowland, etc.). Subbasin parameters are entered in into .sub files, and subbasin level outputs are then routed through a reach (stream) network, with each subbasin having its own reach and corresponding .rch file.

In addition to routing water and water quality constituents through streams, SWAT includes algorithms for simulating four other types of waterbodies: pothole depressions, ponds, wetlands, and reservoirs/impoundments (Neitsch et al., 2011). Although pothole depressions are major features of the landscape in the study area, they are not representative of CREP-style NO₃-N removal wetlands because they have very small drainage areas and do not intercept large volumes of subsurface flow. This is reflected in the SWAT model structure by the fact that input parameters for pothole depressions are located in the .hru files. Therefore, modification of pothole algorithms was not considered in this study.

Ponds and wetlands are simulated at the subbasin level in SWAT, and receive hydrologic and pollutant inputs from a user-specified fraction of the subbasin area. Simulation of ponds and wetlands within subbasins is nearly identical, with inputs for both included in the pond (.pnd) files. Depending on whether a pond or wetland is specified, differing outflow (i.e., discharge) calculation options are utilized (Neitsch et al, 2011). Reservoirs in SWAT are impoundments located along the reach network. They are placed at the outlet of the subbasin in which the impounded reach resides. Therefore, reservoirs receive inflows from the subbasin they are located in as well as all upstream subbasins/reaches.

In summary, the SWAT model structure can be summarized as a system of HRUs (.hru), aggregated at the subbasin (.sub) level, routed through a reach (.rch) network (Figure 4.1). Some portion of a subbasin may drain to a pond or wetland (.pnd). The modified wetland equations were incorporated into the reservoir (.res) module of the SWAT code to take advantage of the model structure and give users the most flexibility in locating treatment wetlands. This allows wetlands to be placed at the outlet of a subbasin, such as a drainage

district tile outlet, which is representative of the placement of NO₃-N removal CREP wetlands in tile-drained regions. Additionally, parameterization of wetlands in the .res file allows the option of intercepting water from multiple subbasins (e.g., drainage districts), which may be useful when trying to optimize NO₃-N removal potential during watershed planning. Another benefit of incorporating new algorithms into the reservoir code is that the improved outflow/discharge equations can be used in the simulation of non-wetland impoundments (e.g., lakes, reservoirs), giving this modification broader utility.

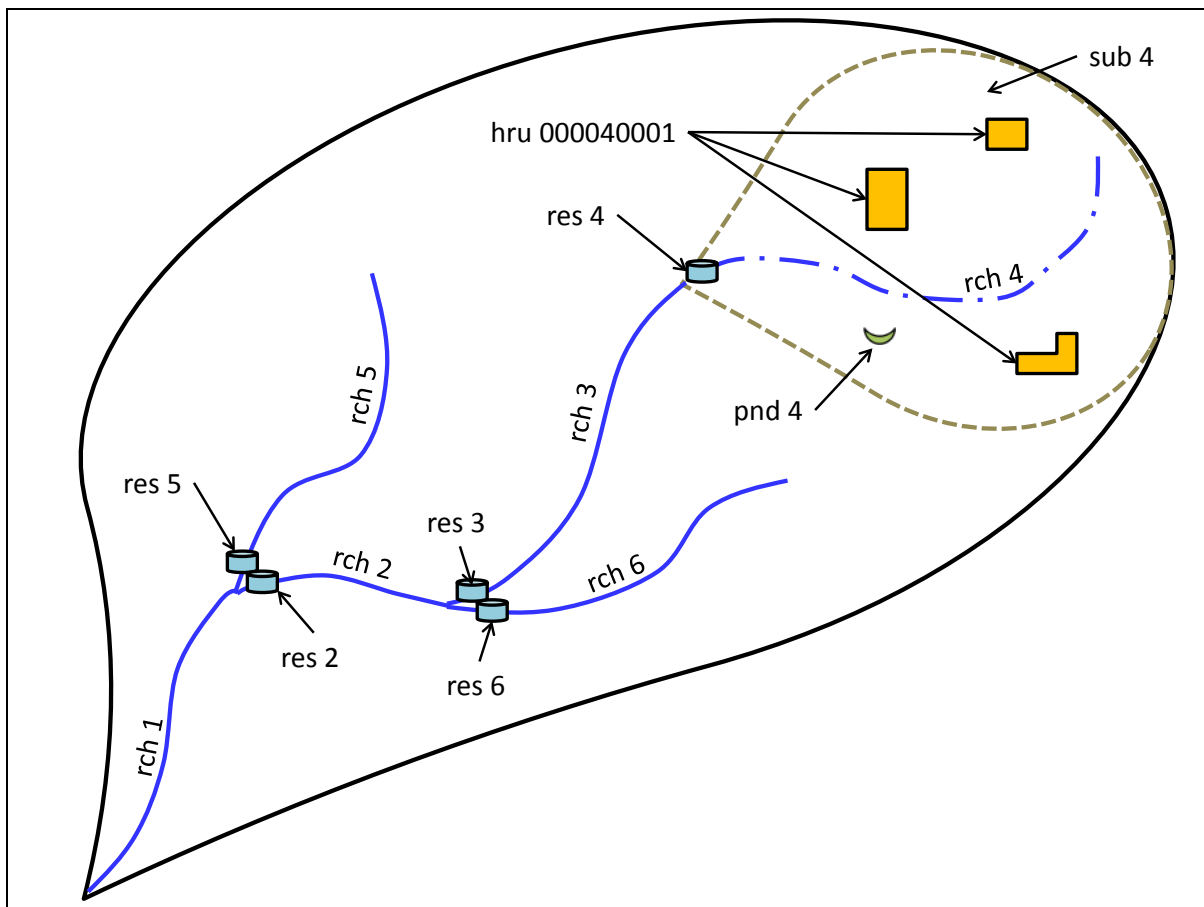


Figure 4.1 SWAT model structure illustrating relationship between subbasins (.sub), reaches (.rch), hydrologic response units (.hru), ponds/wetlands (.pnd) and reservoirs (.res).

4.3.2 *Case study wetlands*

The two wetlands simulated in this study were constructed as part of the Iowa CREP program, with a primary objective of reducing $\text{NO}_3\text{-N}$ exported from tile drainage to surface water in heavily row-cropped areas, particularly within the Des Moines Lobe ecoregion of north-central Iowa. The KS Wetland is located in Story County, Iowa, and receives drainage from a 309-ha watershed before discharging to the headwaters of a first-order tributary to Squaw Creek, a HUC-12 watershed in the Skunk River basin. The AL Wetland is located in Kossuth County and is approximately 120 km northwest of the KS Wetland site (Figure 4.2). The AL Wetland receives drainage from a 227-ha watershed and discharges to a first-order stream that enters Black Cat Creek, a HUC-12 watershed that discharges to the Des Moines River. Both wetlands meet the Iowa CREP criteria and are representative of other sites in the CREP program in terms of land use, drainage intensity, and configuration. One notable difference between sites is the larger wetland-to-drainage-area ratio of 1.1% for the AL wetland compared with only 0.5%, the minimum CREP requirement, for the KS Wetland. Watershed and wetland characteristics for both wetlands are reported in Table 4.1.

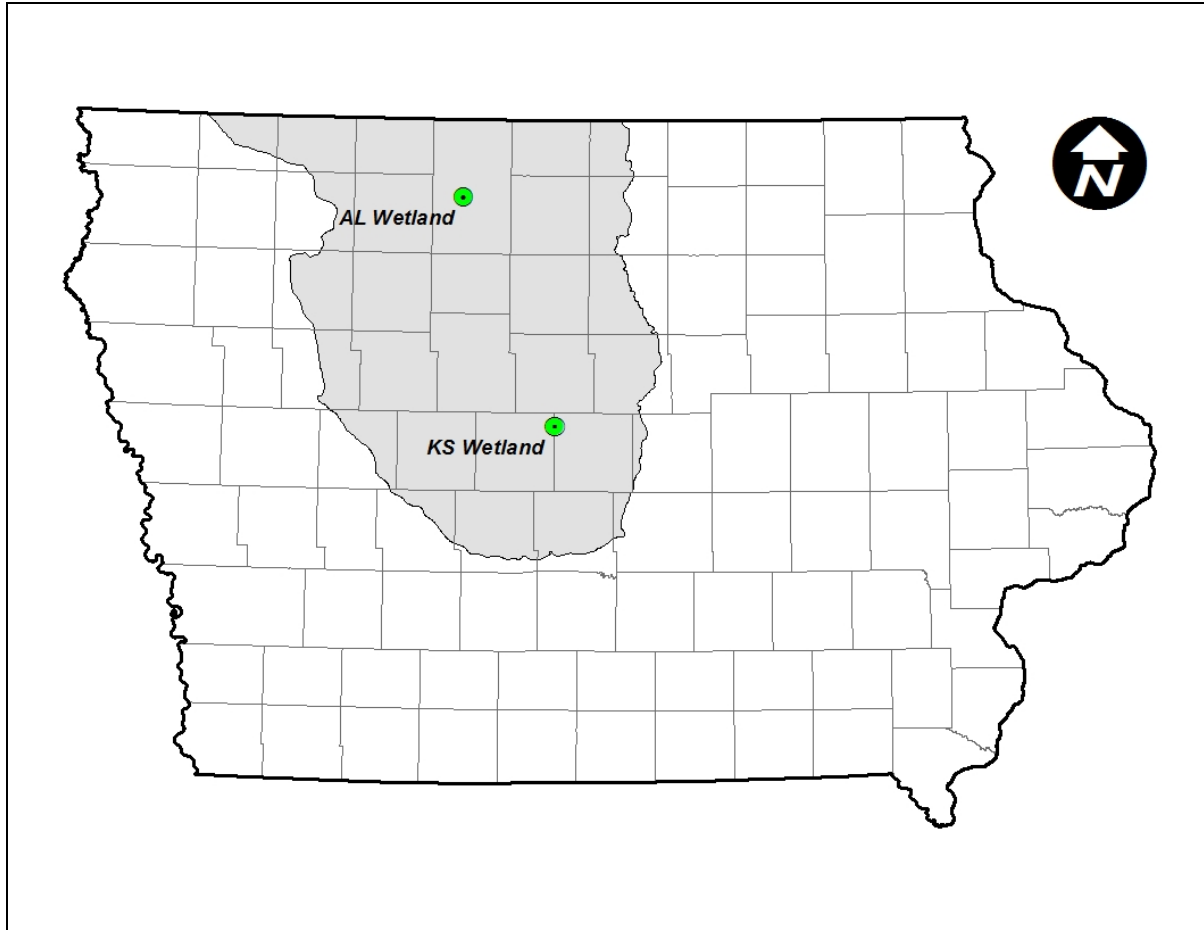


Figure 4.2 Location of case study CREP wetland sites. The shaded region is the Des Moines Lobe ecoregion.

Table 4.1 Watershed and wetland characteristics of case study sites.

Characteristic	KS Wetland	AL Wetland
Drainage area, DA (ha)	309	227
Row crop (% of DA)	93	80
Poor drainage (% of DA) ^[a]	62	77
Annual rainfall (mm) ^[b]	1,081	906
Annual water yield (mm) ^[c]	395	279
Normal pool area (ha)	1.45	2.45
Mean depth (m)	0.67	0.60
Wetland to DA ratio (%)	0.5	1.1

^[a] Row crop areas with slopes < 5% and soils classified as somewhat poor to poorly-drained.

^[b] Average annual rainfall during model simulation period (2008-2011 for KS Wetland, 2007-2010 for AL Wetland).

^[c] Average annual water yield during model simulation period (2008-2011 for KS Wetland, 2007-2010 for AL Wetland).

Inflow to both wetlands is predominantly subsurface (tile) flow, with surface runoff reaching the wetlands during storm events. Flows into and out of the wetlands were measured using Doppler area-velocity meters, which record water depth and velocity on a continuous basis during ice-free conditions (typically late March through November). Flow rates were calculated using these data and a rating curve established for each site using manually measured flow rates. $\text{NO}_3\text{-N}$ concentrations entering and leaving the wetland were measured using automated samplers that collected daily composite samples during the flow-monitoring season. Grab samples were collected approximately weekly at the inflow and outflow locations, and from the wetland itself during periods of zero discharge. Water levels and temperatures in wetlands were also measured continuously using data logging equipment. The monitoring strategy was designed and implemented as part of the CREP wetland monitoring described by Crumpton et al. (2006). This study utilized four years of data at each site: 2008-2011 for the KS wetland, and 2007-2010 for the AL Wetland.

4.3.3 Modified wetland equations

This study was a focused effort to modify and test SWAT for the simulation of $\text{NO}_3\text{-N}$ removal wetlands. Measured flow and $\text{NO}_3\text{-N}$ concentrations entering the case study wetlands were input directly as draining watershed inlets, which are similar to point source inputs in SWAT. Simulated watershed hydrology and water quality outputs were disconnected from the wetland by altering the hydrologic routing structure in the configuration (.fig) file. This eliminated confounding errors associated with watershed and tile processes and allowed focused evaluation of the reservoir/wetland algorithms in SWAT. Three sets of equations were incorporated into the SWAT code to better simulate nutrient

removal wetlands: The first set describes the relationships between wetland area and volume with water level, as follows:

$$SA = PSA \times (1 + A \times H) \quad (4)$$

$$VOL = PVOL \times (A + B \times H + C \times H^2) \quad (5)$$

where

SA = wetland surface area at water level H (m²)

PSA = wetland surface area at normal pool (m²)

H = water level relative to normal pool (m)

VOL = wetland volume at water level H (m³)

PVOL = wetland water volume at normal pool (m³)

A, B, and C = wetland shape coefficients

H is positive when the wetland is above normal pool, zero when the wetland is at normal pool, and negative when the wetland is below full pool. For CREP wetlands similar to those simulated in this study, the following default shape coefficients can be used: 1 m⁻¹ for the A coefficient, 1.75 m⁻¹ for B, and 1 m⁻² for C (William Crumpton, Iowa State University, personal communication, 28 May, 2013). To simulate impoundments that do not conform to typical CREP wetlands, A, B, and C should be adjusted using GIS or other topographic tools to fit local conditions.

An algorithm used to calculate discharge from wetlands using the equation for a non-submerged horizontal weir was also added to the SWAT code. This weir equation takes the following form (Gupta, 1989):

$$Q = C_d \times K \times W \times H^{1.5} \text{ for } H > 0 \quad (6)$$

$$Q = 0 \text{ for } H \leq 0 \quad (7)$$

where

Q = wetland discharge ($\text{m}^3 \text{ day}^{-1}$)

C_d = weir discharge coefficient

K = weir crest coefficient ($\text{m}^{1/2} \text{ day}^{-1}$)

W = width of the weir (m)

H = water level relative to normal pool

The weir discharge coefficient (C_d) can be used to calibrate the discharge equation if sufficient flow data are available; however, a default value of 1.0 is usually appropriate. The weir crest coefficient (K) value is derived from the energy equation, and can be set to $147,000 \text{ m}^{1/2} \text{ day}^{-1}$ for a broad-crested weir, $153,000 \text{ m}^{1/2} \text{ day}^{-1}$ for a sharp-crested weir, or an average value used if weir crest is unknown (Gupta, 1989). Weir width (W) can be measured for existing wetlands or taken from design guidelines for proposed wetlands. Water level (H) is a product of wetland inflow and Equations 4 through 7 above.

A parameter called NOSTEP was added to the model code, which represents the number of subdaily iterations used to calculate wetland outflow. Subdaily iteration is necessary to reflect the dynamic nature of water level fluctuation in small impoundments. The required value of NOSTEP will vary with the size of the system being modeled and the degree of water level fluctuation. The NOSTEP value should be set by assessing the stability of flow and volume predictions, and using the lowest value of NOSTEP that satisfactorily eliminates instability.

To utilize the new wetland flow equations, the user must set the IRESKO parameter equal to 5. These algorithms have been incorporated into the res.f module of the FORTRAN code, and input variables are available in the .res input file of SWAT. These modifications to

SWAT can be used to simulate discharge from any impoundment if water level-area-volume and weir equation parameters can be adequately defined.

The following first-order, temperature-dependent, areal-based mass loss equation (Crumpton, 2001) was added to resnut.f file of the FORTRAN code, with required input variables defined in the reservoir (.lwq) input file:

$$\text{MLR} = \text{SA} \times (\text{C} - \text{C}_o) \times k_{20} \times \theta^{(T-20)} \quad (8)$$

where

MLR = mass removal rate (g day^{-1})

SA = wetland area (m^2)

C = $\text{NO}_3\text{-N}$ concentration in wetland ($\text{g m}^{-3} = \text{mg L}^{-1}$)

C_o = irreducible $\text{NO}_3\text{-N}$ concentration ($\text{g m}^{-3} = \text{mg L}^{-1}$)

k_{20} = areal loss rate at 20°C (m day^{-1})

θ = temperature coefficient (dimensionless)

T = water temperature ($^\circ\text{C}$)

In a typical model application, the $\text{NO}_3\text{-N}$ concentration, C, on a given day will be determined by the simulated flows and $\text{NO}_3\text{-N}$ loads entering the wetland from the watershed and the mass balance resulting from the wetland algorithms. For this study, however, the wetlands were isolated from their watersheds and C is determined using the measured inflow data and wetland algorithms. For $\text{NO}_3\text{-N}$ the irreducible concentration, C_o , is zero and the temperature coefficient, θ , will be between 1.04 and 1.20. The loss rate, k_{20} , is site-specific and if not known is treated as a calibration parameter, varying between 0.05 and 0.50 m day^{-1} ($17\text{-}184 \text{ m year}^{-1}$). Although this study evaluates performance of the modified nutrient equations using only observed $\text{NO}_3\text{-N}$ concentrations, the new equations can also be used to

simulate phosphorus. To utilize the modified nutrient removal equations, model users must set IRES_NUT equal to 1 in the .res input file. The new algorithms were incorporated into a modified version of Rev 636 of the FORTRAN code (obtained from USDA-ARS on June 12, 2015), and are available in subsequent versions of the model.

4.3.4 Hydrologic calibration

The two case study wetlands were simulated using both existing and modified reservoir flow algorithms, with input parameters based on known wetland characteristics. The existing algorithms route flow through wetlands using a simplistic equation that sets outflow equal to the volume above normal pool volume minus normal pool volume divided by the number of days it takes to reach normal pool (NDTARGR). The water level in CREP wetlands in Iowa typically returns to normal pool within 1-2 days after storm events in order to protect the drainage rights of upstream landowners, therefore, daily flow into the case study wetlands is a good proxy for outflow except during extended dry periods when water levels are below the outlet weir at the onset of rainfall and resulting inflow. Because daily outflow data was not available, hydrologic simulations using the original equations were calibrated by varying NDTARGR, an integer value, in order to maximize model fit between observed inflows and simulated outflows. Fit was assessed using linear regression of simulated and observed flows, Nash-Sutcliffe Efficiency (NSE), and percent bias (PBIAS). Performance criteria developed by Moriasi et al. (2015) and listed in Table 4.2 were used to assess performance.

Table 4.2 Performance evaluation criteria^[a].

Statistic	Output	Time Scale ^[b]	Performance Criteria			
			Very Good	Good	Satisfactory	Not Satisfactory
NSE ^[c]	Flow	D-M-A	NSE > 0.80	0.70 < NSE ≤ 0.80	0.50 < NSE ≤ 0.70	NSE ≤ 0.50
	NO ₃ -N	M	NSE > 0.65	0.50 < NSE ≤ 0.65	0.35 < NSE ≤ 0.50	NSE ≤ 0.35
PB ^[d]	Flow	D-M-A	PB < ±5	±5 < PB ≤ ±10	±10 < PB ≤ ±15	PB ≥ ±15
	NO ₃ -N	D-M-A	PB < ±15	±15 < PB ≤ ±20	±20 < PB ≤ ±30	PB ≥ ±30

^[a] Adapted from Moriasi et al. (2015a)

^[b] D = daily, M = monthly, A = annual

^[c] NSE = Nash-Sutcliffe efficiency

^[d] PB = PBIAS = percent bias (%)

The calibrated value of NDTARGR was 2 for the KS Wetland and 1 for the AL Wetland, which is consistent with typical CREP wetland drawdown times. It should be noted that the default value of NDTARG for wetlands is 10 (Neitsch, et al., 2011), which would yield poor outflow simulations of the case study wetlands. The modified routing equations did not require calibration because daily flow was simulated using the wetland area-volume relationships (Equations 4 and 5) and weir discharge equations (Equations 6 and 7), populated with known wetland characteristics.

4.3.5 NO₃-N calibration

Nutrient reduction in ponds, wetlands, and reservoirs in SWAT has been simulated using a simple settling velocity equation (Neitsch, et al., 2011). Although physical settling is not the removal mechanism for NO₃-N in wetlands, it follows the same first-order process as the modified algorithms in defined in Equation 8, but lacks the temperature correction factor and irreducible background concentration. The primary input is the nutrient removal rate (m year⁻¹), which is defined as NSETLR for simulation of nitrogen. SWAT allows for a high and low nutrient removal period (IRES1 and IRES2), which correspond to distinct removal rates, NSETLR1 and NSETLR2. The incorporation of two removal rates into the model is

empirical and lacks a mechanistic basis. Although this input option would likely result in better calibration statistics, simulations were performed using constant removal rates in both original and modified equations. Removal rates were adjusted using the Iowa CREP wetland guidelines, with the goal of minimizing PBIAS and maximizing NSE between predicted and observed daily $\text{NO}_3\text{-N}$ concentrations in the wetlands. Calibrated parameter values for the original nitrogen removal equations are reported in Table 4.3, with Table 4.4 showing parameter values for the modified equations. Both original and modified $\text{NO}_3\text{-N}$ approaches had the same calibrated removal rates of 17 m yr^{-1} for the KS wetland and 40 m yr^{-1} for the AL Wetland.

Table 4.3 Wetland parameters and calibration values using original SWAT equations.

Characteristic	SWAT ID	KS Wetland	AL Wetland
Surface area at normal pool (ha)	PSA	1.45	2.45
Volume at normal pool (m^3)	PVOL	8,690	16,360
Surface area at flood pool (ha)	ESA	3.21	3.64
Volume at flood pool (m^3)	EVOL	21,190	34,214
Drawdown to normal pool (days)	NDTARGR	2 ^[a]	1 ^[a]
Outflow simulation code	IRESCO	2	2
Begin high nitrate removal (month)	IRES1	8 ^[b]	7 ^[b]
End high nitrate removal (month)	IRES2	10 ^[b]	10 ^[b]
Nutrient simulation code	IRES_NUT	0	0
High removal rate (m year^{-1})	NSETLR1	17 ^[c]	40 ^[c]
Low removal rate (m year^{-1})	NSETLR2	17 ^[c]	40 ^[c]

^[a] Hydrologic calibration parameter

^[b] Has no effect if NSETLR1 = NSETLR2

^[c] $\text{NO}_3\text{-N}$ calibration parameter value

4.3.6 Integration of wetlands and watershed/tile drainage

After calibration and performance evaluation of isolated simulation of the CREP wetlands, the KS wetland was integrated with the tile-drained watershed simulations. Watershed simulations were performed using existing soil and tile $\text{NO}_3\text{-N}$ algorithms (Section 3.4.2) as well as the algorithms modified and re-calibrated using additional $\text{NO}_3\text{-N}$ lagging parameters (Section 3.4.4). Both simulations utilized the improved, modified

wetland algorithms and the wetland input parameters for the KS Wetland described in Table 4.4.

Table 4.4 Wetland parameters and calibration values using modified equations.

Characteristic	SWAT ID	KS Wetland	AL Wetland
Surface area at normal pool (ha)	PSA	1.45	2.45
Volume at normal pool (m ³)	PVOL	8,690	16,360
Wetland shape coefficient	ACOEf	1.00	1.00
Wetland shape coefficient	BCOEf	1.75	1.75
Wetland shape coefficient	CCOEf	1.00	1.00
Weir discharge coefficient	WEIRC	1.00	0.25
Weir crest coefficient (m ^{1/2} day ⁻¹)	WEIRK	150,000	150,000
Weir width (m)	WEIRW	6.1	13.0
Number of subdaily flow iterations	NOSTEP	144	96
Outflow simulation code	IRESco	5	5
Begin high nitrate removal (month)	IRES1	1 ^[a]	1 ^[a]
End high nitrate removal (month)	IRES2	1 ^[a]	1 ^[a]
High removal rate (m year ⁻¹)	NSETLR1	17 ^[b]	40 ^[b]
Nutrient simulation code	IRES_NUT	1	1
Low removal rate (m year ⁻¹)	NSETLR1	17 ^[b]	40 ^[b]
Temperature coefficient	THETA_N	1.08 ^[b]	1.08 ^[b]
Irreducible NO ₃ -N conc. (mg L ⁻¹)	CON_NIRR	0.0	0.0

^[a] Has no effect if NSETLR1 = NSETLR2

^[b] NO₃-N calibration parameter value

4.4 Results and Discussion

4.4.1 Simulation of wetland hydrology

The simulation period (2008-2011) for the KS Wetland was wetter than normal, with an average annual rainfall of 1.08 m yr⁻¹. The resulting annual hydraulic loading rate was 84.3 m yr⁻¹. Average rainfall near the AL Wetland during the simulation period (2007-2010) was 0.90 m yr⁻¹, resulting in an annual hydraulic loading rate of 31.4 m yr⁻¹.

The modified equations result in accurate predictions of wetland discharge across wet and dry conditions for the KS Wetland (Figure 4.3) and AL Wetland (Figure 4.4). Although both original and modified equations produced daily outflows with NSE values near 1.0 and PBIAS values less than 1.0% , plots with simulated flows on the Y-axis and observed flows on the X-axis reveal improved flow prediction using the modified equations compared with

the original SWAT equations. As illustrated for the KS wetland in Figure 4.5 and the AL wetland in Figure 4.6, flows predicted using the modified equations consistently match observed flows, while use of the original SWAT equations resulted in several instances of over and under prediction of wetland outflows, even with calibrated values of NDTARGR. Simulation of KS Wetland flows was more accurate than for the AL Wetland, with slightly improved performance using the modified equations in both wetlands. Additionally, the modified equations offer significantly improved simulation of daily wetland volume compared with the original equations. This would have major implications for applications in which wetland volume (and hence, depth and duration of inundation) were important.

Evaluation of wetland hydrology in SWAT revealed poor performance of the original equations using the uncalibrated, default NDTARGR parameter value of 10. Alteration of this parameter to represent the wetlands simulated in this study was made possible by utilizing the .reservoir (.res) file for wetland simulation. SWAT applications using the pond/wetland (.pnd) files for wetland simulation are forced to use the default value of 10, which produced significant over and under estimates of wetland outflows for both the KS Wetland (Figure 4.5) and the AL Wetland (Figure 4.6).

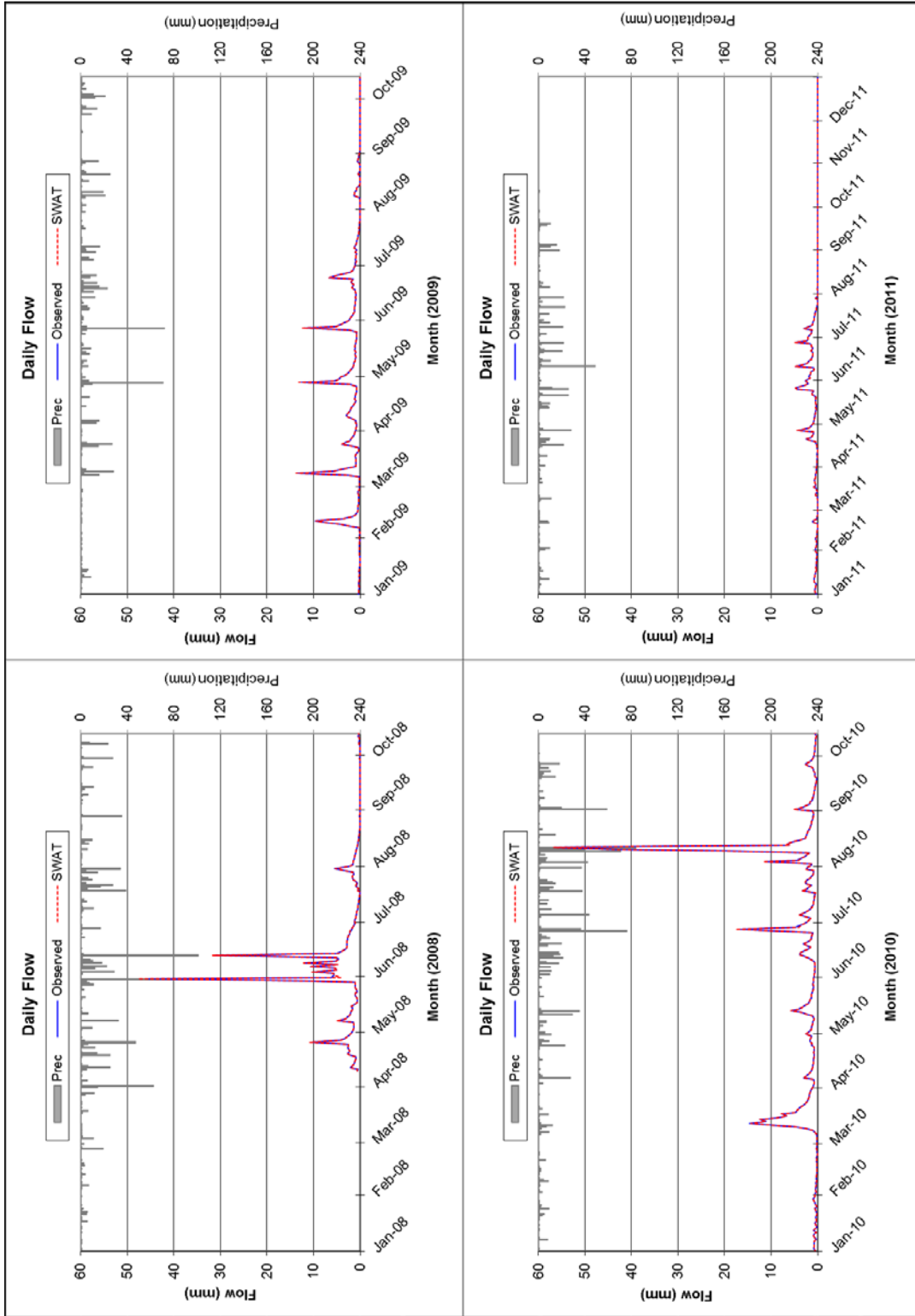


Figure 4.3 Observed flow into the KS Wetland (blue), simulated flow out of the wetland using modified wetland equations, and precipitation (gray bars).

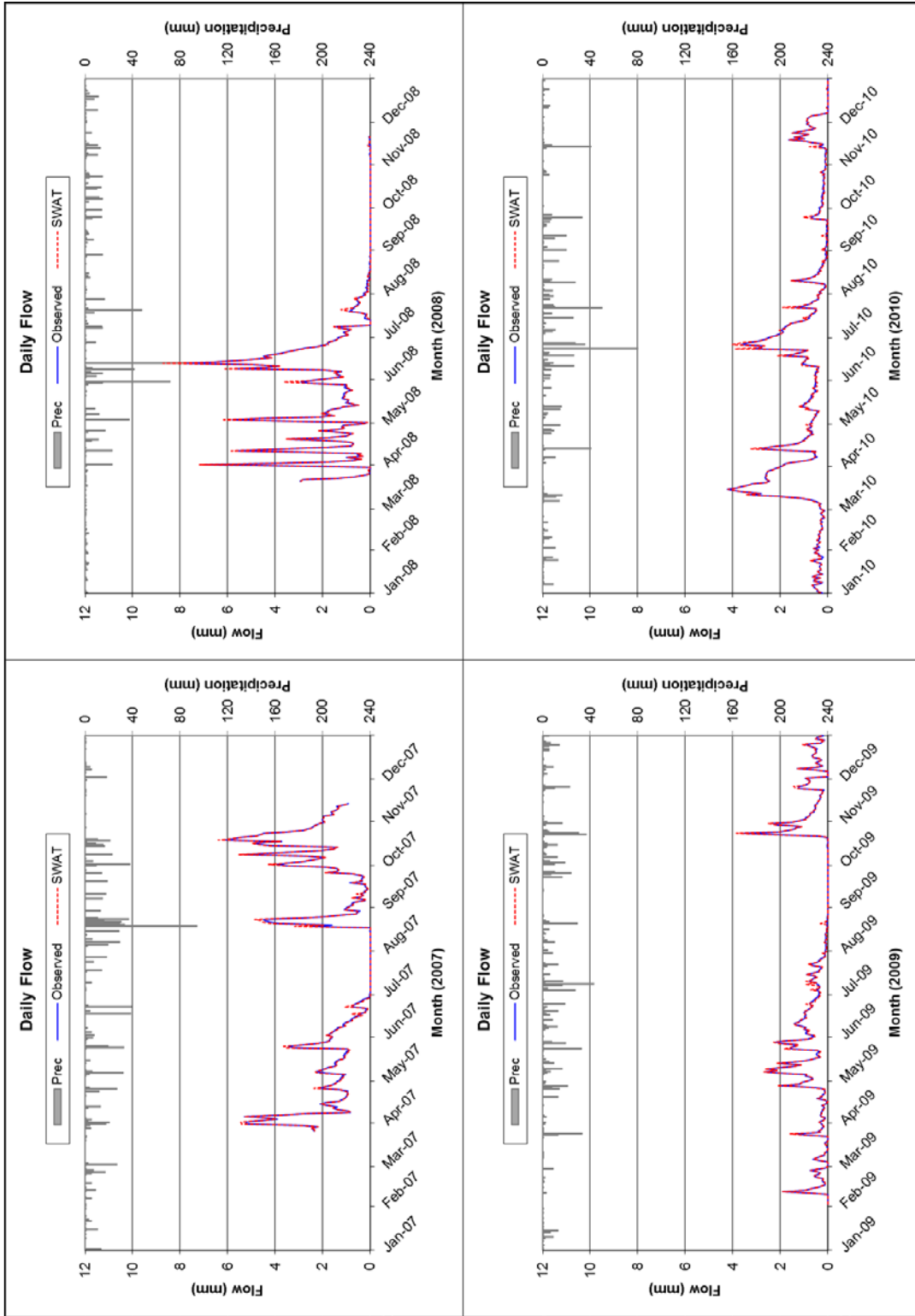


Figure 4.4 Observed flow into the AL Wetland (blue), simulated flow out of the wetland using modified wetland equations, and precipitation (gray bars).

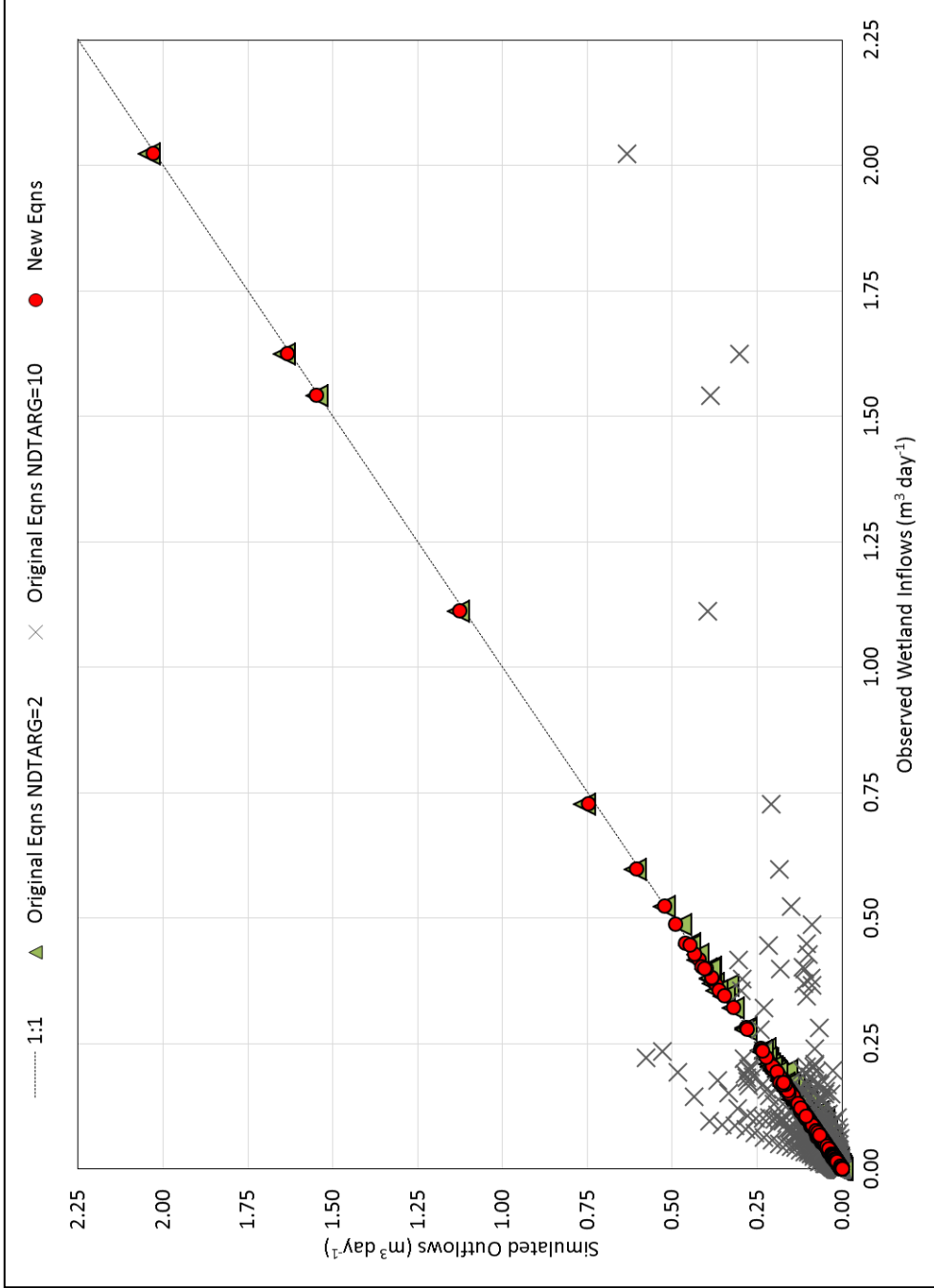


Figure 4.5 KS Wetland simulated outflows vs. measured inflows. Simulated flows using original SWAT equations and NDTARG=10 are plotted as “x” symbols. Original SWAT equation with NDTARGR calibrated value of 2 is illustrated by green triangles. Outflows simulated using the modified wetland equations are shown as red circles.

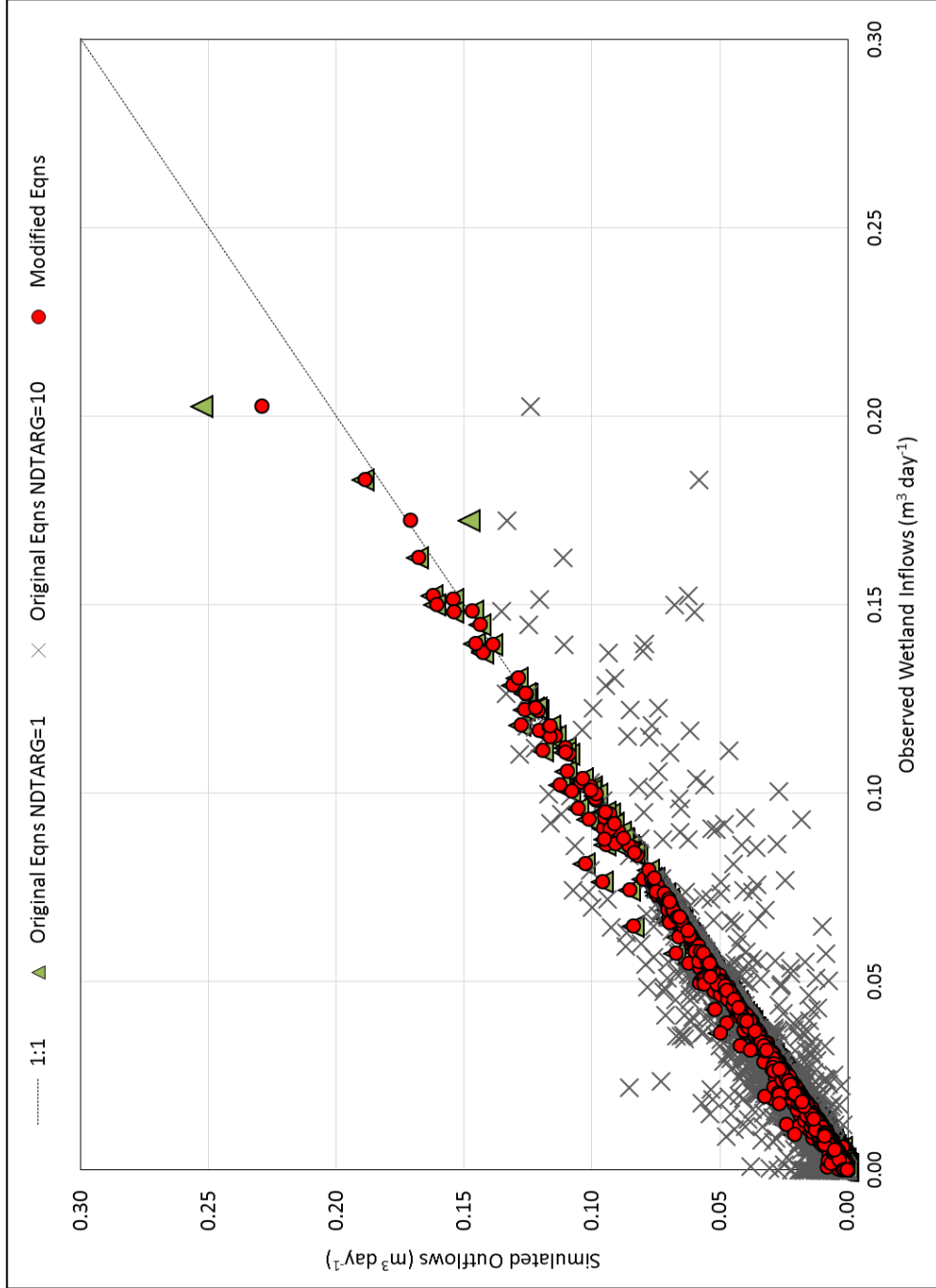


Figure 4.6 AL Wetland simulated outflows vs. measured inflows. Simulated flows using original SWAT equations and NDTARG=10 are plotted as “x” symbols. Original SWAT equation with NDTARG calibrated value of 1 is illustrated by green triangles. Outflows simulated using the modified wetland equations are shown as red circles.

4.4.2 Simulation of wetland $\text{NO}_3\text{-N}$ concentration

The flow-weighted average (FWA) concentration measured in KS Wetland inflow was 10.9 mg L^{-1} , with a FWA outflow concentration of 9.5 mg L^{-1} . The original SWAT equations produced a FWA outflow concentration of 8.9 mg L^{-1} , while the modified wetland equations resulted in a FWA concentration of 9.2 mg L^{-1} . For the AL Wetland, which had a FWA inflow concentration of 12.4 mg L^{-1} and outflow concentration of 7.6 mg L^{-1} , both original SWAT equations and modified equations produced a FWA outflow concentration of 8.2 mg L^{-1} . Daily $\text{NO}_3\text{-N}$ simulations for the KS Wetland using the original equations are reported in Figure 4.7. The original SWAT wetland equations produced very good simulations of daily $\text{NO}_3\text{-N}$ concentrations as indicated by time series plots and performance criteria (Table 4.2). The Nash-Sutcliffe efficiency (NSE) for the calibration period (2008-2009) was 0.84 with a percent bias (PBIAS) of 1.34%, indicating slight under-prediction of observed concentrations. The validation period (2010-2011) resulted in a NSE of 0.87 and PBIAS of 12.11% for daily $\text{NO}_3\text{-N}$ concentrations, the largest bias for either wetland or period. Application of the modified equations to the KS Wetland improved predictions of $\text{NO}_3\text{-N}$ concentrations in terms of the overall FWA and short-term (i.e., daily) fluctuations (Figure 4.8). The NSE for the calibration period using the modified equations was 0.85, with PBIAS of -2.76%. The validation period NSE was 0.90 with a PBIAS of 8.29%, both improved compared with validation using the original equations.

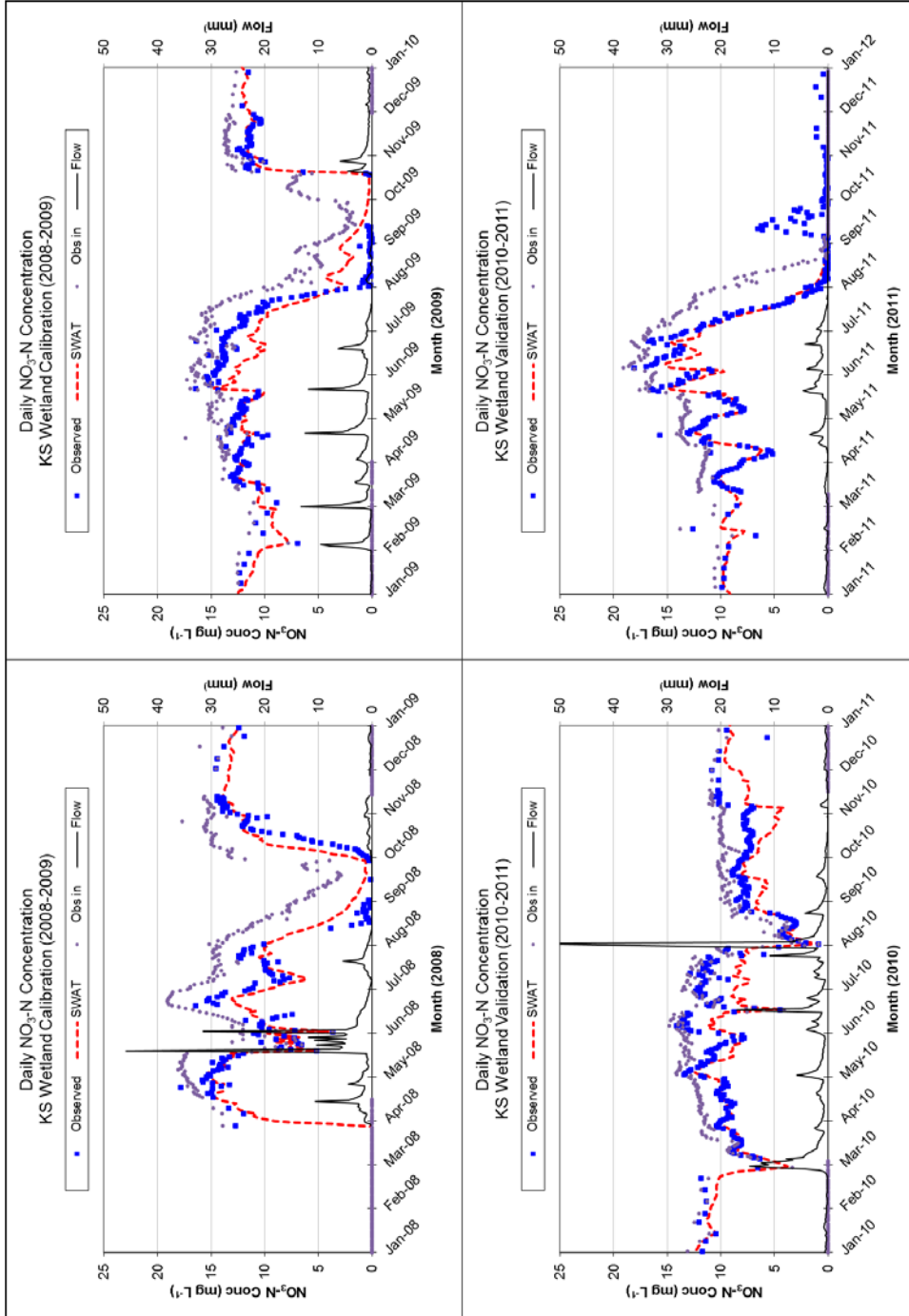


Figure 4.7 Calibration (2008-2009) and validation (2010-2011) results for KS Wetland $\text{NO}_3\text{-N}$ concentration using original SWAT equations. Larger, blue dots are observed concentrations, red dashed line is simulated concentration, small, purple dots represent observed inflow concentration, and black line is simulated flow out of the wetland.

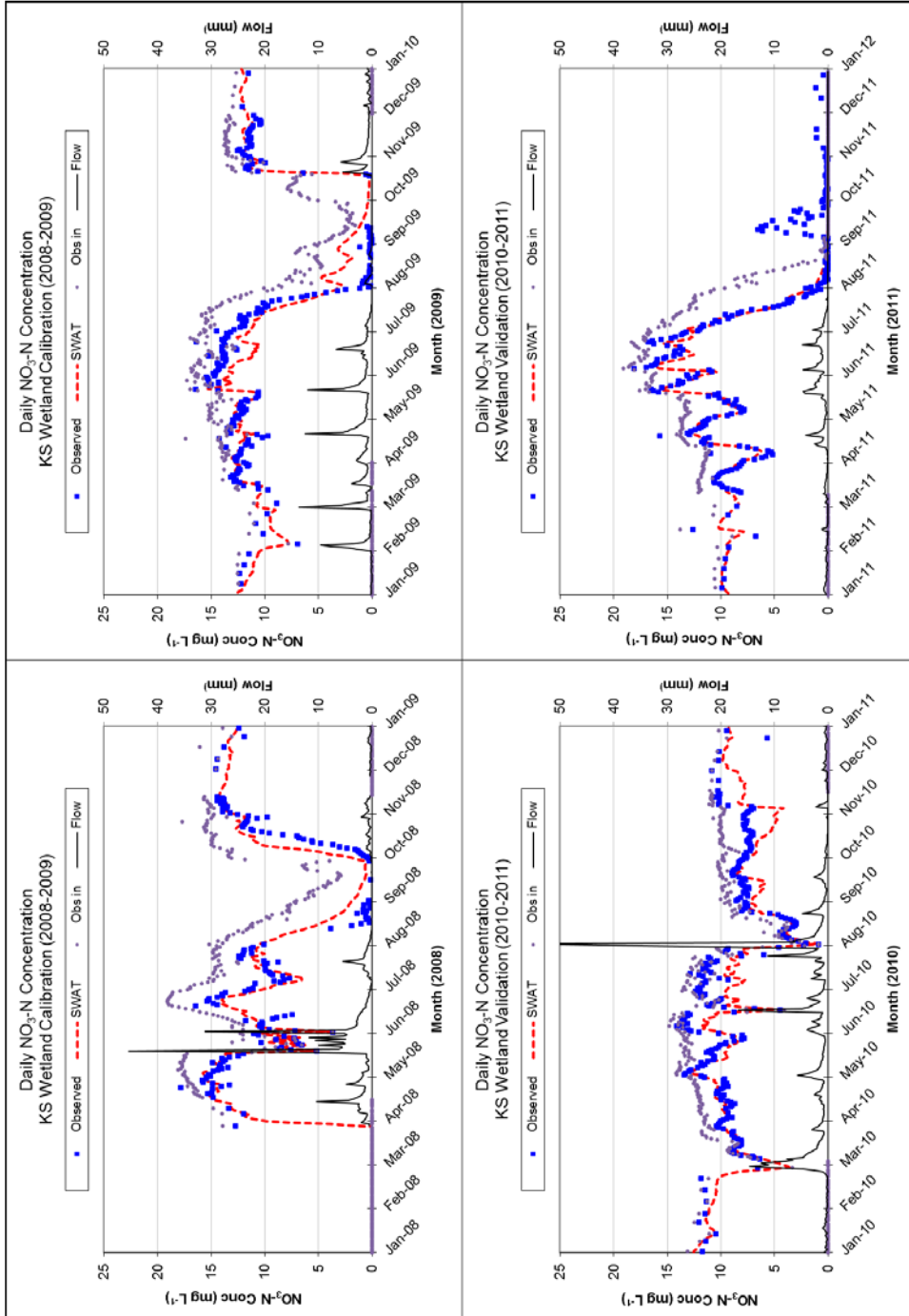


Figure 4.8 Calibration (2008-2009) and validation (2010-2011) results for KS Wetland $\text{NO}_3\text{-N}$ concentration using modified wetland equations. Larger, blue dots are observed concentrations, red dashed line is simulated concentration, small, purple dots represent observed inflow concentration, and black line is simulated flow out of the wetland.

Performance of the original SWAT equations (Figure 4.9) and modified wetland equations (Figure 4.10) simulating $\text{NO}_3\text{-N}$ concentration in the AL Wetland was nearly identical, with no discernible difference in calibration or validation statistics. The calibration NSE was 0.84 and the validation NSE was 0.77 for both sets of equations. Calibration period PBIAS was slightly better using the original equations (1.53%) than the modified equations (1.61%). Conversely, validation PBIAS was slightly better using the modified equations (-1.12%) compared with the original equation PBIAS of -1.21%. All statistics meet the performance criteria established by Moriasi et al. (2015) as very good.

4.4.3 Simulation of wetland $\text{NO}_3\text{-N}$ loads

As illustrated by the overlapping time series plots of measured and simulated $\text{NO}_3\text{-N}$ loads in the KS wetland, both the original SWAT equations (Figure 4.11) and modified wetland equations (Figure 4.12) provided close agreement with daily loads. Loads under both high and low flow conditions are well-represented with few exceptions, and model performance statistics are better for load predictions than concentration predictions in the KS Wetland (Table 4.5). The modified wetland equations did outperform the original SWAT equations in terms of daily $\text{NO}_3\text{-N}$ load predictions, as indicated by lower PBIAS values (Table 4.5) and the XY scatter plot shown in Figure 4.13. The relationship between simulated and observed loads more closely follows the 1:1 line in Figure 4.13, and deviations from observed loads are generally smaller when utilizing the modified equations (Figure 4.14).

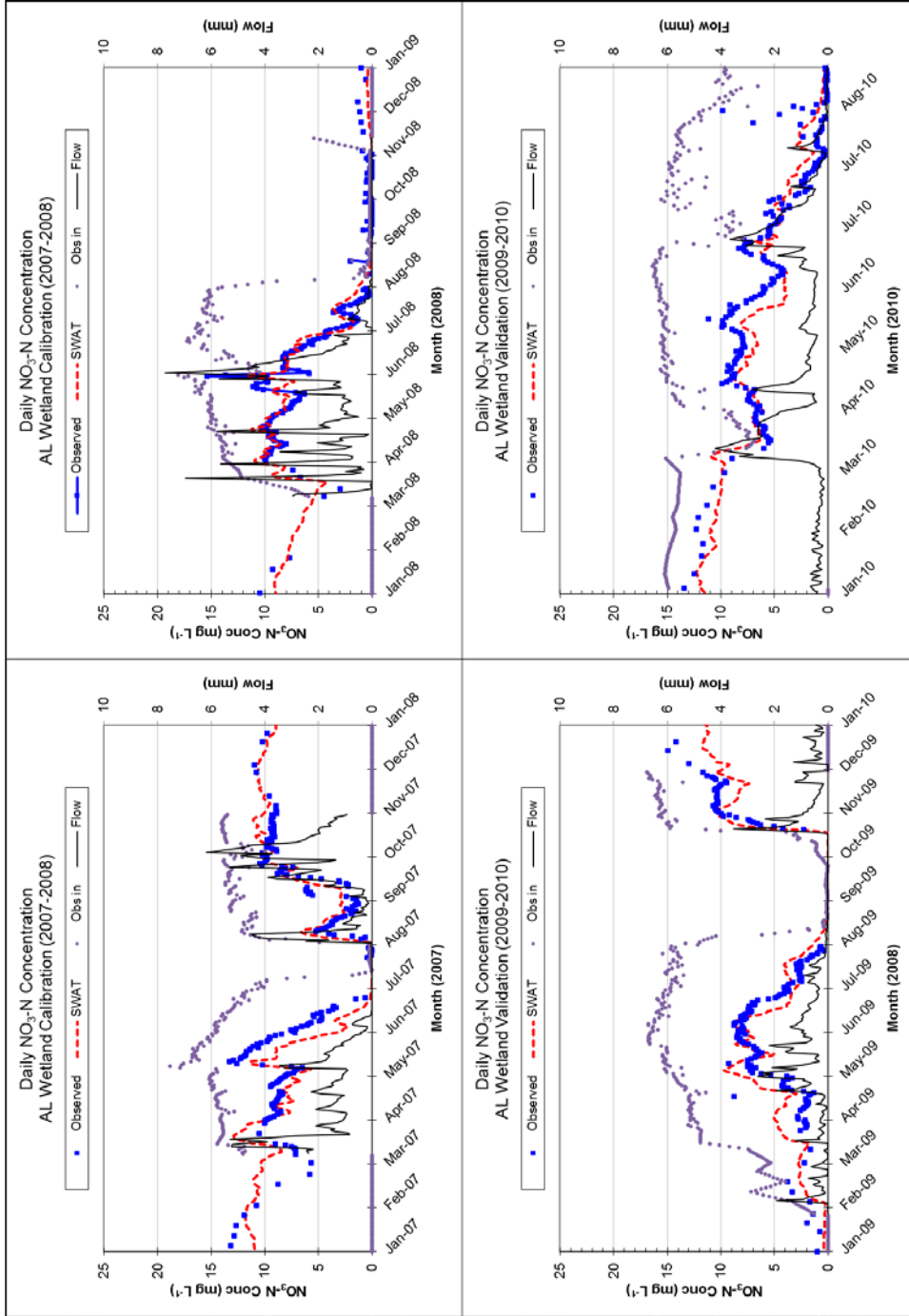


Figure 4.9 Calibration (2007-2008) and validation (2009-2010) results for AL Wetland $\text{NO}_3\text{-N}$ concentration using original SWAT equations. Larger, blue dots are observed concentrations, red dashed line is simulated concentration, small, purple dots represent observed inflow concentration, and black line is simulated flow out of the wetland.

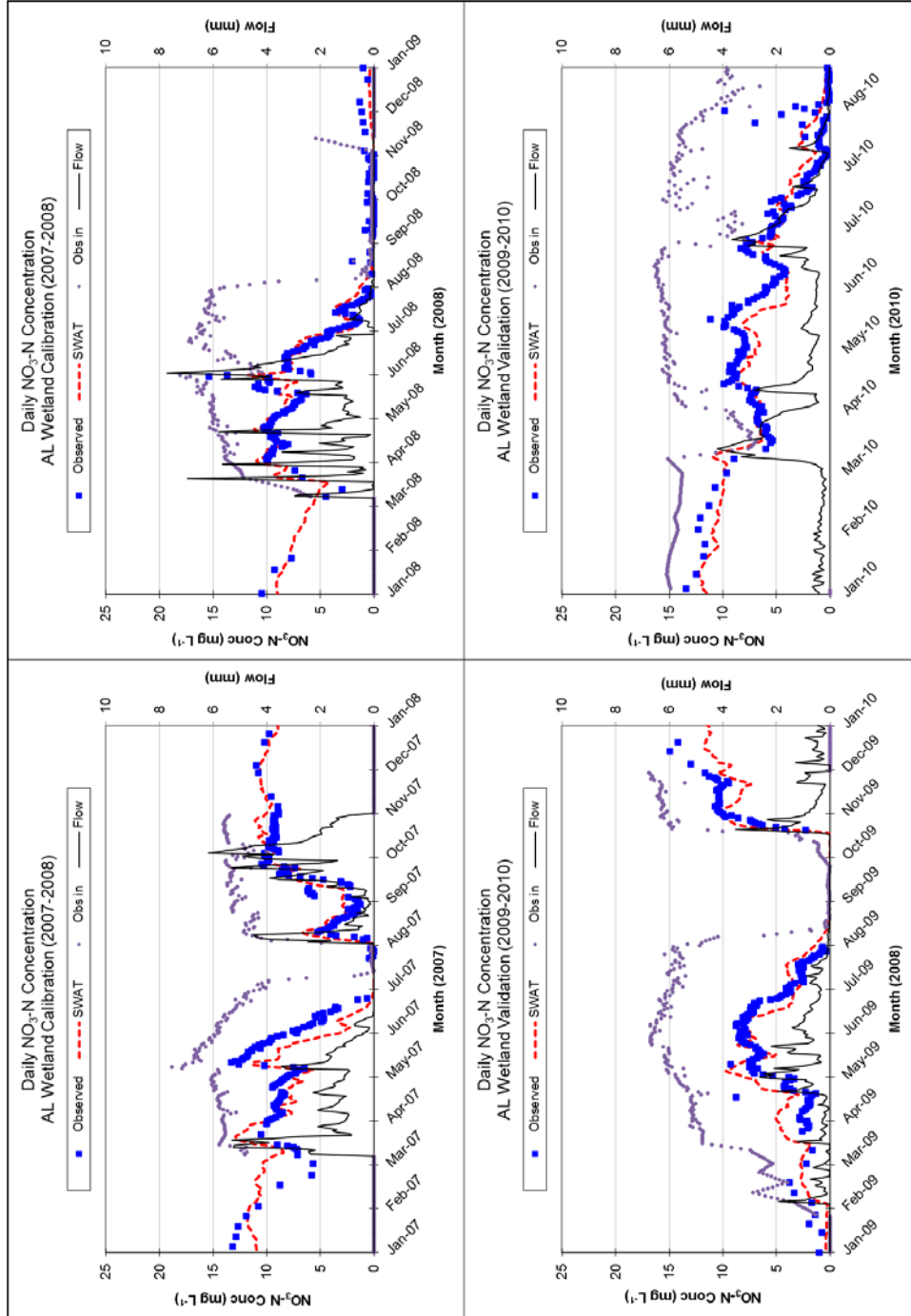


Figure 4.10 Calibration (2007-2008) and validation (2009-2010) results for AL Wetland $\text{NO}_3\text{-N}$ concentration using modified wetland equations. Larger, blue dots represent observed concentrations, red dashed line is simulated concentration, small, purple dots represent observed inflow concentration, and black line is simulated flow out of the wetland.

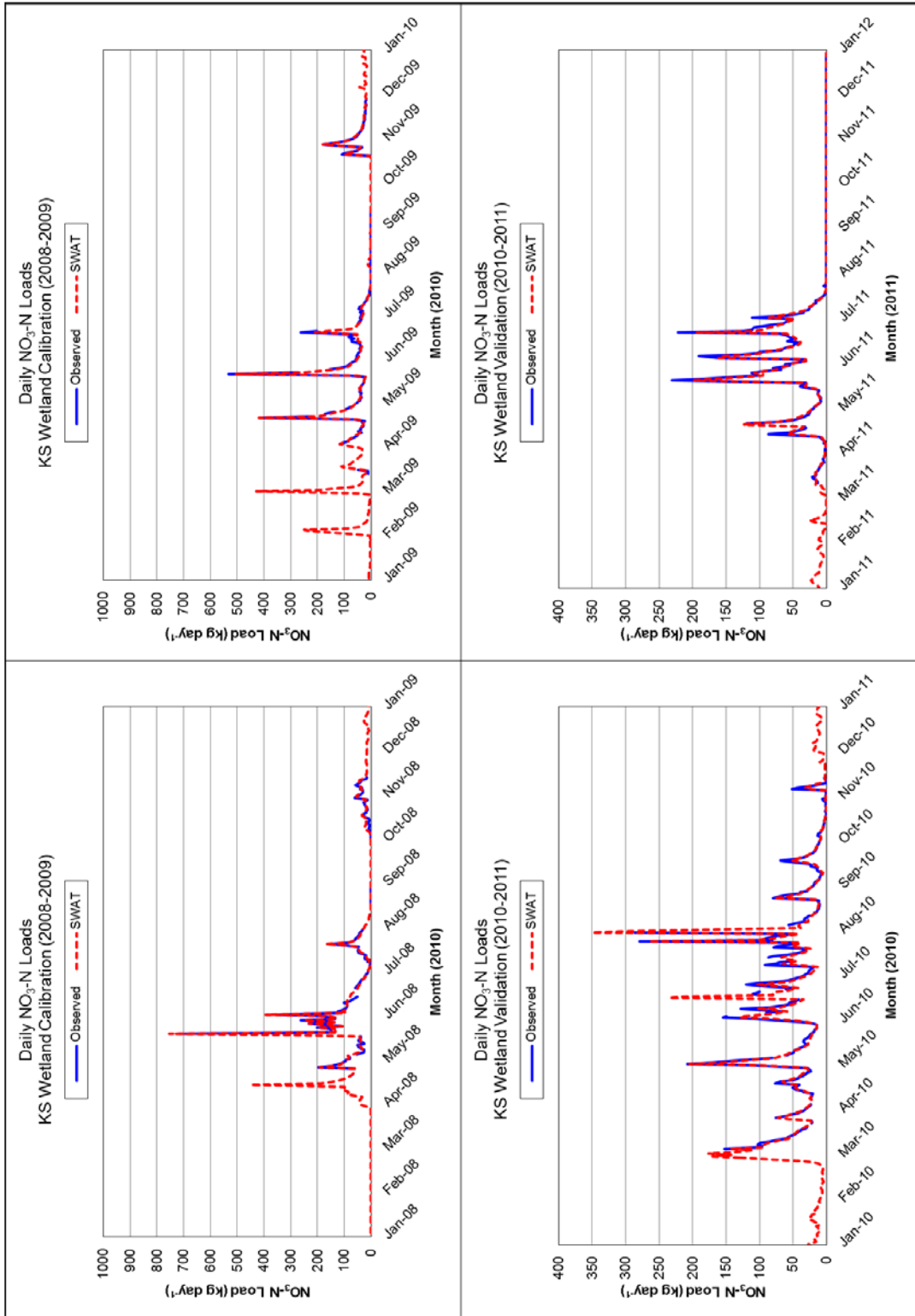


Figure 4.11 Calibration (2008-2009) and validation (2010-2011) results for KS Wetland $\text{NO}_3\text{-N}$ loads using original SWAT equations. Blue line is observed and red dashed line is simulated load out of the wetland.

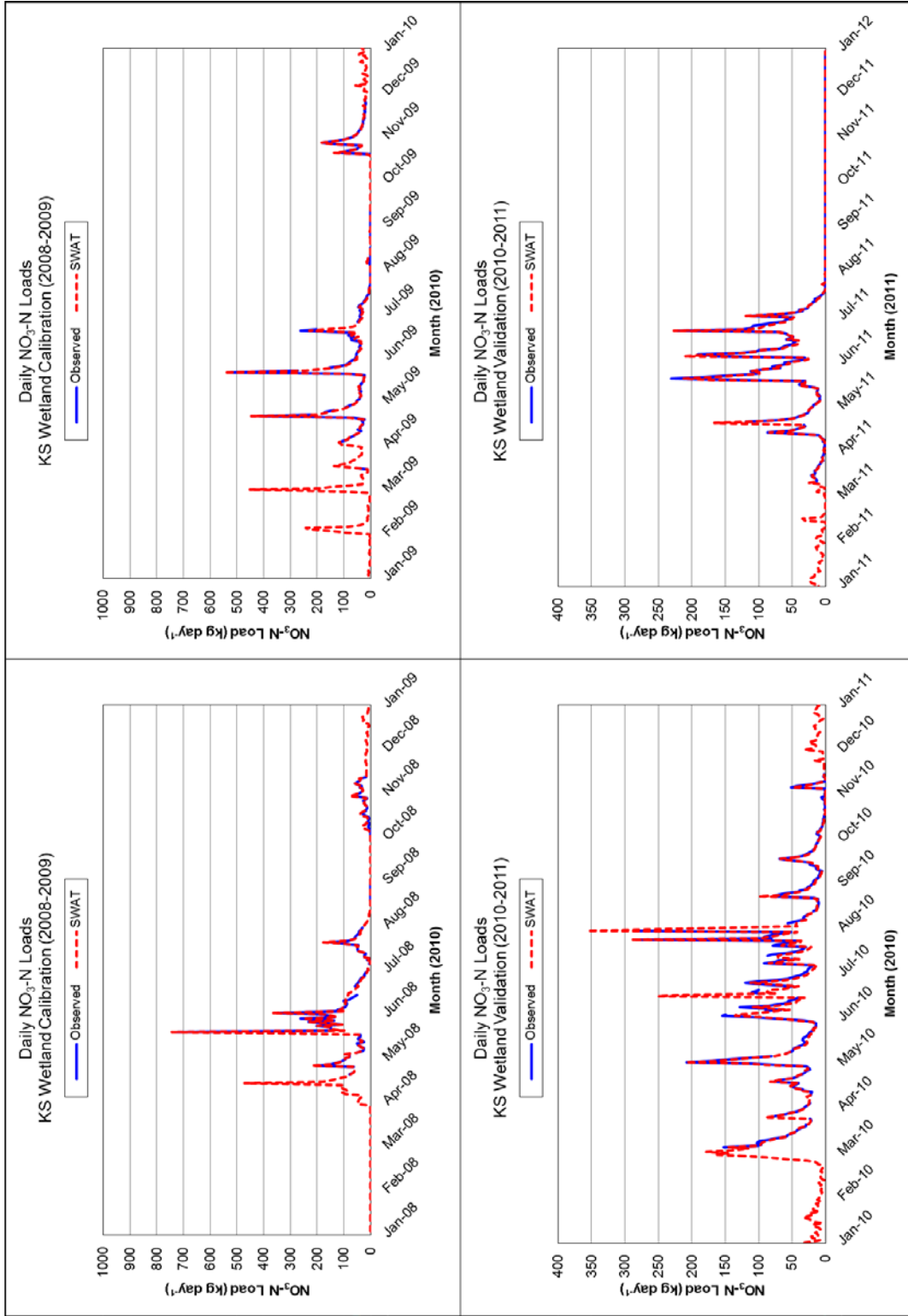


Figure 4.12 Calibration (2008-2009) and validation (2010-2011) results for KS Wetland $\text{NO}_3\text{-N}$ loads using modified wetland equations. Blue line is observed and red dashed line is simulated load out of the wetland.

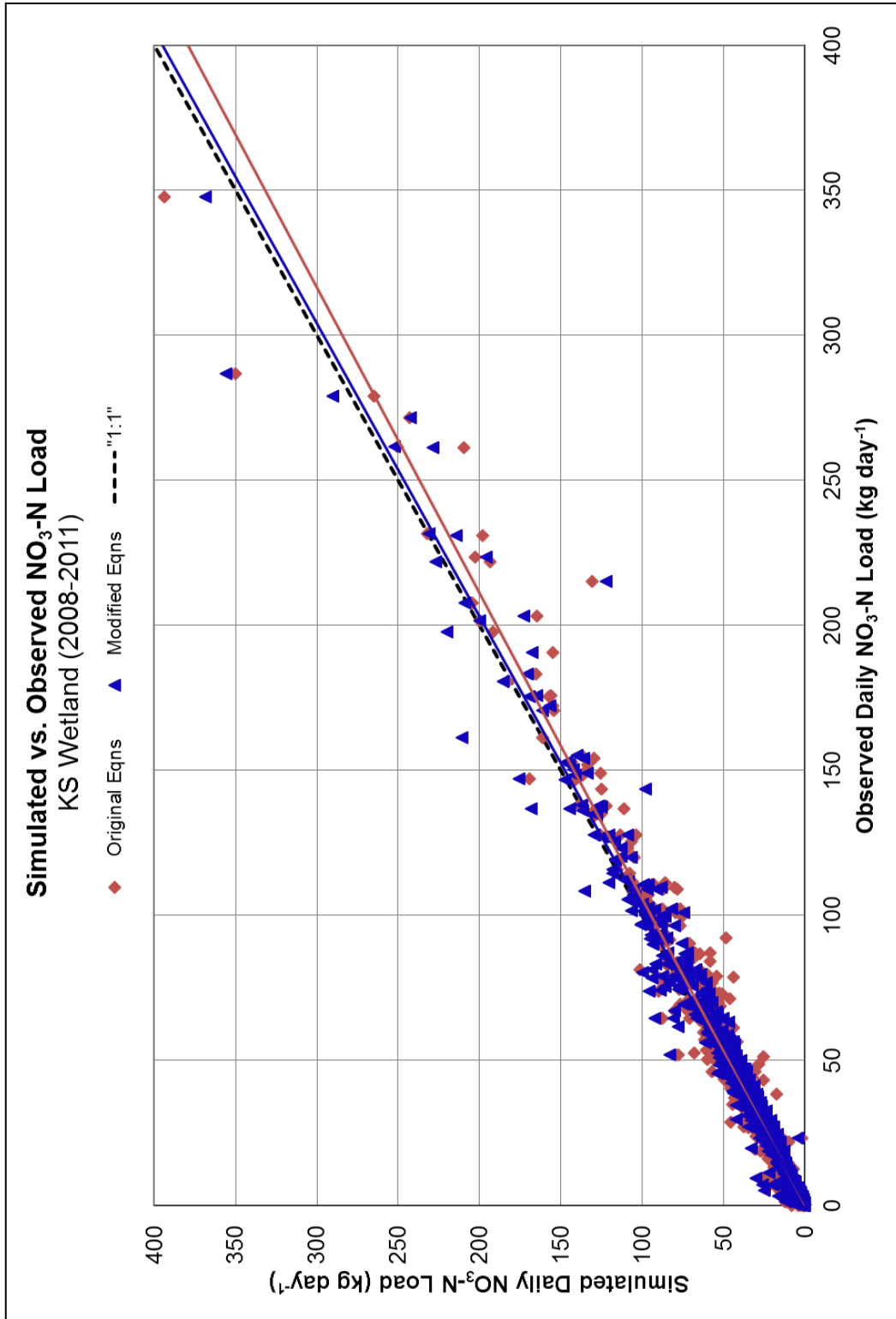


Figure 4.13 Simulated vs. observed $\text{NO}_3\text{-N}$ load for the KS Wetland (2008-2011) using original SWAT equations (red diamonds) and modified wetland equations (blue triangles).

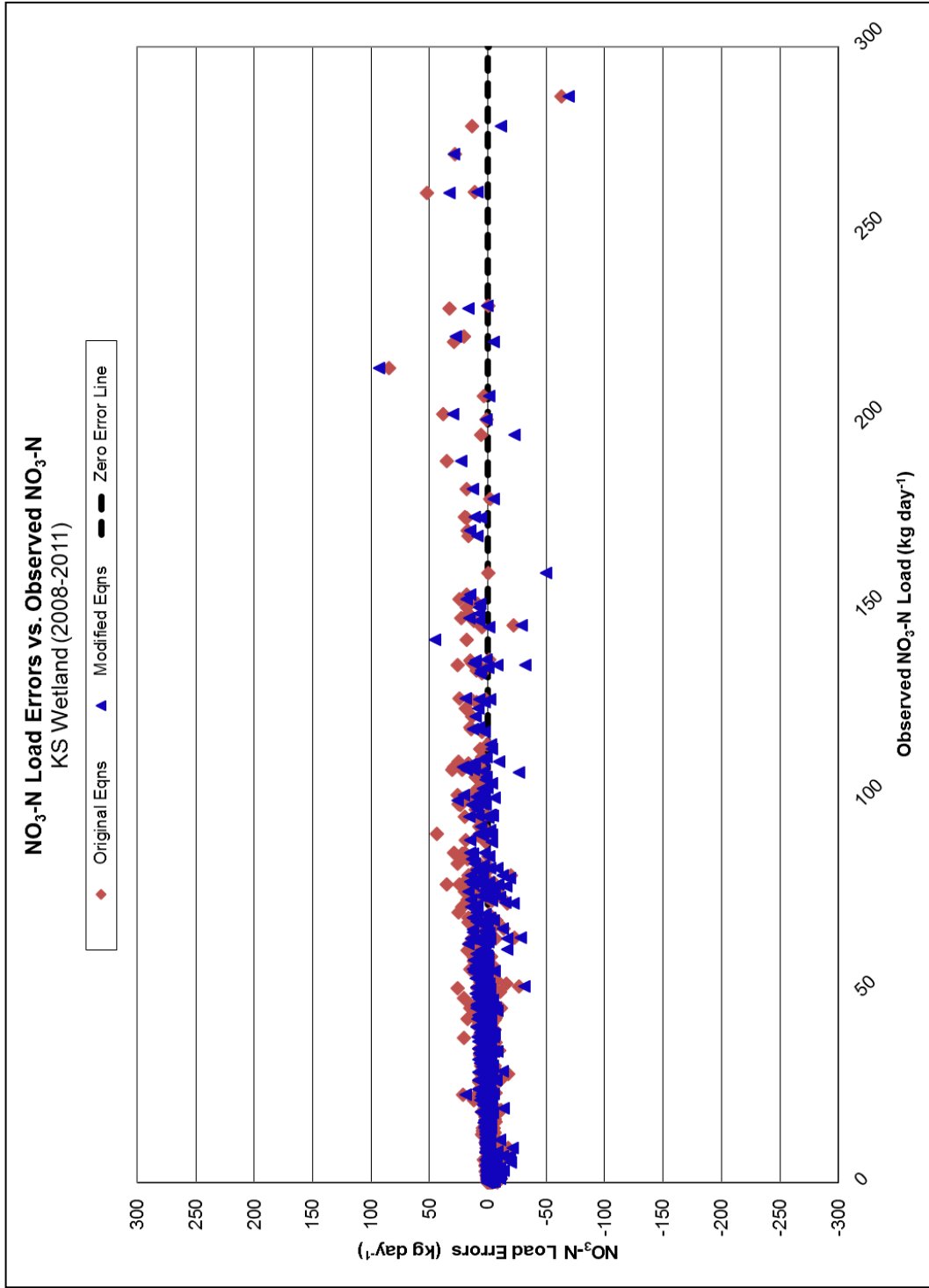


Figure 4.14 Plot of NO₃-N load errors (observed minus simulated) against observed loads for KS Wetland (2008-2011) using the original SWAT equations (red diamonds) and modified wetland equations (blue

Similar to the KS Wetland, time series plots of measured and simulated NO₃-N loads in the AL Wetland illustrate very good agreement between measured and predicted loads using both the original SWAT equations (Figure 4.15) and modified wetland equations (Figure 4.16). However, there were periods where both equations produced noticeable errors in load predictions. For example, in June of 2008 and May of 2009, the models over-predicted NO₃-N loads, while the large events in July of 2010 were under-estimated by the models. Model performance in the AL Wetland was better for loads than concentrations, as implied by NSE values; however PBIAS was actually larger for loads (Table 4.5). This indicates that daily load fluctuations are captured better despite a larger error in the overall load predictions.

There was little difference in model performance between the original and modified equations for load prediction in the AL Wetland. Both NSE and PBIAS values are nearly identical between versions (Table 4.5), and the XY scatter plot (Figure 4.17) and error plot (Figure 4.18) reveal significant overlap in deviations between predicted and measured loads using both algorithms. One exception is the approximately 20 kg day⁻¹ larger error using the original equations when both models significantly over-predict an observed load of just over 100 kg day⁻¹. This large error occurred in June of 2008, when peak load in both models occurred the day after the measured peak. The magnitude of error in the peak load for the event was not large but was shifted by a day, resulting in a large error for the daily load.

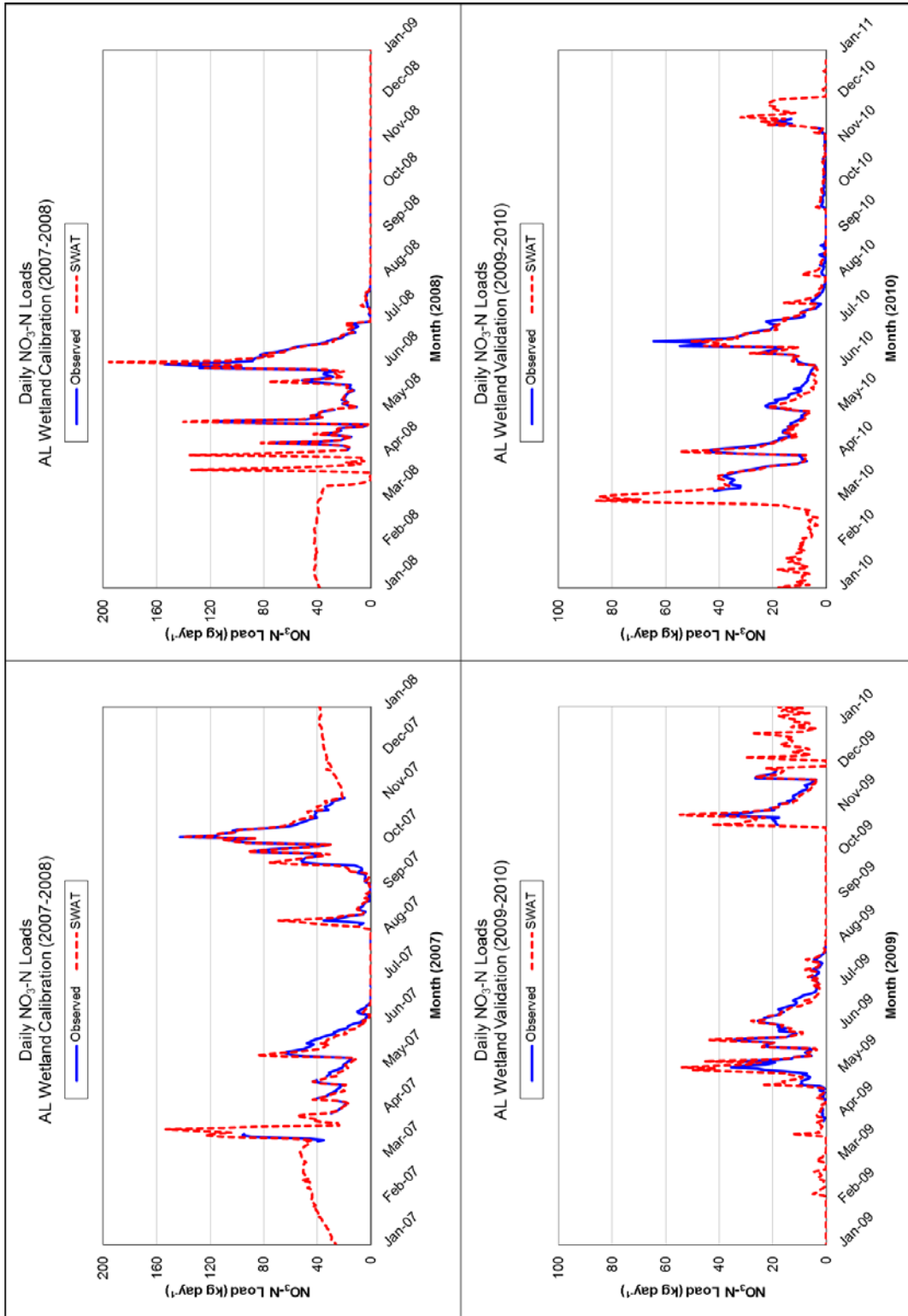


Figure 4.15 Calibration (2007-2008) and validation (2009-2010) results for AL Wetland $\text{NO}_3\text{-N}$ loads using original SWAT equations. Blue line is observed and red dashed line is simulated load out of the wetland.

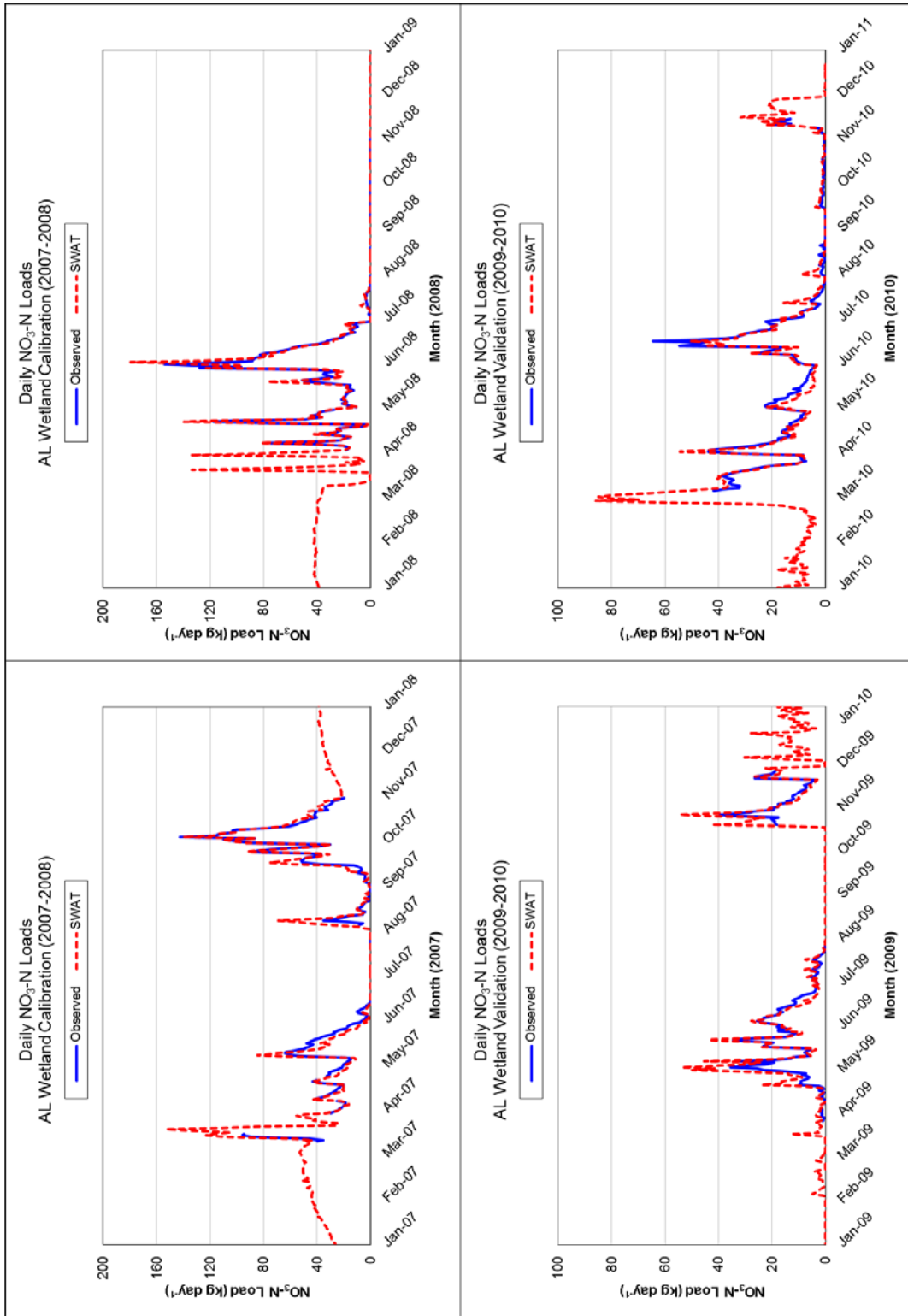


Figure 4.16 Calibration (2007-2008) and validation (2009-2010) results for AL Wetland $\text{NO}_3\text{-N}$ loads using modified wetland equations. Blue line is observed and red dashed line is simulated load out of the wetland.

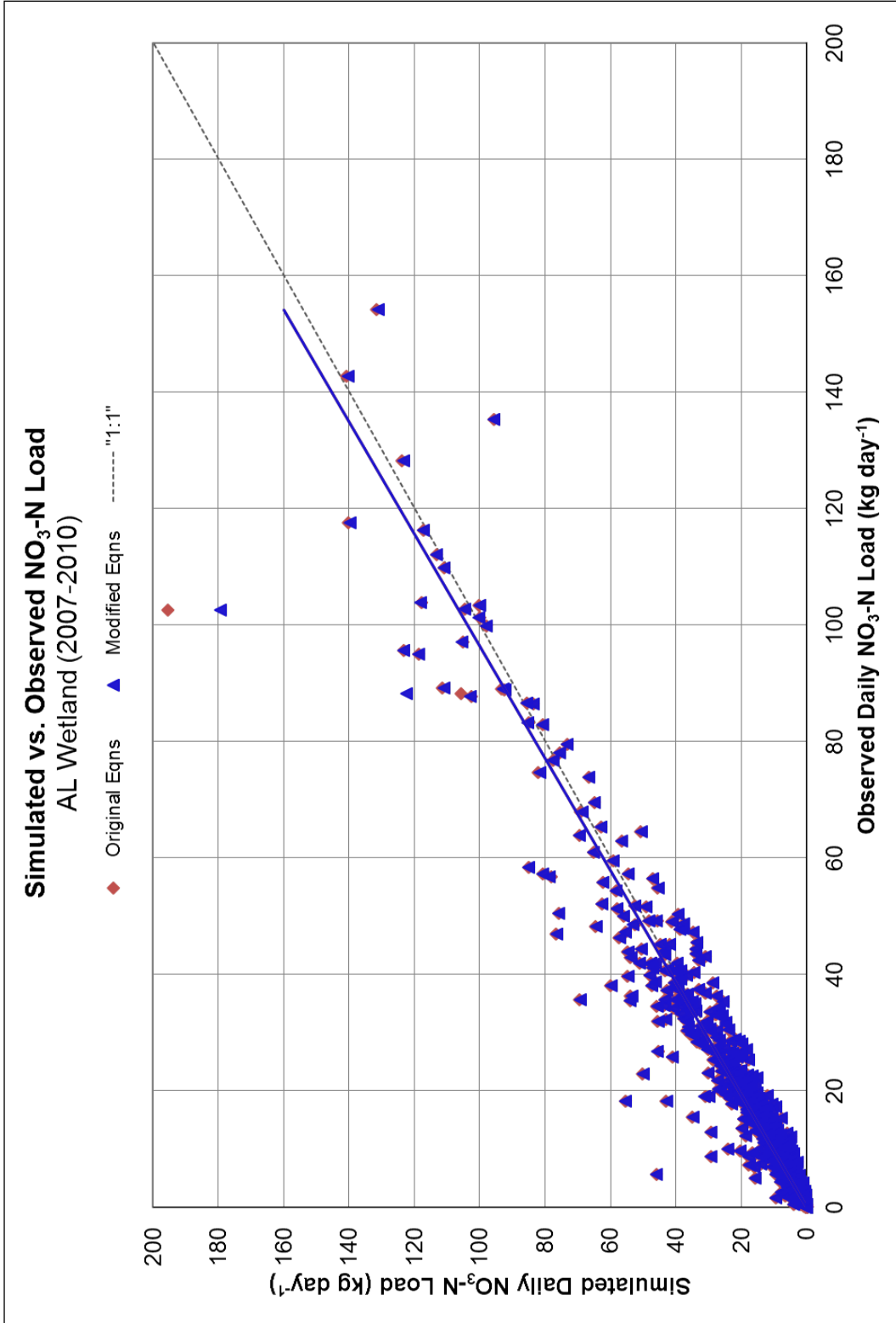


Figure 4.17 Simulated vs. observed NO₃-N loads for the AL Wetland (2007-2010) using original SWAT equations (red diamonds) and modified wetland equations (blue triangles).

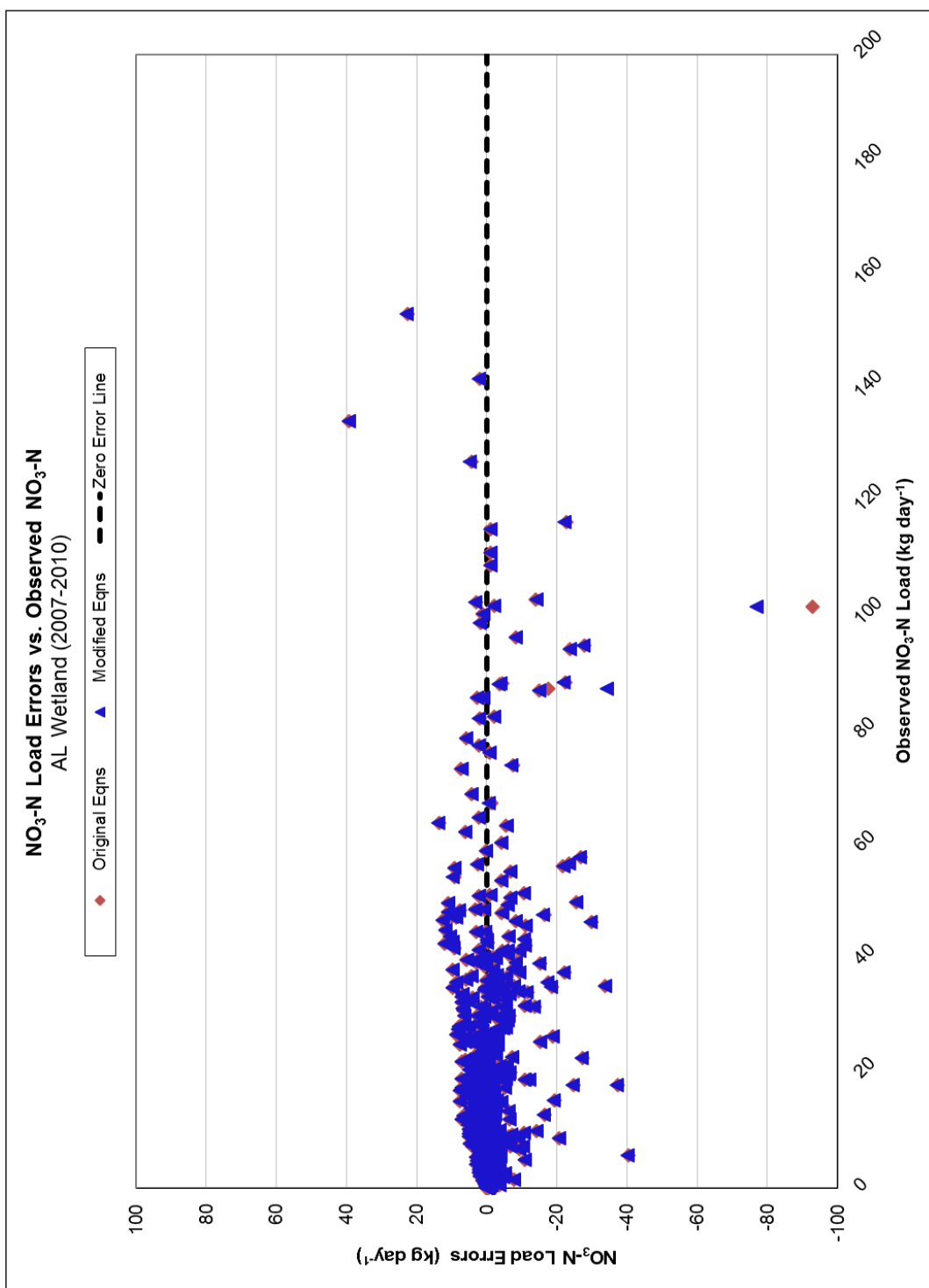


Figure 4.18. Plot of NO₃-N errors (observed minus simulated) against observed loads for the AL Wetland (2007-2010) using original SWAT equations (red diamonds) and modified wetland equations (blue triangles).

Table 4.5 Comparison of NO₃-N simulation performance using original and modified equations.

	KS Wetland NSE ^[a]		AL Wetland NSE	
	Calibration (2008-2009)	Validation (2010-2011)	Calibration (2007-2008)	Validation (2009-2010)
NO₃-N concentration				
Original equations	0.84	0.87	0.84	0.77
Modified equations	0.85	0.90	0.84	0.77
NO₃-N load				
Original equations	0.98	0.96	0.91	0.87
Modified equations	0.99	0.97	0.92	0.88
	KS Wetland PBIAS ^[a]		AL Wetland PBIAS ^[b]	
NO₃-N concentration				
Original equations	1.34	12.11	1.53	-1.21
Modified equations	-2.76	8.29	1.61	-1.12
NO₃-N load				
Original equations	2.29	8.60	-4.45	-3.97
Modified equations	0.03	5.41	-4.38	-3.92

^[a] Nash-Sutcliffe efficiency

^[b] Percent bias (negative indicates over-estimation)

4.4.4 Sensitivity analysis using modified wetland equations

A sensitivity analysis was also performed using the modified wetland equations. The rate (NSETLR) was varied from 0.05 m day⁻¹ to 0.50 m day⁻¹ (17 to 184 m yr⁻¹), with the temperature correction factor (THETA_N) held constant at 1.08. This range of NSETLR was based on typical ranges observed in Iowa CREP wetlands (Crumpton, unpublished data). The resulting range of simulated NO₃-N concentrations in KS Wetland outflow is illustrated in Figure 4.19. For the KS Wetland, the range of simulated concentrations is large, with removal rates near the low-end of the allowable range required for accurate predictions.

The sensitivity of NO₃-N concentrations to the temperature correction factor was also assessed by varying THETA_N while holding NSETLR constant at the calibrated value of 17 m yr⁻¹ (Figure 4.20). Predicted NO₃-N concentrations in the KS Wetland are not as sensitive to changes in N_THETA as NSETLR, as indicated by narrow concentration bands throughout the simulation period. Relatively minor sensitivity was observed in the summer months of each year, with almost no variation in predicted concentrations outside the

growing season. However, there are several instances in which changes in N_THETA resulted in variations of NO₃-N concentration exceeding 5 mg L⁻¹, such as June and July of 2011.

The results of the sensitivity analyses using the modified wetland equations for the AL Wetland are illustrated in Figure 4.21 (NSETLR sensitivity) and Figure 4.22 (N_THETA sensitivity). Sensitivities to both parameters were similar to the KS Wetland, with the exception that the AL Wetland is less sensitive to N_THETA, as indicated by a smaller band of NO₃-N concentrations in Figure 4.22.

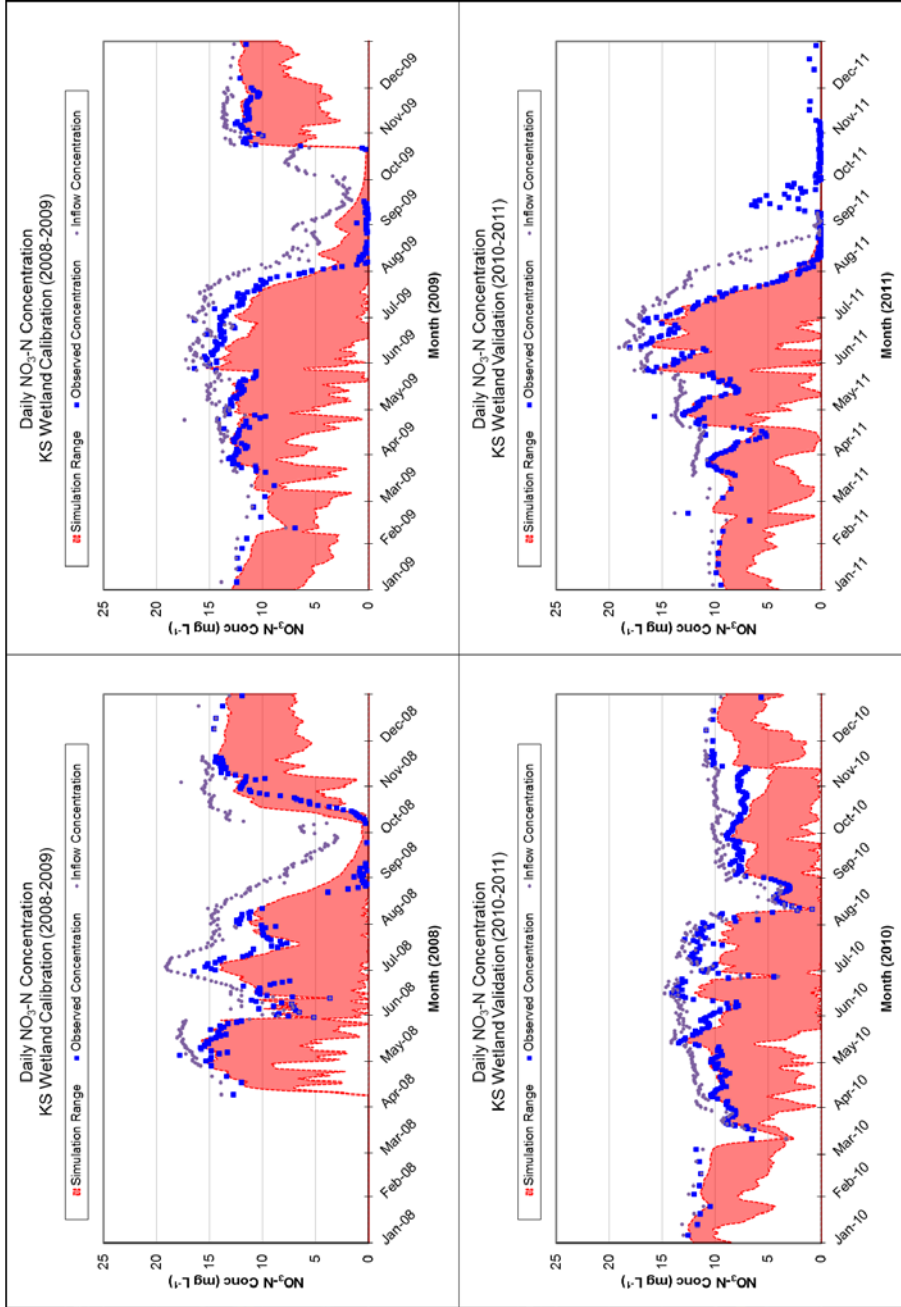


Figure 4.19. Sensitivity of $\text{NO}_3\text{-N}$ concentrations in the KS wetland with variation of removal rate, NSETLR, from 17 m yr^{-1} to 184 m yr^{-1} , using the modified wetland equations. The temperature coefficient, N_THETA , was held constant at the calibrated value of 1.08. The dots illustrate measured inflow concentrations, the solid blue line represents observed outflow concentrations, and the red-shaded band illustrates the range of predicted $\text{NO}_3\text{-N}$ concentration.

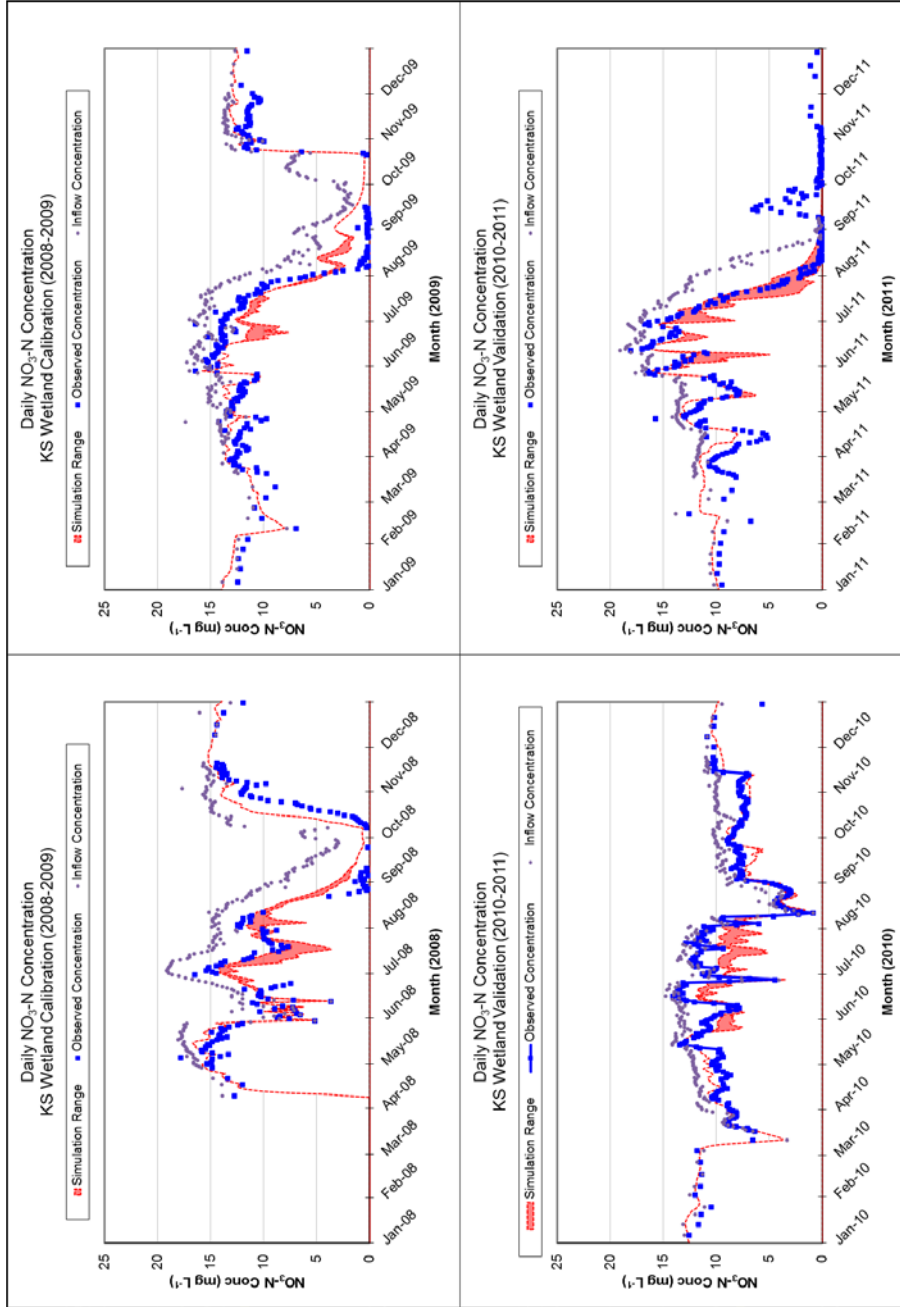


Figure 4.20. Sensitivity of $\text{NO}_3\text{-N}$ concentrations in the KS wetland with variation of temperature coefficient, N_THETA , from 1.04 to 1.20. The removal rate, $NSETLR$, was held constant at the calibrated value of 17 m yr^{-1} . The dots illustrate measured inflow concentrations, the solid blue line represents observed outflow concentrations, and the red-shaded band illustrates the range of predicted $\text{NO}_3\text{-N}$ concentration.

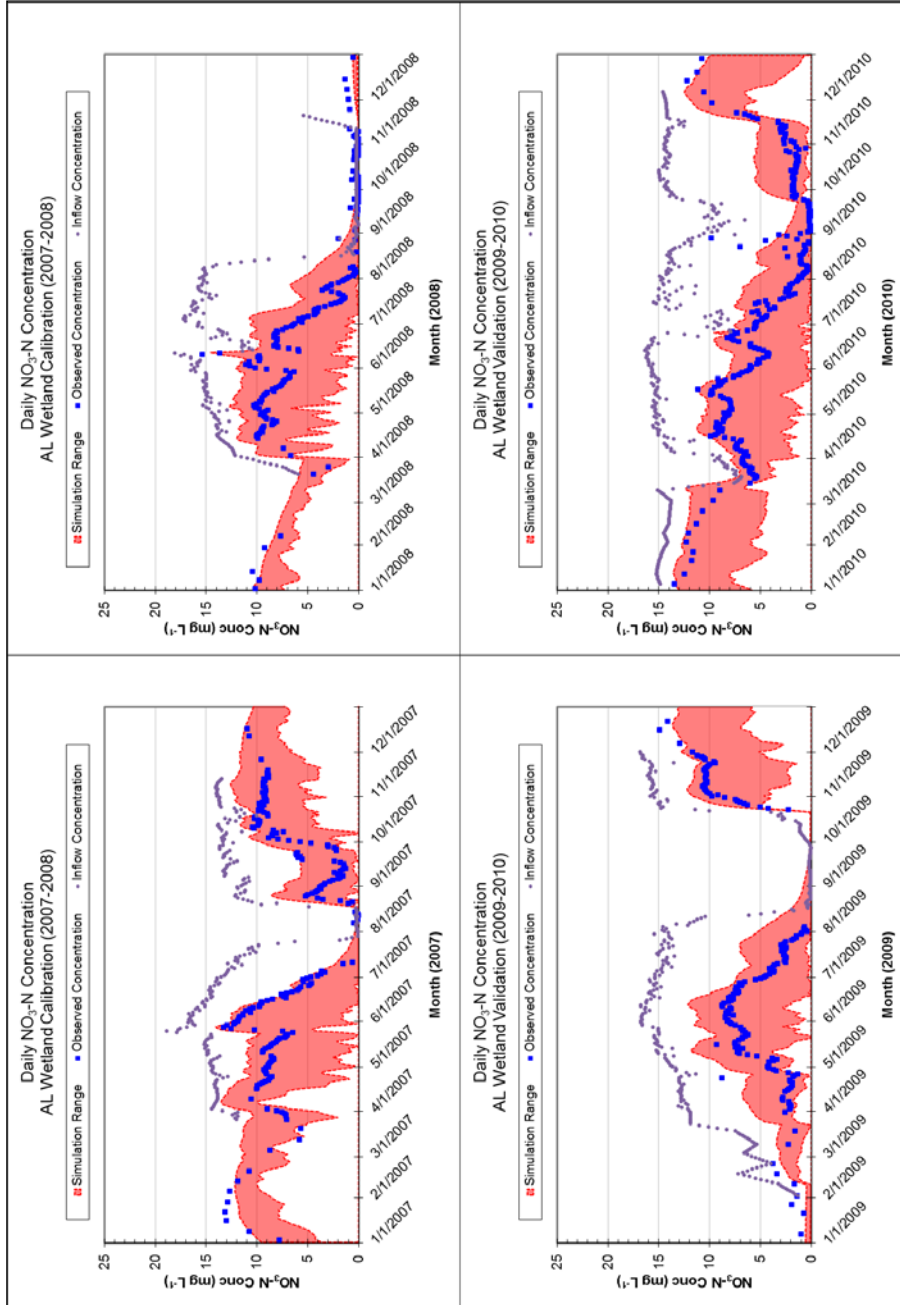


Figure 4.21. Sensitivity of $\text{NO}_3\text{-N}$ concentrations in the AL wetland with variation of removal rate, NSETLR, from 17 m yr^{-1} to 184 m yr^{-1} , using the modified wetland equations. The temperature coefficient, N_THETA , was held constant at 1.08. The dots illustrate measured inflow concentrations, the solid blue line represents observed outflow concentrations, and the red-shaded band illustrates the range of predicted $\text{NO}_3\text{-N}$ concentration.

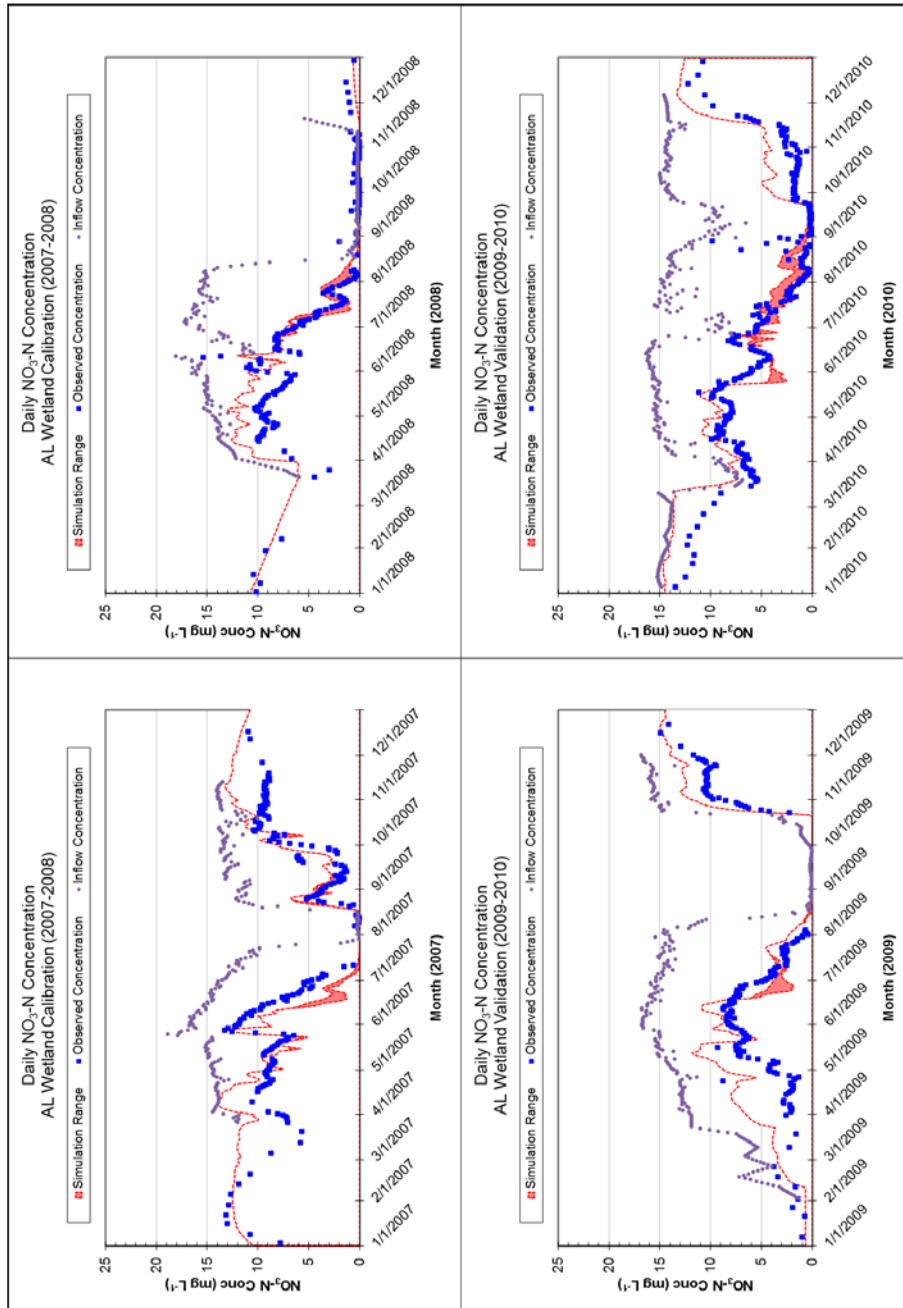


Figure 4.22. Sensitivity of $\text{NO}_3\text{-N}$ concentrations in the AL wetland with variation of temperature coefficient, N_THETA , from 1.04 to 1.20. The removal rate, $NSETLR$, was held constant at the calibrated value of 40 m yr^{-1} . The dots illustrate measured inflow concentrations, the solid blue line represents observed outflow concentrations, and the red-shaded band illustrates the range of predicted $\text{NO}_3\text{-N}$ concentration.

Simulation of $\text{NO}_3\text{-N}$ in wetlands using the SWAT model was improved using the modified wetland equations developed for Iowa CREP wetlands, but improvements were not as dramatic as expected due to the reasonably good simulations obtained using the original equations. However, it is important to realize that the performance of the original SWAT model equations benefited from the availability of information used for parameterization not normally available for SWAT wetland applications. The modified equations simulate flow based on established relationships between wetland size and volume combined with the use of weir discharge equations and known weir characteristics. Hence, they did not require calibration. Conversely, the original equations utilize the empirical NDTARGR parameter to predict wetland discharge, for which the default value is 10 days – too large for CREP wetlands – and required calibration.

To illustrate the importance of this, the sensitivity of $\text{NO}_3\text{-N}$ dynamics to NDTARGR in the original equations was evaluated by comparing simulated concentrations in the KS Wetland using the calibrated value of NDTARGR and the default value of 10 days (Figure 4.23). With NDTARGR equal to 10, SWAT consistently significantly under-estimated $\text{NO}_3\text{-N}$ concentration. Calibrating to observed concentrations would have required using NSETLR values outside of the range recommended for Iowa CREP wetlands. Further, because the default NDTARGR parameter affected concentration and outflow, subsequent errors in predicted $\text{NO}_3\text{-N}$ loads exported from the KS Wetland were quite large, especially during times of high flows (Figure 4.24).

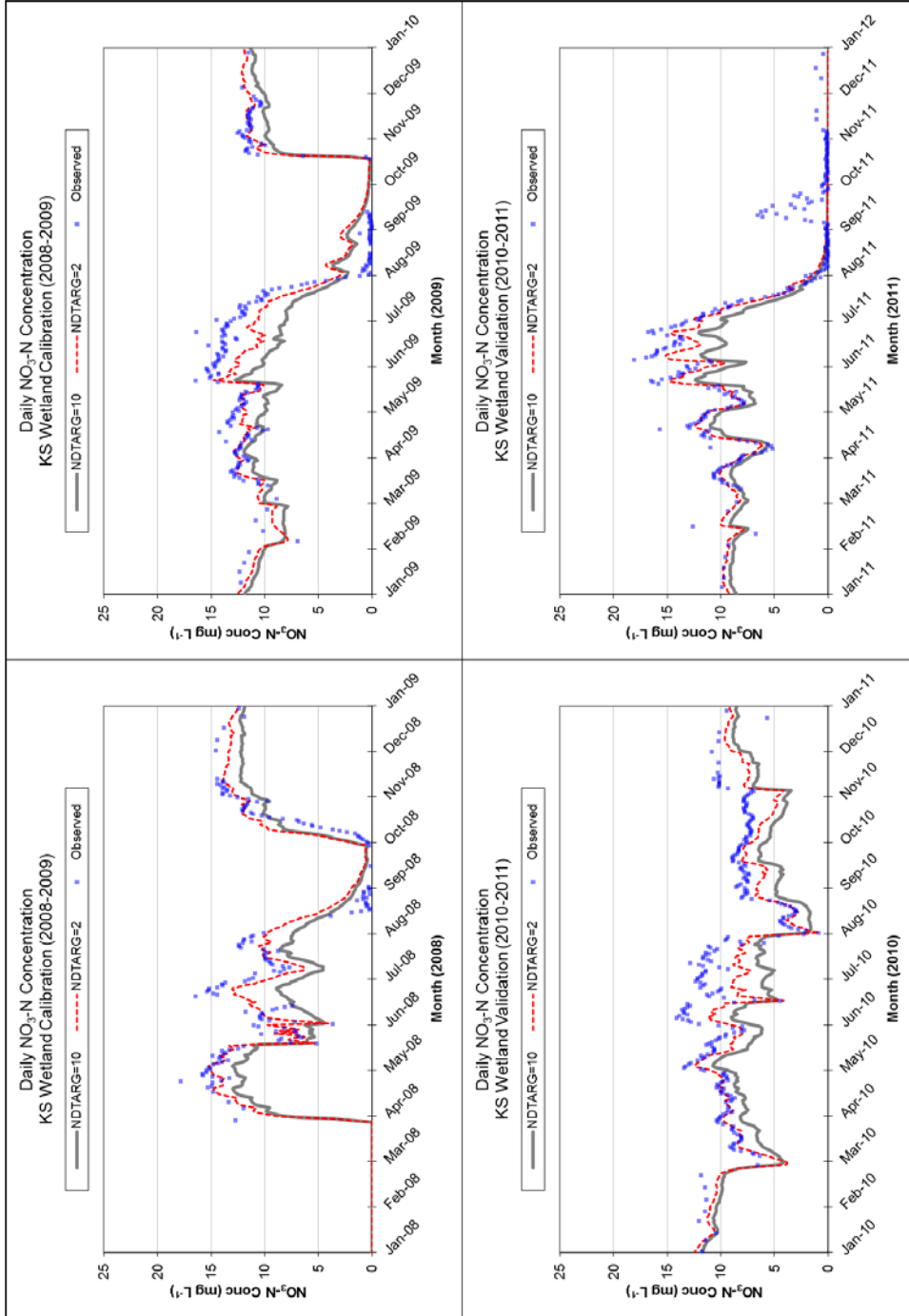


Figure 4.23. Simulation of NO₃-N concentrations in the KS wetland with variation of NDTARGR from 2 (calibrated value) to 10 (SWAT default value) using the original equations. The red, dashed line represents daily NO₃-N concentration with NDTARGR=2. The gray, solid line illustrates concentrations simulated with NDTARGR=10. Blue dots represent observed concentrations.

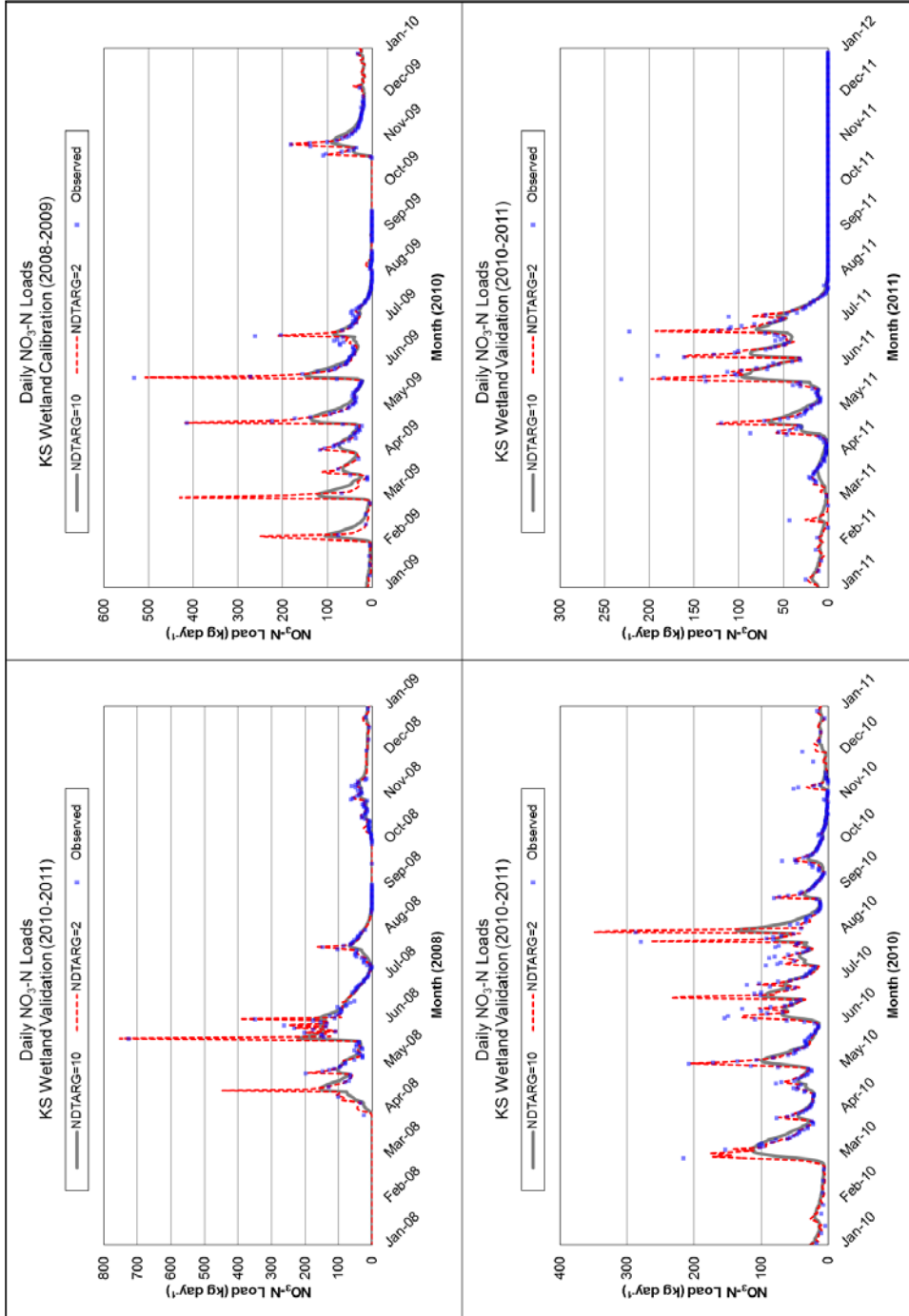


Figure 4.24. Simulation of $\text{NO}_3\text{-N}$ loads exported from the KS wetland with variation of NDTARGR from 2 (calibrated value) to 10 (SWAT default value) using the original equations. The red, dashed line represents daily $\text{NO}_3\text{-N}$ load with $\text{NDTARGR}=2$. The gray, solid line illustrates loads simulated with $\text{NDTARGR}=10$. Blue dots represent observed loads. Note varying y-axis scale.

4.4.5 *Integrated watershed/wetland simulation*

The CREP wetland at the outlet of the KS watershed was integrated with KS watershed model (described in Chapter 3) using the modified and re-calibrated NO₃-N parameters (best results) as well as the original NO₃-N calibration results (worst results). The resulting NSE and PBIAS values for NO₃-N loads exported from the wetland were 0.44 (satisfactory) and 18.6 (good), respectively, for the best-case scenario. These are significantly lower than the NSE value of 0.98 (very good) and PBIAS of 2.6 (very good) obtained when simulating only the wetland. Percent NO₃-N removal in the wetland was increased from 15.1% in the wetland-only simulation to 15.7% in the best-case integrated simulation, but mass removal of NO₃-N was reduced by 1,221 kg over the 4-year simulation period (305 kg yr⁻¹) due to underestimation of watershed NO₃-N export. For the worst-performing KS model, integrated simulation of the watershed and CREP wetland (prior to modification of lagging parameters), the resulting NSE value was 0.30 (not satisfactory) and the PBIAS was 53.3 (not satisfactory), with predicted mass removal of NO₃-N under-predicted by 4,202 kg (1050 kg yr⁻¹).

Measured and simulated NO₃-N loads leaving the wetland are illustrated in Figure 4.25 (best-case) and Figure 4.26 (worst-case). These results show the potential errors introduced to NO₃-N prediction in wetlands arising from errors in watershed/tile simulation, with particularly large errors at times of high export (i.e., high flows). This finding validates the importance of evaluating short-term (i.e., daily) performance of models intended to simulate water quality improvement BMPs such as wetlands.

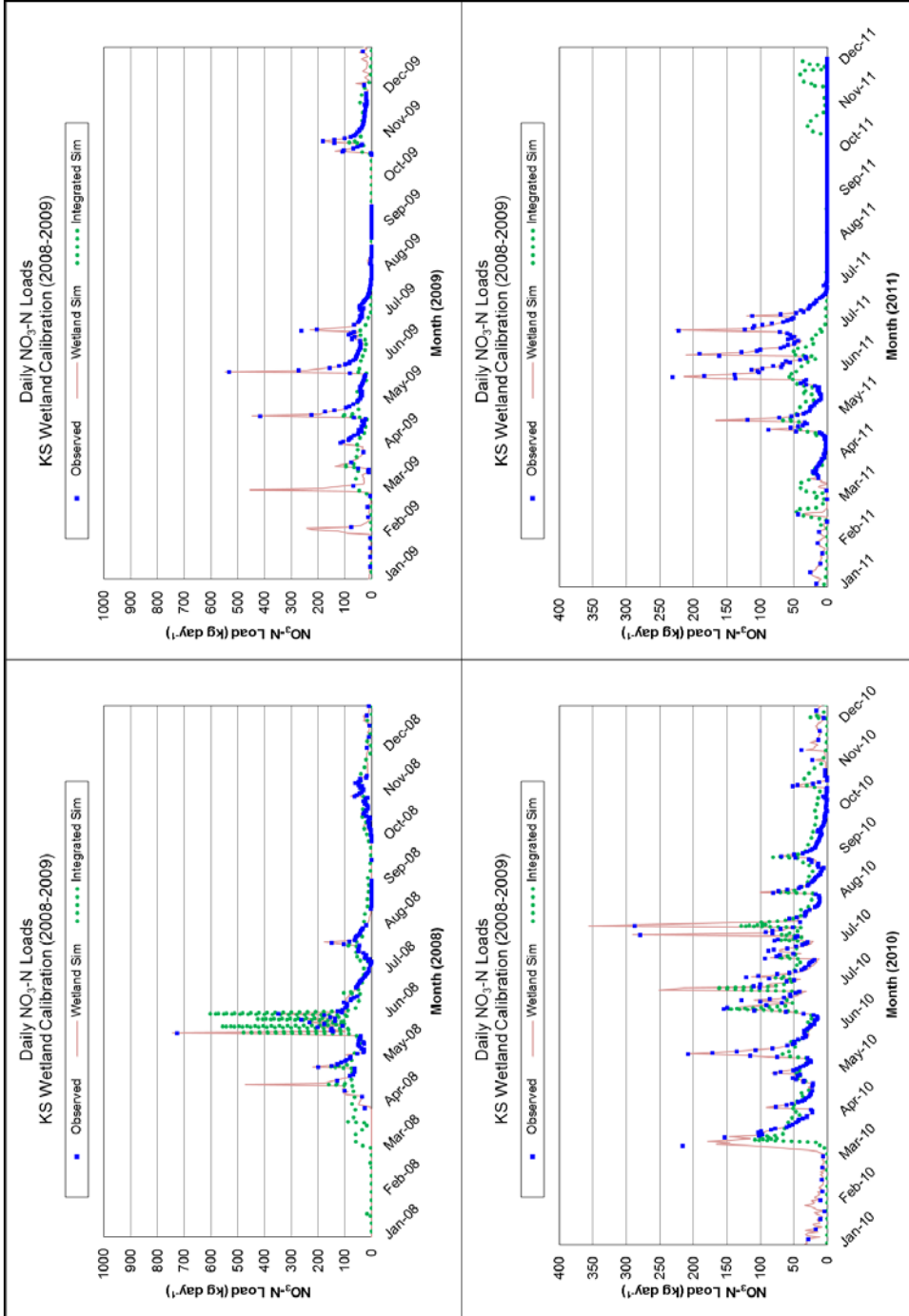


Figure 4.25 Simulated $\text{NO}_3\text{-N}$ loads in wetland outflow for the best simulation of the KS watershed using modified lagging parameters. Blue dots represents measured data, dashed green line is model output resulting from integrating watershed/tile and wetland simulations, and solid red line is reflects isolated wetland simulation.

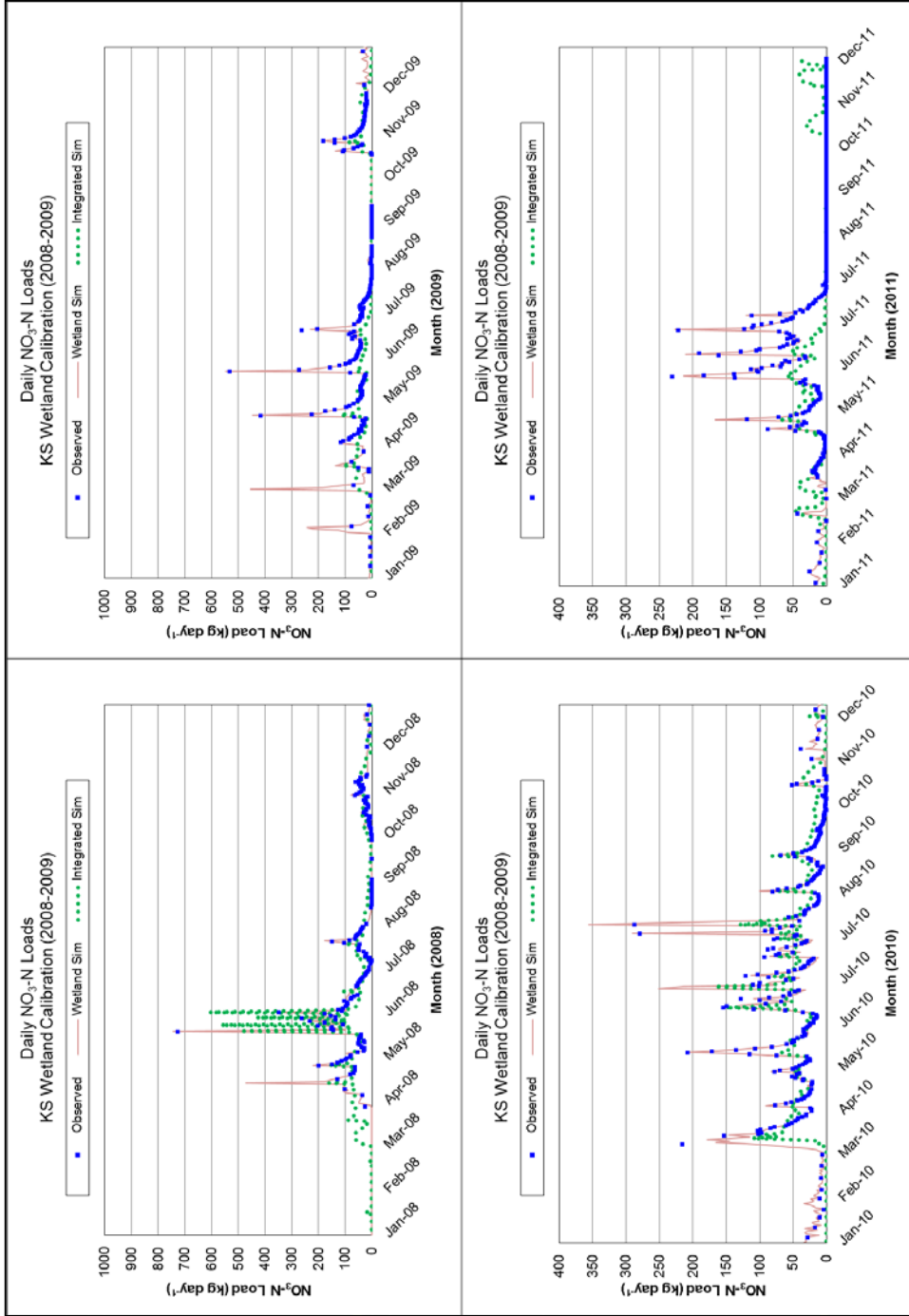


Figure 4.26 Simulated NO₃-N loads in wetland outflow for the KS watershed using the original NO₃-N algorithms. Blue dots represents measured data, dashed green line is model output resulting from integrating watershed/tile and wetland simulations, and solid red line is reflects isolated wetland simulation.

4.5 Conclusions

Overall, both the original and modified wetland equations simulated wetland outflow, $\text{NO}_3\text{-N}$ concentrations, and $\text{NO}_3\text{-N}$ loads well at the daily time step. The modified wetland equations provided better simulation of wetland hydrology and hence, $\text{NO}_3\text{-N}$ loads, compared with the original SWAT equations. This is likely due to the introduction of physically-based weir discharge equations in the modified approach in lieu of the simplistic drawdown and mass balance approach in the original equations. Simulation of wetland volume fluctuation was particularly improved, which may have significance for model applications in which volume, ET, and duration of inundation are of interest. Perhaps more importantly, the modified equations are more physically-based and objectively informed, making them more readily applied to other wetlands. Additionally, the modified wetland equations incorporated into the SWAT model have broad utility and are useful for simulating other impoundments in addition to CREP wetlands, provided that the stage-area-volume relationships of the impoundment of interest can be derived.

The improvements in $\text{NO}_3\text{-N}$ simulation using the modified equations were not as dramatic due to reasonably good calibration of the original equations using observed flow and $\text{NO}_3\text{-N}$ data. However, in the absence of such data, errors produced using the original equations may be much larger, since the NDTARGR parameter required calibration and concentration and load predictions were both influenced by this parameter. Conversely, the modified equations did not require hydrologic calibration, which simplified the calibration process to adjustment of the $\text{NO}_3\text{-N}$ removal rate (NSETLR) and temperature correction factor (N_THETA). For both equations, NSE values ranged from 0.77 to 0.90 for daily

concentrations, and 0.87 to 0.98 for daily loads. PBIAS ranged from -2.76% to 12.11% for simulation of NO₃-N concentration, and from -4.45 to 8.60 for NO₃-N load simulations.

Although this study evaluated wetland flow and NO₃-N simulation, the new/modified equations are also available for phosphorus (P) simulation. Further parameterization guidance is needed, since removal of P in wetlands is more variable and uncertain than NO₃-N reduction. The primary limitation of the modified wetland equations that were incorporated into the SWAT model is the availability of site-specific topographic and weir outlet data. These characteristics are needed to parameterize the new equations. Selection of appropriate removal rates (NSETLR) is critical, given the sensitivity of model predictions to this parameter.

Simulation of NO₃-N in the KS watershed CREP wetland revealed the impacts of errors in watershed/tile simulation on wetland simulations. Isolating the wetland from the watershed resulted in an NSE of 0.98 and PBIAS of 2.6% for NO₃-N load at the wetland outlet. When the wetland was integrated with the watershed simulations using the existing soil and tile NO₃-N algorithms, the NSE decreased to 0.30 and PBIAS increased to 53.3%. Additionally, the mass removal of NO₃-N in the wetland was under-predicted by 1,050 kg yr⁻¹ in the integrated watershed/wetland simulation. These findings verify that simulation of NO₃-N removal in wetlands is limited by the ability of the model to predict subsurface flow and NO₃-N concentrations in tile drainage.

4.6 Acknowledgements

This study was made possible through funding by EPA's Initiative Enhancing State and Tribal Wetland Programs grant program (Grant Agreement Number CD-97723301-0). Flow and water quality monitoring data used for model testing and evaluation were collected

as part of the Iowa CREP program, a state, federal, local, and private partnership that helps establish and monitor wetlands for water quality improvement in the tile-drained regions of Iowa. Data compilation and dissemination by Greg Stenback in the Department of Ecology, Evolution, and Organismal Biology (EEOB) at Iowa State University, is greatly appreciated. SWAT model FORTRAN code modification and testing was conducted in collaboration with Jeff Arnold and Nancy Sammons in the Grassland, Soil, and Water Research Laboratory of USDA-ARS in Temple, Texas.

4.7 References

- Alexander, R. B., Smith, R. A., Schwarz, G. E., Boyer, E. W., Nolan, J. V. Nolan, and Brakebill, J. W. 2008. Differences in phosphorus and nitrogen delivery to the Gulf of Mexico from the Mississippi River basin. *Environ. Sci. Technol.*, 42:822–830.
- Arnold, J. G., Allen, P. M., Morgan, D. S. 2001. Hydrologic model for design and constructed wetlands. *Wetlands*, 21(2):167-178.
- Bingner, R. L., & Theurer, F. D. 2005. AnnAGNPS technical processes documentation for version 3.2. United States Department of Agriculture (USDA). National Sedimentation Laboratory. Oxford, Miss.
- Bishop, R. A., and A. G. van der Valk. 1982. Wetlands. pp. 208-229. In T.C. Cooper (ed.) *Iowa's Natural Heritage*. Iowa Natural Heritage Foundation and Iowa Academy of Science. Des Moines, Iowa, USA.
- Borah, D. K., Yagow, G. Saleh, A., Barnes, P. L., Rosenthal, W., Krug, E. C., & Hauck, L. M. 2006. Sediment and nutrient modeling for TMDL development and implementation. *Trans ASABE*, 49(4):967-986.
- Crumpton, W. G. & Goldsborough, L. G. 1998. Nitrogen transformation and fate in prairie wetlands. *Great Plains Research*, 8(1):57-72.
- Crumpton, W.G. 2001. Using wetlands for water quality improvement in agricultural watersheds; the importance of a watershed scale approach. *Water Sci. and Tech.*, 44(11-12):559-565.
- Crumpton, W. G., Stenback, G. A., Miller, B. A., and Helmers, M. J. 2006. Potential benefits of wetland filters for tile drainage systems: impact on nitrate loads to Mississippi River subbasins. Ames, Iowa. Final report to the U.S. Department of Agriculture (USDA).
- Crumpton, W. G., M. J. Helmers, G. A. Stenback, D. W. Lemke, and S. Richmond. 2012. Integrated Drainage Wetland Systems for Reducing Nitrate Loads from Des Moines Lobe Watersheds. Agricultural and Biosystems Engineering Project Reports. Paper 13. http://lib.dr.iastate.edu/abe_eng_reports/13
- Dinnes, D. L., Karlen, D. L., Jaynes, D. B., Kaspar, T. C., Hatfield, J. L., Colvin, T. S., & Cambardella, C. A. 2002. Nitrogen management strategies to reduce nitrate leaching in tile-drained Midwestern soils. *Agron J.*, 94:153-171.

- Douglas-Mankin, K. R., Srinivasan, R., & Arnold, J. G. 2010. Soil and water assessment tool (SWAT) model: current developments and applications. *Trans. ASABE.*, 53(5): 1423-1431.
- Gassman, P. W., Reyes, M. R., Green, C. H., & Arnold, J. G. 2007. The soil and water assessment tool: Historical development, applications, and future research directions. *Trans. ASABE*, 50(4): 1211-1250.
- Goolsby, D. A., Battaglin, W. A., Aulenbach, B. T., & Hooper, R. P. 2000. Nitrogen flux and sources in the Mississippi River basin. *Sci. of the Total Environ.*, 248:75-86.
- Ingersoll, T. L., & Baker, L. A. 1998. Nitrate removal in wetland microcosms. *Water Res.*, 32(3): 677-684.
- Kadlec, R. H. & Knight, R. L. 1996. *Treatment Wetlands*. Lewis Publishers, Boca Raton, Fla.
- Kalcic, M. M., J. Frankenberger, and I. Chaubey. Spatial optimization of six conservation practices using SWAT in tile-drained agricultural watersheds. *Journal of the American Water Resources Association*. 51(4):956-972.
- Kovacic, D. A., David, M. B., Gentry, L. E. , Starks, K. M., & Cooke, R. A. 2000. Effectiveness of constructed wetlands in reducing nitrogen and phosphorus export from agricultural tile drainage. *J. Environ. Qual.*, 29:1262-1274.
- Lin, Y. F., Jing, S. R., Wang, T. W., & Lee, D. Y. 2002. Effects of macrophytes and external carbon sources on nitrate removal from groundwater in constructed wetlands. *Environ. Pollution*, 119:413–420. Doi:10.2489/jswc.67.6.513.
- Miller, B. A., W. G. Crumpton, and A. G. van der Valk. 2009. Spatial distribution of historical wetland classes on the Des Moines Lobe, Iowa. *Wetlands*. 29(4):1146-1152.
- Moriasi, D. N., Rossi, C. G., Arnold, J. G., & Tomer, M. D. 2012. Evaluating hydrology of the Soil and Water Assessment Tool (SWAT) with new tile drain equations. *J. Soil Water Cons. Soc.*, 67(6):513-524
- Moriasi, D. N., Gowda, P. H., Arnold, J. G., Mulla, D. J., Srinivasulu, A., Steiner, J. L., & Tomer, M. D. 2013. Evaluation of the Hooghoudt and Kirkham tile drain equations in the Soil and Water Assessment Tool to simulate tile flow and nitrate-nitrogen. *J. Environ. Qual.*, 42:1699-1710. doi:10.2134/jeq2013.01.0018.
- Moriasi, D. N., M. W. Gitau, N. Pai, and P. Daggupati. 2015. Hydrologic and water quality models: Performance measures and evaluation criteria. *Trans. of the ASABE* 58(6):1763-1785.
- McCorvie, M. R. & Lant, C. L. 1993. Drainage district formation and the loss of Midwestern wetlands, 1850-1930. *Agric. Hist.*, 67(4):13-39.
- Neitsch, S. L., Arnold, J. G., Kiniry, J. R., & Williams, J. R. 2011. Soil and water assessment tool theoretical documentation version 2009. Texas Water Resources Institute Technical Report No. 406. Texas A&M University. College Station, Texas.
- Phipps, R. G. & Crumpton, W. G. 1994. Factors affecting nitrogen loss in experimental wetlands with different hydrologic loads. *Ecol. Eng.*, 3:399-408.
- Records, R. M. M. Arabi, S. R. Fassnacht, W. G. Duffy, M. Ahmadi, and K. C. Hegewisch. 2014. Climate change and wetland loss impacts on a western river's water quality. *Hydro. Earth Syst. Sci.* 18:4509-4527. doi:10.5194/hess-18-4509-2014

- Singh, J., Knapp, H. V., Arnold, J. G., & Demissie, M. 2005. Hydrological modeling of the Iroquois River watershed using HSPF and SWAT. *J. Amer. Water Resources. Assoc.*, 41(2):343-360.
- Skaggs, R. W., Breve, M. A., & Gilliam, J. W. 1992. Environmental impacts of agricultural drainage. In *Proc. Irrigation & Drainage: Saving a threatened resource – in search of solutions* (pp. 19-24). Baltimore, Md.: ASCE
- Tomer, M. D., Crumpton, W. G., Bingner, R. L., Kostel, J. A., & James, D. E. 2013. Estimating nitrate load reductions from placing constructed wetlands in a HUC-12 watershed using LiDAR data. *Ecol. Eng.*, 56:69-78.
- United States Environmental Protection Agency (EPA). 1998. Comparison of model capabilities. Scientific Advisory Panel Meeting. July 29-30, 1998. Retrieved from <http://www.epa.gov/scipoly/sap/meetings/1998/july/matrix.htm>
- Urban, M.A. 2005. An uninhabited waste: transforming the Grand Prairie in nineteenth century Illinois, USA. *Jour. Hist. Geog.*, Vol. 31:647-665.
- van der Valk, A. G., & Jolly, R.W. 1992. Recommendations for research to develop guidelines for the use of wetlands to control rural NPS pollution. *Ecological Engineering*, 1(1):115-134.
- Water Pollution Control Federation (WPCF). 1990. *Natural Systems for Wastewater Treatment, Manual of Practice FD-16*. Alexandria, VA: Water Environment Federation.
- Xue, Y., Kovacic, D. A., David, M. B., Gentry, L. E., Mulvaney, R. L., & Lindau, C. W. 1999. In site measurements of denitrification in constructed wetlands. *J. Environ. Qual.*, 28:263-269.
- Yuan, Y., Mehaffey, M. H., Lopez, R. D., Bingner, R. L., Bruins, R., Erickson, C., & Jackson, M. A. 2011. AnnAGNPS model application for nitrogen loading assessment for the future Midwest landscape study. *Water*, 3:196-216.

CHAPTER 5. GENERAL CONCLUSIONS

5.1 Review of central themes

The central theme of this dissertation is the evaluation and simulation of hydrology and nitrate-nitrogen ($\text{NO}_3\text{-N}$) in small watersheds in tile-drained landscapes. Subsurface tile drainage systems have played a critical role in the agricultural and economic success of the Upper Midwest, but have also dramatically reduced wetland ecosystems and increased loss of $\text{NO}_3\text{-N}$ to surface water. The watersheds evaluated in this dissertation are representative of agricultural drainage districts on the Des Moines Lobe ecoregion. In recent years, the export of $\text{NO}_3\text{-N}$ from drainage districts such as these has garnered much attention, as nutrient transport has negatively impacted drinking water supplies and hypoxia in the Gulf of Mexico.

Watershed management for nutrient reduction requires accurate and reliable information about $\text{NO}_3\text{-N}$ transport pathways and processes. Models capable of simulating hydrology, nutrient fate and transport, and the effects of BMPs at watershed scales are needed to better support planning and implementation efforts. This dissertation describes three studies undertaken to improve our ability to predict hydrology and nutrient transport in tile-drained watersheds. The first study explored the magnitude and patterns of measured $\text{NO}_3\text{-N}$ exports from drainage districts to downstream river basins. The second study evaluated the simulation of two drainage-district scale watersheds using SWAT and focused on model performance for pathway-specific flow and daily $\text{NO}_3\text{-N}$ concentrations. The third study evaluated and improved the simulation of $\text{NO}_3\text{-N}$ removal in SWAT using detailed monitoring data collected at two Conservation Reserve and Enhancement Program (CREP) wetlands.

5.2 Review of the magnitude and patterns of NO₃-N exports from drainage districts to downstream river basins

The objectives of this study were to quantify hydrology and NO₃-N export patterns from three tile-drained catchments and the downstream river over a 5-yr period, compare results to prior plot-, field-, and watershed-scale studies, and discuss implications for water quality improvement in these landscapes. The tile-drained catchments had an annual average water yield of 247 mm yr⁻¹, a flow-weighted NO₃-N concentration of 17.1 mg L⁻¹, and an average NO₃-N loss of nearly 40 kg ha⁻¹ yr⁻¹, with substantial spatial variation in NO₃-N exports between watersheds. Overall, water yields were consistent with prior tile drainage studies in Iowa and the upper Midwest, but associated NO₃-N concentrations and losses were among the highest reported for plot studies and higher than those found in small watersheds. More than 97% of the nitrate export occurs during the highest 50% of flows at both the drainage district and river basin scales. Findings solidified the importance of working at the drainage district scale to achieve nitrate reductions necessary to meet water quality goals, and also indicate the importance of accurately predicting NO₃-N transport at this scale for the purpose of watershed planning.

5.3 Review of simulating short-term fluctuations in subsurface flow and NO₃-N in small, tile-drained watersheds using SWAT

The objectives of this study were to develop and calibrate SWAT models for small, tile-drained watersheds, evaluate model performance for pathway-specific flow and NO₃-N simulation at monthly and daily intervals, and document important intermediate processes and N-fluxes. Model calibration and evaluation revealed that it is possible to meet generally accepted performance criteria (Moriassi et al., 2015a) for simulation of monthly total flow

(WYLD), subsurface flow (SSF), and $\text{NO}_3\text{-N}$ loads in both case study watersheds. In the final calibration simulations for the KS and AL watersheds, Nash-Sutcliffe Efficiency (NSE) values were 0.79 and 0.71, respectively, for monthly WYLD; 0.55 and 0.66 for monthly SSF; and 0.72 and 0.60 for monthly $\text{NO}_3\text{-N}$ load (using the modified $\text{NO}_3\text{-N}$ lagging algorithms). Simulation of daily SURQ and SSF proved more challenging and were generally not satisfactory. Simulation of daily $\text{NO}_3\text{-N}$ concentration was not satisfactory even after modifying $\text{NO}_3\text{-N}$ algorithms to lag flushing from the soil profile.

Differences in hydrology and $\text{NO}_3\text{-N}$ transport between watersheds were not reflected by the model, which suggests that parameterization may not be transferable across watersheds and that models calibrated at larger scales may not accurately reflect hydrology and nutrient transport at drainage district scales. These limitations are especially important for simulation of $\text{NO}_3\text{-N}$ removal wetlands.

When calibrated to $\text{NO}_3\text{-N}$ concentration in flow, the model tracks soil- NO_3 levels reasonably well over time, but over-estimates depletion from the soil during summer months. Analysis of soil- $\text{NO}_3\text{-N}$ fluxes revealed that simulated mineralization and plant uptake rates are generally reasonable compared to literature values; however, these fluxes are highly variable in space and time and heavily influence $\text{NO}_3\text{-N}$ transport via tile drainage. Soil-N fluxes should therefore be evaluated and reported as standard practice when applying the SWAT model for simulation of $\text{NO}_3\text{-N}$ transport. Better parameterization methods and supporting data for model inputs related these processes are needed, and if possible, related inputs and soil-N fluxes should be constrained within reasonable ranges.

5.4 Review of the modification of SWAT to improve simulation of NO₃-N removal wetlands.

The objectives of this study were to modify existing algorithms in SWAT by adapting proven CREP wetland models, compare model performance using original SWAT algorithms and modified wetland equations to simulate two Iowa CREP wetlands, and ramifications of watershed/tile simulation errors on prediction of NO₃-N in Iowa CREP wetlands. The modified equations improved simulation of hydrology and NO₃-N in the wetlands, with NSE values of 0.88 to 0.99 for daily load predictions, and percent bias (PBIAS) values generally less than 6%. The applicability of the modified equations to wetlands without detailed monitoring data was improved over the original SWAT equations due to more objectively-informed parameterization, reduced need for hydrologic calibration, and incorporation of an irreducible nutrient concentration and temperature correction factor. The NO₃-N removal rate (NSETLR) is the critical input parameter for NO₃-N reduction and strongly influences model performance.

Simulation of NO₃-N in the KS watershed CREP wetland revealed that isolating the wetland from the watershed resulted in an NSE of 0.98 and PBIAS of 2.6% for NO₃-N load at the wetland outlet. When the wetland was integrated with the watershed simulation, the NSE decreased to 0.30 and PBIAS increased 53.3%, indicating that simulation of NO₃-N removal wetlands is limited by the ability of the model to simulate NO₃-N in suburface tile drainage.

5.5 Implications/recommendations

The findings of these studies reveal that manner in which watershed models are developed and calibrated may limit the utility of a model for its intended purpose, consistent

with recent hydrologic and water quality model calibration guidelines. Parameterization methods and input values may not be transferrable across small watersheds and models calibrated at large watershed scales may not be suitable for predicting small watershed hydrology and $\text{NO}_3\text{-N}$ exports or optimizing BMPs placement at drainage-district outlets.

Findings also indicate that model applications in which the impacts of water quality BMPs with removal rates driven by inflow concentrations (e.g., wetlands) will be simulated should include calibration and assessment of nutrient concentrations, not just nutrient loads. Accuracy of predicted nutrient simulation within the BMP will be only as accurate as simulation of concentrations entering the BMP. Furthermore, the practice of calibrating flow and load simultaneously may actually worsen model reliability by masking deficiencies or errors in the simulation of concentration.

A third key finding is that although the SWAT has the ability to estimate soil-N dynamics reasonably well, the processes are highly variable and significantly affect $\text{NO}_3\text{-N}$ transport to surface water. This is particularly true of denitrification, which is highly sensitive to input parameters in SWAT. This implication is that better parameterization methods are needed, and the development of appropriate parameter and N-flux constraints would facilitate improved model performance. This will likely require the collaboration between model developers and agronomists and soil scientists.

5.6 Recommendations for future research

- Using all available CREP wetland monitoring data, a methodology should be developed to inform selection of nutrient removal rates in SWAT (NSETLR, PSETLR) based on known wetland and/or watershed characteristics to better inform

application of the new wetland algorithms to wetlands for which monitoring data do not exist.

- The effect of the lumped nature of HRUs in SWAT on the simulation of tile flow should be further evaluated. This could be done by applying to model to plot and/or field-scales for which detailed tile flow and NO₃-N data are available. Additionally, comparison of SWAT with DRAINMOD and/or RZWQM simulations at field or plot scales would be instructive.
- Simulation of tile drainage in SWAT and other watershed models would benefit from more model applications in which detailed calibration data are available. This type of monitoring is typically cost-prohibitive, therefore integrated monitoring and model improvement studies are needed so that model algorithms, parameterization methods, and constraints on model processes (such as intermediate nutrient fluxes) can be improved to address current model limitations.
- Soil-N fluxes and process in SWAT need further evaluation using available agronomic research related to mineralization, denitrification, and plant uptake rates. Related algorithms may require modification/improvement, but at a minimum, better parameterization methods and parameter constraints are needed to assist with model calibration. Crop growth parameters in SWAT may need updating to reflect current crop genetics related to things such as nitrogen use efficiency and drought tolerance.

APPENDIX A

FORTRAN CODE MODIFICATIONS FOR CHAPTER 3

Modified nutrient uptake (NUP.F):

```

unmx = uno3d * (1. - Exp(-n_updis * gx / sol_rd)) / uobn
  uno3l = Min(unmx - nplnt(j), sol_no3(1,j))
  uno3l = up_reduc * uno3l  !! line in question ☐this line was
commented

```

Modified tile drain NO₃-N transport (NUP.F):

```

co_p(j) = co_p(j) * (1. - alph_e(j)) + vno3_c * alph_e(j)
  tileno3(j) = co_p(j) * qtile  !Daniel 1/2012 ☐originally co(j)
  tileno3(j) = Min(tileno3(j), sol_no3(jj,j))
  sol_no3(jj,j) = sol_no3(jj,j) - tileno3(j)

```

APPENDIX B

FORTRAN CODE MODIFICATIONS FOR CHAPTER 4

New wetland flow equations (RES.F):

```

case (5)
  resflwo = 0.
  do jj = 1, nostep
    !! solve quadratic to find new depth
    !testing relationship res_vol(jres) = float(jj) * .1 * res_pvol(jres
  )
    x1 = bcoef(jres) ** 2 + 4. * ccoef(jres) * (1. -
&                                res_vol(jres) / res_pvol(jres))
    if (x1 < 1.e-6) then
      res_h = 0.
    else
      res_h1 = (-bcoef(jres) - sqrt(x1)) / (2. * ccoef(jres))
      res_h = res_h1 + bcoef(jres)
    end if
    !! calculate water balance for timestep with new surface area
    ressa = res_psa(jres) * (1. + acoef(jres) * res_h)
    resev = 10. * evrsv(jres) * pet_day * ressa
    ressep = res_k(jres) * ressa * 240.
    respcp = sub_subp(res_sub(jres)) * ressa * 10.
    if(res_h <= 1.e-6) then
      res_qi = 0.
      res_h = 0.
    else
&      res_qi = weirc(jres) * weirk(jres) * weirw(jres) *
&                                (res_h ** 1.5)
    end if
    resflwo = resflwo + res_qi
    res_vol(jres) = res_vol(jres) + (respcp + resflwi - resev
&                                - ressep) / nostep
  enddo

```

New wetland nutrient equations (RESNUT.F):

!! settling rate/mean depth

```

!! part of equation 29.1.3 in SWAT manual
if (iresco(jres) == 5) then
  phosk = ressa * 10000. * (conc_p - con_pirr(jres)) *
&   theta(psetlr(iseas,jres), theta_p(jres), tmpav(res_sub(jres)))
  nitrok = ressa * 10000. * (conc_n - con_nirr(jres)) *
&   theta(nsetlr(iseas,jres), theta_n(jres), tmpav(res_sub(jres)))
else
  phosk = psetlr(iseas,jres) * ressa * 10000. /
&   (res_vol(jres) + resflwo)
  phosk = Min(phosk, 1.)
  nitrok = nsetlr(iseas,jres) * ressa * 10000. /
&   (res_vol(jres) + resflwo)
  nitrok = Min(nitrok, 1.)
endif
!! remove nutrients from reservoir by settling
!! other part of equation 29.1.3 in SWAT manual
res_solp(jres) = res_solp(jres) * (1. - phosk)
res_orgp(jres) = res_orgp(jres) * (1. - phosk)
res_orgn(jres) = res_orgn(jres) * (1. - nitrok)
res_no3(jres) = res_no3(jres) * (1. - nitrok)
res_nh3(jres) = res_nh3(jres) * (1. - nitrok)

res_no2(jres) = res_no2(jres) * (1. - nitrok)

```